Torque Measurement on Wind Turbines and its Application in the Determination of Drivetrain Efficiency

Von der Fakultät für Maschinenbau

der Gottfried Wilhelm Leibniz Universität Hannover

zur

Erlangung des akademischen Grades

Doktor-Ingenieur

- Dr.-Ing. -

genehmigte Dissertation

von

M. Sc. Hongkun Zhang

2021

Abstract

The input torque of a wind turbine contains an abundance of information about the operating conditions of the turbine. At the same time it is also a critical input for the efficiency determination of the drivetrain. An appropriate method of torque measurement plays an important role in wind turbines research and helps to further reduce the COE (cost of energy) of the wind turbines. However, a number of challenges are currently restricting the breadth and depth of torque measurement applications in the testing and operation of wind turbines. The research described in this dissertation studies the major challenges posed by the different aspects of torque measurement, including the measuring principle, the calibration and the uncertainty. The efficiency determination of the drivetrain is also studied as an important application, which has the highest demand on the accuracy of torque measurement and its calibration among applications in the wind energy industry.

The research proposes new approaches and improvements to cope with the above mentioned challenges. A new method of torque measurement based on the rotary encoders is proposed and realised during a test campaign. During the same test campaign, improvement of the traditional torque measurement based on strain gauges is also demonstrated, where the influence of non-torque loads is greatly reduced by having more measuring points for the torque measurement. A new method is also proposed to address the problem of insufficient accuracy in the drivetrain efficiency determination of a wind turbine on the test bench. With the proposed method, the dependency of the determined efficiency on the accuracy of torque and electrical power measurement can be effectively reduced. As a result, the efficiency can be determined with an uncertainty considerably lower than that of the torque measurement. The method takes advantage of a specially designed test sequence whereby the test bench and the wind turbine drivetrain take turns to run in motor mode and drive the other one which operates in generator mode. The same test sequence is also adopted to develop a method of torque calibration. The method establishes a relationship between the torque and the electrical power using measurements from the two tests where the turbine drivetrain operates in different modes. The calibration uncertainty introduced by the power loss in the drivetrain is thus reduced. Detailed uncertainty analysis for the efficiency determination and torque calibration is carried out in this research to confirm the benefit as well as quantify the effectiveness of the methods proposed. Future work and further applications of the methods proposed are presented at the end of the dissertation.

Kurzfassung

Das Eingangsdrehmoment einer Windenergieanlage enthält eine große Menge an Informationen über ihre Betriebsbedingungen und ist gleichzeitig ein kritischer Eingangsparameter für die Effizienzbestimmung des Antriebsstrangs. Ein geeignetes Verfahren zur Drehmomentmessung spielt daher eine wichtige Rolle in der Windenergieforschung und -entwicklung und kann dazu beitragen, die COE (Energiekosten) von Windenergieanlagen weiter zu verringern. Eine Reihe von Herausforderungen beschränken aber bisher die Anwendungsbreite und -tiefe der Drehmomentmessung in der Prüfung und dem Betrieb von Windenergieanlagen. Die in dieser Dissertation beschriebenen Forschungsarbeiten widmen sich den Hauptherausforderungen, die sich durch die unterschiedlichen Aspekte der Drehmomentmessung stellen, einschließlich des Messprinzips, der Kalibrierung und der Messunsicherheit. Zudem wird die Anwendung zur Effizienzbestimmung des Antriebsstranges untersucht, die von allen Anwendungen in der Windenergieindustrie die höchsten Anforderungen an die Genauigkeit der Drehmomentmessung und seiner Kalibrierung stellt.

Im Rahmen der vorliegenden Dissertation werden neue Ansätze und Verbesserungen vorgeschlagen, um die genannten Herausforderungen zu meistern. Ein neues Verfahren zur Drehmomentmessung, das auf Drehgebern beruht, wird vorgestellt und in einer Versuchsreihe angewendet. Das Verfahren besitzt großes Potenzial für Langzeitmessungen an einer Windenergieanlage während des Betriebs. In derselben Versuchsreihe wird ebenfalls eine Verbesserung der traditionellen Drehmomentmessung gezeigt, die auf Dehnungsmessstreifen beruht, wobei der Einfluss von Lasten, die nicht auf dem Drehmoment beruhen, stark verringert wird, indem mehr Messpunkte für die Drehmomentmessung zur Verfügung stehen. Um die Problematik der unzureichenden Genauigkeit bei der Wirkungsgradbestimmung des Antriebsstrangs einer Windenergieanlage zu adressieren, wird in der vorliegenden Dissertation ein neues Verfahren auf einem Prüfstand vorgeschlagen, um die Abhängigkeit des bestimmten Wirkungsgrads von der Messgenauigkeit beim Drehmoment und der elektrischen Leistung zu verringern. Dabei kann der Wirkungsgrad mit einer Unsicherheit bestimmt werden, die beträchtlich unter der der Drehmomentmessung liegt. Das Verfahren nutzt einen speziell ausgelegten Prüfablauf aus, bei dem sich der Prüfstand und der Antriebsstrang der Windenergieanlage im Motorbetrieb miteinander abwechseln, wobei der Motor die andere Maschine antreibt, die als Generator arbeitet, und umgekehrt. Der gleiche Prüfablauf wird verwendet, um ein Verfahren der Drehmomentkalibrierung zu entwickeln. Das Verfahren stellt eine Beziehung zwischen dem Drehmoment und der elektrischen Leistung mithilfe der Messungen aus den zwei

Prüfungen her, in denen der Antriebsstrang in unterschiedlichen Betriebsarten läuft. Die Kalibrierungsunsicherheit, die durch den Leistungsverlust im Antriebsstrang eingetragen wird, wird so verringert. In dieser Forschungsarbeit wird eine detaillierte Analyse der Unsicherheit für die Wirkungsgradbestimmung und die Drehmomentkalibrierung durchgeführt, um den Nutzen der vorgeschlagenen Verfahren zu bestätigen und ihre Leistungsfähigkeit quantifizieren. Zukünftige Arbeiten und weitere Anwendungen der vorgeschlagenen Verfahren werden gegen Ende dieser Doktorarbeit dargestellt.

Schlagwörter: Windenergieanlage, Drehmomentmessung, Drehmomentkalibrierung, Wirkungsgradbestimmung, Antriebsstrang, Unsicherheit.

Acknowledgements

<div align="right">

Hongkun Zhang

January 2021, Bremen

</div>

Contents

Abbreviations

BIPM	Bureau International des Poids et Mesures
CPR	Counts per Revolution
COE	Cost of Energy
COG	Centre of Gravity
DAQ	Data Acquisition
DOF	Degree of Freedom
DUT	Device Under Test
ECD	Extreme Coherent gust with change in Direction
EMI	Electromagnetic Interference
EMPIR	European Metrology Programme for Innovation and Research
EOG	Extreme Operating Gust
EOG1	Extreme Operating Gust, with a recurrence period of 1 year
EWEA	European Wind Energy Association
FBG	Fibre Bragg Grating
FEM	Finite Element Method
FLS	Force Lever System
HSS	High Speed Shaft
IPC	Individual Pitch Control
IR	Infrared
JCGM	Joint Committee for Guides in Metrology
LAU	Load Application Unit

LiDAR	Light Detection And Ranging
LNE	Laboratoire national de métrologie et d'essais
LSS	Low Speed Shaft
NIST	National Institute of Standards and Technology
NMI	National Metrological Institute
NPL	National Physical Laboratory
NREL	National Renewable Energy Laboratory
NTP	Network Time Protocol
PPR	Pulse Per Revolution
PTB	Physikalisch-Technische Bundesanstalt
SI	Système International (d'unités)
TSM	Torque Standard Machine
TTS	Torque Transfer Standard
VIM	Vocabulaire International de Métrologie

1 Motivation

Wind energy has experienced rapid and significant development in the past decades. It is now a major source of renewable energy and supplied close to 6 % of the world's entire electricity demand in 2018[1]. Wind energy has overtaken coal as the second largest power generating capacity in the European Union and covered 14 % of the electricity demand in the EU in 2018. About 48 % of the newly installed power capacity in the EU came from wind energy in the same year[2]. WindEurope (formerly the European Wind Energy Association EWEA) expects that more than 20 % of the electricity demand in the EU could be satisfied by wind energy by 2030[3]. An important reason of this success lies in the strong competition in the wind energy industry which drives the continuous technological progress and the reduction in the energy cost[4]. In the visible future, this competition is expected to remain intense, especially as the subsidy policies for wind energy are being phased out in major world markets.

The ultimate goal of the competition in the wind energy industry is to reduce the cost of energy (COE), and this can be achieved through better performance and less downtime of the wind turbines. Various types of sensors and sensing technologies have provided important foundations for new technologies that help reduce the COE. For example, the individual pitch control (IPC) technology uses the rotor bending moment as a key input signal[5], which can be measured by strain gauges on the roots of the blades[6]. Similarly, Light Detection And Ranging (LiDAR) technology measures the wind field in front of the turbine and provides a new foundation for better control strategies of wind turbines[7]. Condition monitoring systems on different levels and different components of the turbine gather information by means of numerous sensors and carry out assessment during the operation of the wind turbine. In principle, new measurement signals on the wind turbine could provide more information about the turbine and make new technologies possible. An example of such a signal is the mechanical torque in the wind turbine drivetrain. It is a result of the load balance between the aerodynamic torque of the rotor and the generator's magnetic torque on both sides, coupled with the structural dynamics of the drivetrain and the rotor. As a result, the drivetrain torque contains an abundance of information about the turbine operation. For example, the level of torque in the drivetrain represents the output power level from the rotor and the input power level to the nacelle, while the oscillations of the torque signal contain the dynamic behaviours of the whole drivetrain.

Measuring the torque is interesting both for an operating wind turbine in the wind

farm and also for a turbine under test on a test bench. Therefore, the first task of the research undertaken for this dissertation was to study possible ways of torque measurement. A good opportunity for the study was afforded by a comprehensive test campaign of an 8-MW wind turbine on the nacelle test bench "DyNaLab"[8], shown in Figure 1.1. The test campaign lasted more than one year and three turbines of the Adwen AD-8 type with different configurations were tested.

Figure 1.1: Adwen test campaign in DyNaLab[9] at Fraunhofer IWES

Wind turbines have some of the largest torque levels found in modern industries because of the low rotating speed of the rotor. Taking the NREL 5-MW reference turbine as an example, the turbine has a rated mechanical power of 5.3 MW and a rated speed of 12.1 rpm. The rated input torque on the low speed shaft (LSS) side is therefore greater than 3.9 MN·m. In most cases, it is inconceivable from both a technical and an economical point of view to measure torque at this level with commercial torque transducers. As a result, the common practice is to measure the input torque of the wind turbine with strain gauges applied to the main shaft of the turbine. If the turbine is on a test bench, the strain gauges could also be applied to the test bench output shaft or to the connecting shaft between the test bench and the turbine drivetrain. To obtain torque measurement from the raw measured signal, the relationship between the raw signal and the torque needs to be determined. This process is generally referred to as "calibration" in the wind energy industry. In practice, there are a number of ways to calibrate the torque for a wind turbine. One method is to calibrate using the measurements of electrical power and rotating speed, with the drivetrain efficiency taken into consideration. Another method, also known as analytical calibration, is to determine the relationship between torque and the raw signal with analyses of all the elements in the whole measurement chain. Unfortunately, all the methods and their variants have a common drawback — the large uncertainty in

the calibration. The calibration using the electrical power is based on the unknown or estimated drivetrain efficiency, while the analytical calibration can easily accumulate a high level of uncertainty through the large number of analysis or assumptions in the process. As a result, there is a a great demand for better accuracy in the torque calibration for a wind turbine, especially when the turbine drivetrain is under test on a test bench. Therefore, the second task of the research presented here is to develop a new calibration method that can be easily carried out on a test bench and can notably improve the accuracy compared with the other methods which are commonly available.

One of the most important applications of the torque measurement on the wind turbine is to determine the drivetrain efficiency. The efficiency characteristic of a wind turbine is of great importance, both because better efficiency gives the turbine a big advantage in the market competition and also because the efficiency information provides the turbine manufacturer with valuable feedbacks about the design and helps to further optimise the design. However, to ensure that the determined efficiency delivers clear and meaningful information, the efficiency must have sufficient accuracy, or in another term, have the uncertainty below a certain level. The most direct way to determine the drivetrain efficiency is to compare the electrical output power with the mechanical input power. The uncertainty in the determined efficiency is thus a result of the measurement uncertainties in the both. While the electrical power can be measured relatively easily with good accuracy, the accuracy of the mechanical power is often insufficient due to the high level of uncertainty in the torque measurement. Since the drivetrain efficiency of a wind turbine is normally above 90 % at rated operation, the accuracy requirement for the determined efficiency is often very high. The uncertainty within 1 % or even smaller is often desired from the industry. In contrast, an efficiency result of 95 % ± 5 %, for instance, would not provide much useful information. Under the current technical circumstances in the wind energy branch, it is extremely difficult to improve the torque measurement so that sufficient accuracy could be achieved in the efficiency determination. Therefore, the third task of the research is to develop a new method of efficiency determination which is not sensitive to the accuracy of the torque measurement. With the new method, it should be possible to determine the drivetrain efficiency at sufficient accuracy level with the commonly adopted torque measurement methods.

2 State of the Art

2.1 Methods of torque measurement

In discussion of the possible ways of torque measurement, a large number of methods and their variants can be taken into consideration. According to their measuring principles, the methods can be generally divided into three groups: measurements based on the local strain or stress on the structure, measurements based on the structure deformation, and the measurements based on the transmission or reaction forces. For each group, different forms of solutions are also available. This section discusses a number of solution forms that are commonly adopted or have the potential to be adopted for a wind turbine drivetrain.

2.1.1 Measurement with load cells

Measuring the torque with strain gauges is a very mature technique which has a wide range of applications in different industries. Certain strain gauge full-bridge configurations are available for measuring the shear strain caused by the torque while at the same time compensating the influence of the loads in other directions[10]. Strain gauges are also commonly used in commercial load cells and transducers, including torque transducers of different types and ranges[11,12]. The transducer manufacturers consider all major factors that affect the measurement uncertainty of the measurement and take necessary approaches to compensate or reduce the uncertainty. As a result, measurements with torque transducers can normally achieve the highest accuracy level among all the solution forms. A drawback, however, is that the transducers often allow only low levels of the non-torque loads on the shaft[13], in order to guarantee the accuracy and protect the internal structure. Moreover, for applications in a drivetrain, the transducer has to be integrated into the drivetrain and connected in tandem with other components. The integration of the transducer requires reconfiguration of the drivetrain layout and incurs hereby additional costs. This is especially true when the transducer needs to be disassembled regularly for re-calibration. A research project undertaken in the 1980s, has used a torque transducer placed directly in the wind turbine for the torque measurement[14]. However, as the rated power of new wind turbines continues to increase, it is unimaginable today to have torque transducers installed in a similar way on the low-speed side of the multi-MW wind turbines[15]. The input torque of such turbines easily extends into the multi-MN·m range, with extreme values up to 10 MN·m. No commercial serial-produced transducer has a comparable capacity at the moment. The cost of developing a multi-MN·m range

torque transducer would be very high, especially if the transducer has to be developed specifically for a certain type of wind turbine or just for a project. Furthermore, the even larger non-torque loads, which commonly occur in wind turbines, make it even more difficult to apply the torque transducer directly to the low-speed side of the wind turbine. For a drivetrain that includes a gearbox, the high-speed side may have a much lower torque level, which makes it theoretically possible to have a torque transducer integrated to the high-speed shaft. However, this also presents several challenges: the positions of the components need to be reordered for the transducer; telemetry or similar systems need to be instrumented for the power supply and data transfer of the transducer; the rotating balance and dynamic stability of the high-speed shaft must be checked again after the transducer is integrated.

2.1.2   Measurement directly with strain gauges

In cases where the use of commercial torque transducers is not realistic, strain gauges can also be applied directly to the available structure. This is common practice in the industries especially in cases when the accuracy of the measurement is not of crucial interest. In the wind energy branch, the IEC 61400-13 standard recommends the drivetrain torque be measured with strain gauges on the main shaft or on top of the tower, where the material and geometry are favourable for the measurement[15]. For tests of a drivetrain on the test bench, strain gauges can also be applied to the shaft adapter between the test bench and the drivetrain. Compared to a commercial transducer, the application of strain gauges on available structures is more practical and requires lower cost, which makes the torque measurement in many cases possible. However, the measurement with this method is more prone to environmental influences and instrumentation errors, and as a result normally has a much lower accuracy than the torque transducers. Important environmental influences come, for example, from the temperature change[16] and the humidity penetration through the protective cover[17,18].

In most the cases, main shaft is the best option of torque measurement in a wind turbine. However, as the main shaft is a rotating part, the power supply and data transfer for the strain gauges can be challenging. The common solution is to use an additional slip ring[19] or a telemetry system[19–22] to supply power and transfer data, which also drives up the cost of the instrumentation. In some cases, the main shaft is a hollow structure and has a inner diameter large enough for applying the strain gauges to the inner surface of the shaft. Here the strain gauges may be connected directly to the measurement system in the hub without the slip ring or telemetry system. For applications on a test bench where the hub is not included in the test layout, the rotational measurement system of the test bench may be used instead. A drawback of the traditional metallic strain gauges is their long-term stability and reliability. As the design life of a wind turbine is normally 20 years or longer, stable and reliable

measurement is very important for the turbine operation and condition monitoring. Owing to the commonly occurring signal drift over time[23] and the frequent failure reports, traditional strain gauges are normally not supposed for long-term measurement in the wind energy industry[24]. As an alternative, optical strain gauges, or Fibre Bragg Grating (FBG) sensors can be considered for applications requiring long-term measurement.

2.1.3   Measurement with FBG sensors

FBG sensors use an array of reflectors in an optical fibre to reflect light of particular wavelength, while the reflected light can be measured by an interrogation unit. When the optical fibre is subjected to deformations introduced by strain, temperature change, acceleration or other factors, the wavelength of the reflected light will change accordingly. This makes the measurement of corresponding variables possible. For strain measurement, the FBG sensors have some obvious advantages over the traditional metallic strain gauges. Since the FBG sensors are based on optical principles, they are immune to electromagnetic interferences (EMI) and are not subjected to errors due to long cable distances. FBG sensors can measure strain upto a much higher level and can be easily integrated into composite materials. Additionally, multiple sensors can be integrated into one single fibre, with each sensor using a specific range of wavelength in the light spectrum. Most importantly, the of the FBG sensors has an excellent long-term stability[25]. The major drawbacks of FBG sensor applications is the high cost of the interrogation unit. To measure the torque, FBG sensors can be affixed to a shaft in a similar way to normal strain gauges, so that the shear strain produced by the torque can be measured and processed[26,27].

In the wind energy industry, FBG sensors are often used on the rotor blade for condition monitoring and load measurement[28,29]. For example, FBG technology is a good option for measuring the bending moment on the blade for the IPC control strategy[30–32]. Apart from on the rotor blade, FBG sensors are also adopted by many approaches for the health monitoring of the tower and supporting structure of a wind turbine[33–35]. However, as for measurement in the drivetrain, FBG sensors are not often discussed or preferred. An important reason is the high cost of the interrogation unit for the FBG sensors.

2.1.4   Measurement based on structure deformation

Apart from exerting strain on the structures, torque transmission through the drivetrain also causes structural deformation. Therefore, deformation is another principle that can be utilised for torque measurement. For the measurement, the angular deformation of two positions along a shaft is measured and the torque can be determined from the angular deformation with the stiffness of the shaft segment. The stiffness can be obtained through either analytical calculation, finite element method (FEM) analy-

sis, or through calibration. Depending on the layout of the instrumentation, there are two ways of measuring the angular deformation:

- Measure the absolute angular positions of two sections on the shaft and determine the deformation by comparing the measured angular positions. The sensors are installed on a stationary structure and targeting the rotating shaft, where units with angular marks are installed. A number of different measurement principles can be adopted here for the position measurement, including optical[36,37], magnetic[38] and inductive[39] principles. One drawback of this concept is that the deflection of the shaft as well as the deformation of the stationary structure, where the sensors are attached to, can cause relative displacement between the sensors and the shaft. This displacement will be then interpreted by the measurement system as angular movement of the shaft. Therefore, small shaft deflection and structure deformation is a prerequisite for a good accuracy of the measurement. This is normally true in the marine industry, where the propeller shaft of a ship is typically long and not subjected to large bending moments. On wind turbines however, the opposite is the case - the main shaft is relatively short and subjected to high level of non-torque loads at the same time. Therefore, it is generally difficult to adopt this method on the main shaft of wind turbines.

- Measure the relative angular deformation between two sections directly. To overcome the drawback of the influence from structure deformations, the relative angular movement between a shaft segment can be measured directly using a device sitting on the shaft and sensing the angular movement of each position with, e.g., a clamp. The angular deformation between the two clamps can be captured by a sensor with the help of a special mechanism linking the two clamps. A telemetry system is needed for the power and data transmission. This concept is already used in the marine industry, where the torque measurement is very important for the motor control of a ship. Two commercial suppliers of this solution are VAF Instruments with its T-Sense product[40], and LEUTERT with the EVOthrust system[41]. In principle, it is possible to apply this method on wind turbines with main shaft of enough length. However, it needs to be investigated how sensitive is the measurement to the non-torque loads on the shaft. Additionally, the measuring device must be adapted to fit the shape of the main shaft, whose diameter often varies along the axis.

2.1.5   Measurement through forces over lever arms

The torque signal can also be determined through the multiplication of the force and the length of the lever arm, both of which are basic variables and can be measured with good accuracy under favourable conditions. This principle is also adopted by

many torque standard machines[42–44], which provide the national standard for the traceable torque calibrations. To measure torque with this principle in a drivetrain, there are generally two types of set-up available: the direct in-line measurement and the measurement through the equilibrium torque.

In a direct in-line torque measurement, the forces are normally measured by load cells, which are integrated as load transmission parts into the drivetrain. The torque can be calculated with the measured forces and the lever arms with known length. Measurement with this method captures all information of the torque, including the dynamic behaviour, since the torque is directly transmitted through the load cells. However, the instrumentation of the method demands additional efforts, especially when the bending moments also have to be transmitted at the same time. One application of the method is reported in the work of Kyling et al.[45], where a test campaign carried out at Fraunhofer IWES is presented. Figure 2.1 shows the layout of this application during the test. Similarly, the concept of a 5 MN·m torque transducer for wind turbine test benches is proposed by Kock et al.[46,47], whereas the design in this concept also enables the transmission of the non-torque loads.
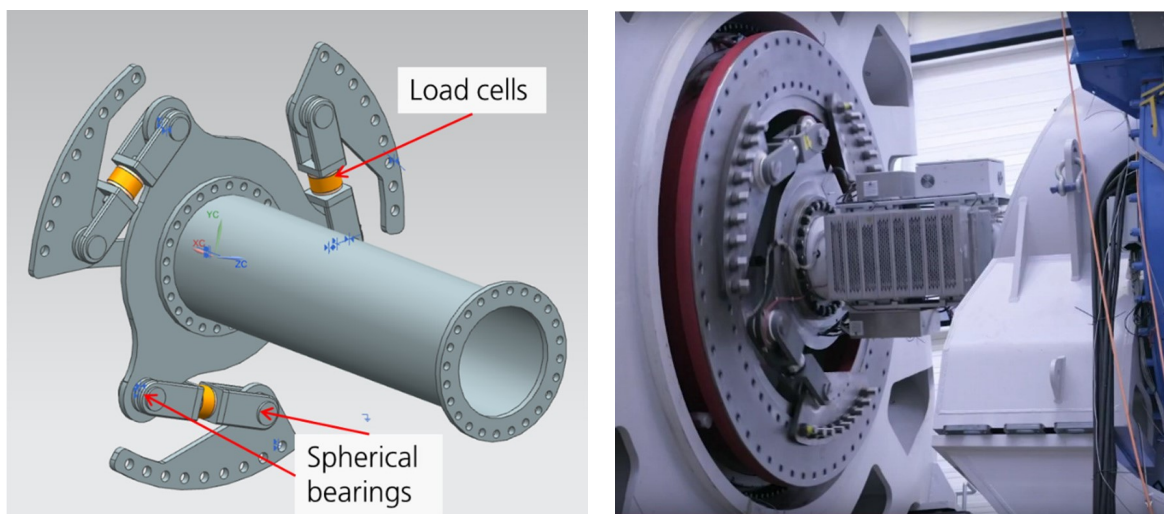
Figure 2.1: An approach of in-line torque measurement with load cells during a test campaign of a 3.6-MW wind turbine drivetrain at Fraunhofer IWES[45]

Different from in-line measurement, the equilibrium torque measurement focuses on the reaction of the stator of the machine. A typical example is the dynamometer, which is designed to determine the mechanical power of the shaft by measuring the torque and rotational speed at the same time[48]. Although in-line torque measurement is also available on some dynamometers[49], the input torque is traditionally determined on a dynamometer using a load cell to measure the equilibrium torque on the stator. To make this possible, the dynamometer is normally supported with bearings so that the tilt motion of the stator is constrained only through the load cell by means of a lever arm. One example of this layout is shown in Figure 2.2. This type

of dynamometers are also known as cradle-mounted dynamometers.

Figure 2.2: The DT type hydraulic dynamometer from HORIBA[50]

Compared to the in-line torque measurement, the measurement with the cradle-mounted dynamometers has several advantages[51]. For example, the load cell is not subjected to mechanical shock loads on the rotating shaft; the measurement provides a more stable signal thanks to the mechanical damper of the stator and can therefore achieve better accuracy of the averaged value; the measuring device does not rotate, and is thus not subjected to the influence of the rotation and the centrifugal force. However, one fundamental weakness of cradle-mounted dynamometers is their poor ability to measure the dynamic torque, since the lever arm and the measuring load cell are mechanically separate from the rotating shaft in the rotational degree of freedom.

The torque measurement method used by the cradle-mounted dynamometers can theoretically be applied to the wind turbine drivetrain on a test bench. This requires the main frame of the turbine to be placed on a certain form of bearing support, so that the turbine is able to tilt along the drivetrain axis. The tilt movement must be constrained by one or more load cells over a lever arm of known length. One challenge of such applications lies in the instrumentation of the supporting parts and the structure reconfiguration of the turbine itself, especially considering the size of the wind turbine. Another drawback of the application is again the ability to measure the dynamics in the torque. Given the stochastic nature of the loads on a wind turbine, this is an important disadvantage in the torque measurement.

2.1.6 Applications of torque measurement on wind turbines

In the wind energy industry, torque measurement in the drivetrain is one of the tasks defined by the IEC 61400-13 standard[15] for mechanical load measurements, which is an important part of the conformity testing of the turbine. It offers a possibility to validate the design loads of the turbine and is therefore required for the type

certification[52] of the wind turbine. As a result, torque measurement is often carried out on wind turbine prototypes for the purposes of certification.

Additionally, torque measurement has also been studied for condition monitoring systems of the wind turbines[53,54]. However, for reasons of cost and reliability, the commonly used methods of torque measurement are still not suitable for long-term and wide use on the wind turbines[55,56].

Torque measurement is also one of the key measurements when testing a wind turbine drivetrain on test benches in a laboratory environment[57,58]. Torque measurement provides a reliable information of the mechanical interaction between the test bench and the turbine drivetrain, and helps to analyse the dynamic behaviours in the rotational degree of freedom. It is also a necessary measurement for calculating the input mechanical power to the drivetrain and hence important in determining the drivetrain efficiency.

2.2 Calibration of torque measurement

Depending on the principle employed, the raw signal from a torque measurement can be strain, displacement or simply the analog voltage or current outputs. To convert the raw signal into torque, it is first necessary to determine the relationship between torque and measured raw signal. In principle, the relationship is assumed to follow a linear behaviour, and the task of the calibration is to determine the slope and offset parameters of this linear relationship. The slope is also known as the sensitivity or gain of the relationship. The slightly non-linear behaviour of the relationship is normally considered as a source of error in the measurement, which contributes to the measurement uncertainty. The slop and offset parameters of the relationship can be obtained through a calibration process. The definition of "calibration" is given by Joint Committee for Guides in Metrology (JCGM) in Vocabulaire International de Métrologie (VIM, 2.39)[59] as:

"Operation that, under specified conditions, in a first step, establishes a relation between the quantity values with measurement uncertainties provided by measurement standards and corresponding indications with associated measurement uncertainties and, in a second step, uses this information to establish a relation for obtaining a measurement result from an indication."

In this definition, the "indication" refers to the direct reading or raw signal of the measurement, while the "measurement standard" is in this case the reference torque, against which the raw signal is to be calibrated. According to the definition, the assessment of measurement uncertainty is a vital task of the calibration. The uncertainty comes both from the measured raw signal (the indication) and from the torque reference (measurement standard). To ensure the uncertainty assessment of the mea-

surement is carried out correctly in accordance with the international standard based on the SI[60] system (international system of units), the term of metrological traceability is introduced to evaluate whether the measurement can be traced back through a set of calibrations to the international standard[61]. It is defined in VIM (2.41)[59] as:

"Property of a measurement result whereby the result can be related to a reference through a documented unbroken chain of calibrations, each contributing to the measurement uncertainty."

The unbroken chain of calibrations is composed of calibrations from different levels of the calibration hierarchy shown in Figure 2.3.
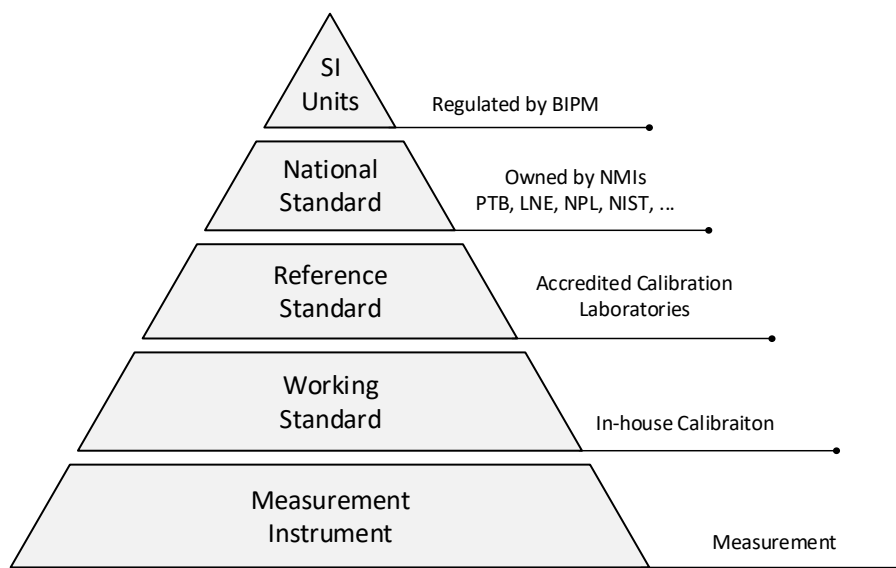
Figure 2.3: The calibration hierarchy

At the top of the hierarchy is the definition of the units — the SI system of units, which is regulated by the International Bureau of Weights and Measures BIPM. The base and derived units based on the SI system are usually realised by the National Metrological Institutes (NMI) with the highest achievable level of accuracy[62]. As NMIs provide traceability to the international standards and maintain an overview of the national calibration hierarchy, a traceable measurement is therefore often referred to as being traceable to the national standard owned by the NMIs (e.g. the PTB in Germany, the LNE in France and the NIST in the United States).

2.2.1 Torque standards and calibration

Although torque has been widely utilised throughout the entire industrial history, a separate national standard for torque became available only very recently. In the 1990s, addressing industry's need for better accuracy and traceability of the torque measurement, Germany was the first to start the research and to establish a national

torque standard[63,64]. It was then quickly followed by a number of NMIs in other countries[65–68]. As an example, the first torque national standard in the UK was realised by means of a 2 kN·m torque standard machine (TSM), which was commissioned at the end of 2005[69]. The TSMs have the highest level of accuracy, and are normally owned by the national metrological institutes and accredited calibration laboratories. Currently, the largest TSM capacity available in the world is 1.1 MN·m[42], which is owned by the PTB of Germany. A larger capacity of 5 MN·m[70] is under development in PTB.

To distribute the standard of the TSMs to other calibration laboratories, torque transducers of sufficient accuracy are often needed to "carry" the standard. Such transducers are called torque transfer standards (TTS). They act as torque references and are very important for the traceability of the torque calibration system[71]. The TTS is also often used to compare the measurements of different laboratories and for the "key comparisons" between NMIs[72,73].

Apart from the standards for the torque itself (as variable torque), there are also standards regulating the calibration process and the uncertainty assessment[74], including the DIN 51309, EA-10 and VDI/VDE2639[75–77]. The standards require a set of loading procedures during the calibration in order to chart important behaviours of the transducer, including non-linearity, repeatability, hysteresis and creep[78]. For the traceable torque measurement, suitable calibrations and documentation in accordance with the calibration standard are necessary.

2.2.2 Torque calibration for wind turbines

As mentioned in Chapter 1, the nominal torque on a modern wind turbine can easily reach a multi-MN·m level. This is well above the highest TSM capacity in the world, which is only 1.1 MN·m. As a result, a torque measurement traceable to national standards on the LSS side of a modern multi-megawatt wind turbine is still not available. To address the need for traceable torque measurement in the wind turbine industry, especially on a nacelle test bench for wind turbines, an EMPIR project "Torque measurement in the MN·m range" was launched in 2015[79,80]. One approach of the project for traceable torque measurement is the 5 MN·m TTS acquired and developed by the PTB, which is partially calibrated to 1.1 MN·m on the PTB's torque standard machine and then extrapolated to the full range of 5 MN·m[81,82]. Test data analysis and FEM simulation are used to develop the the extrapolation process and calculate the uncertainty budget[83,84]. As an application, the developed 5 MN·m TTS is deployed in the calibration of the built-in torque transducer of a 4-MW wind turbine nacelle test bench[57] at Center for Wind Power Drives (CWD) of RWTH Aachen University, as shown in Figure 2.4. The calibration is carried out with the TTS mounted in-line in the test drivetrain between the test bench and the device under test (DUT). Since all

the available standards for the calibration process are designed for calibration in a static situation while both the test bench and the DUT operate in rotation, a calibration process based on the constant rotation of the drivetrain has been developed[85–87]. Another approach employed in the project is the force lever system (FLS). A number of studies have proposed different designs of FLS, aiming at a traceable torque measurement and calibration based on a traceable force measurement and lever arms of known length[88–90].
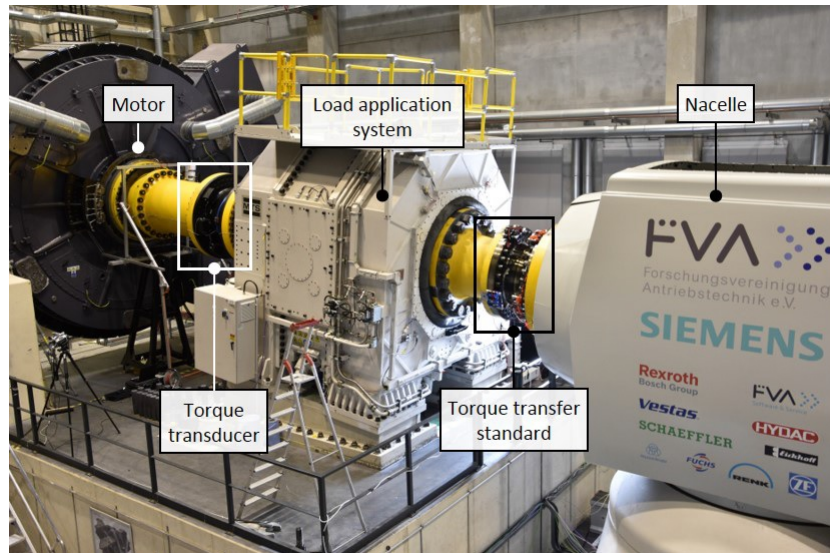
Figure 2.4: The 5 MN·m TTS deployed for torque calibration on the 4-MW wind turbine nacelle test bench at CWD in Aachen[86]

Apart from the work undertaken in the EMPIR project, traceable calibration of torque measurement is still rarely discussed in the wind energy community due to the high expense and the challenge involved, especially for the industry. Correspondingly, traceable torque calibration is not explicitly mentioned in the major industrial guidelines for wind turbine certification and load measurement[15,91,92].

The IEC 61400-13 standard proposes four methods for torque calibration on wind turbines in the field: analytical calibration, calibration through gravity loads (single blade), calibration through external load, and calibration through electrical power and rotational speed. These are explained in the following:

- The term "analytical calibration" is used in IEC 61400-13 to refer to the process of determining the relationship between the torque and the measured raw-signal by means of analysis instead of through a test sequence. Strictly speaking, the process of pure analysis does not fit the definition of the metrological term "calibration" given in Section 2.2 of the VIM. However, under the specific circumstances found in a wind turbine, the process is meaningful and practical in establishing a measurement function between the torque and the measured raw signal. Similarly, the term "analytical calibration" is commonly used in the

research field of analytical chemistry[93]. For the analytical calibration of the torque measurement, the whole measurement chain is analysed in detail in order to determine the measurement function. This usually requires the measurement to be located at a favourable position and on a favourable structure, for example at the middle of a circular shaft. Depending on the complexity of the structure and how accurate the calibration is expected to be, the analysis can be carried out either manually or with the aid of the FEM analysis. Since analytical calibration can be undertaken without any additional instrumentation and test procedures, it is very often used on an operating wind turbine in the field. This calibration method is also very attractive for the wind turbine on a test bench. Even in cases where another torque calibration method is adopted on the test bench, the analytical calibration result can be used as a beneficial verification. The drawback of the method is obviously the uncertainty through the various analysis and assumptions in the process.

- Torque calibration through the gravitational load of a single blade is possible when the blade is being installed to the wind turbine in the wind farm. The calibration takes advantage of the self-weight and centre of gravity (COG) position of the blade when only one blade is mounted on the rotor hub. By turning the rotor to different azimuth angles, the blade applies different levels of torque to the rotor and the main shaft of the turbine. This method is highly dependent on the opportunity afforded by the rotor imbalance during the installation, and thus cannot be implemented during drivetrain test on a test bench. The uncertainty in the calibration is dependent on the wind disturbance during the calibration as well as the uncertainty in the weight and COG of the blade.

- Instead of utilising the self-weight of the blade, the torque can also be generated by means of an external force applied to a lever arm. In the field, such a calibration can be carried out with one of the blades acting as the lever arm, while the force can be applied from a crane and measured by a load cell when the crane is dragging or lifting the blade[94]. The uncertainty in such a calibration depends to a great extent on the accuracy of the load cell as well as the accuracy in the length calculation of the lever arm. The lever arm is dependent on the force application position on the blade as well as the force direction. A study by Lekou et al.[95] shows that the calibration through external load tends to provide better accuracy than the analytical calibration. It is also pointed out in the same study, that the implementation of this method faces strong challenges with the increase in blade length and tower height. In principle, this method can also be applied on a nacelle test bench. However, due to the length limit of the lever arm allowed by the testing hall, the forces used to generate the torque would be much larger than that used during the calibration in the field. Additionally,

in order to avoid the torque measurement being influenced by the stress concentration caused by the lever arm, a designed structure may be necessary to be used for transferring the loads from the lever arm "evenly" to the part of torque measurement.

- Calibration with electrical power and rotational speed: For the drivetrain of a wind turbine, the torque is the source of the input mechanical power, and can therefore be calibrated according to energy equilibrium through the electrical output power and the rotational speed of the shaft. The electrical power and rotational speed can normally be easily measured and the calibration process can be carried out during a series of normal operations of the system. No reconfiguration in the drivetrain is necessary to be carried out for the calibration. However, the unknown drivetrain efficiency forms part of the calculation in calibration, which can introduce large uncertainties. The calibration uncertainty is further dependent on the uncertainty in the electrical power measurement, which is discussed in Section 2.3. Similar to the analytical calibration, the method is often used on wind turbines both in the field and on test benches.

The methods proposed in IEC 61400-13 as above focus on the torque calibration on wind turbines that are already installed or during their installation in a wind farm. Although some of the methods can also be adopted for calibrations on a test bench, the applications are often restricted.

2.3 Efficiency determination of wind turbine drivetrains

The efficiency behaviour of the drivetrain from the main shaft input to the electrical output is an important property for wind turbines. It is also a very interesting point to be investigated during a test campaign on the test bench. The drivetrain efficiency is by definition the result of the output electrical power divided by the input mechanical power on the main shaft. It is therefore influenced by all the mechanical and electrical power losses throughout the energy transmission and conversion. It is worthwhile to mention that a drivetrain normally has different levels of efficiency at different working points. Therefore the efficiency behaviour is not a single value but a function of the working point. Nevertheless, the efficiency must be determined during a test at a particular working point. A correctly determined efficiency offers a basis for the design validation, and increase the confidence of the market of the wind turbine. To determine the drivetrain efficiency, several ways can be considered: measuring the mechanical input and electrical output powers of the drivetrain; measuring the overall efficiency of a back-to-back set-up composed of two drivetrains with identical design; and measuring the thermal emission of the drivetrain that results from the power loss. For all the methods, the accuracy of the determined efficiency is of great concern.

The demand for higher accuracy (or lower uncertainty) is especially strong when the efficiency itself is at a high level. This is usually the case for a wind turbine operating near the rated point, where the drivetrain efficiency can be well above 90 %[96,97].

2.3.1 Determination with direct method

The most direct way to determine the drivetrain efficiency is to determine according to the definition, namely the output power divided by the input power. For wind turbines, the output electrical active power from the generator or converter and the input mechanical power to the low speed shaft are necessary for the efficiency calculation. For the sake of simplicity, the electrical active power will be referred to below as "electrical power".

Depending on whether the converter is included as part of the drivetrain, the electrical power measurement can be carried out on the output cables of either the generator or the converter. At the measurement position, voltage and current sensors are instrumented to obtain the corresponding signals. The signals from the sensors are often forwarded to the data acquisition system (DAQ) of the so-called "power analyser" unit, which calculates the electrical power based on the voltage and current signals. Usually, the sampling rate of the DAQ system is set to be high enough that enough details of the signal shape can be captured, which makes high accuracy power measurement possible. Many power analysers on the market can have sampling rates above 1 MHz[98,99]. This is normally more than enough to build up the detailed shape of the 50 or 60 Hz voltage and current signals. With these signals, the power analyser can carry out a number of analyses of the power output. For example, the instant and the root mean square (RMS) values of the power output, the power factor, along with other power quality analyses. The uncertainty in the measured power output depends mainly on three parameters[100–102]: the accuracy of the measured voltage signals, the accuracy of the measured current signals and the phase shift between the voltage and current signals. For each parameter, the accuracy results from both the accuracy of the sensor and that of the DAQ system. With the state-of-the-art solutions in the industry, both voltage and current can be measured with very high accuracy. Taking the 50 Hz AC output as an example, the amplitude and phase errors of a fluxgate current sensor can be controlled within 0.01 % (of the nominal value) and 0.04°[103], while the errors of a voltage divider can be achieved within 0.1 % (of nominal) and 0.06°[104]. On the DAQ system side, the amplitude error can be well below 0.05 %[98,99]. Of course, individual cases are also influenced by the sensor cables and other environmental factors. Taking all the factors into consideration, it is not difficult to measure the output electrical power of a wind turbine with an error of less than 0.5 % of the rated power. For many the efficiency measurements, this accuracy can be considered to be sufficient.

Although the electrical power can be measured with sufficient accuracy, the measurement of the mechanical power is proven to be the real challenge in the determination of the efficiency. Theoretically, the mechanical power can be easily calculated as a product of the torque and the rotational speed. The rotating speed is usually measured with instrumental or absolute rotary encoders, which is a mature technology and provides excellent accuracy. However, as outlined earlier, it is very difficult to achieve sufficient accuracy in the torque measurement on the input shaft of a wind turbine. This can lead to a great uncertainty in the determined efficiency, following the uncertainty propagation[105] principles. Depending on the level of the efficiency, a large uncertainty usually means that the efficiency obtained is not useful. One example is given in a NREL report[97] where the obtained drivetrain efficiency of the same working point varies between 91 % and 98 % over different tests. Different ways of torque measurement on wind turbines have been discussed in Section 2.1 of this dissertation. Almost the only way to ensure sufficient accuracy, when using the direct method, is to use a multi-MN·m torque transducer for the torque measurement, in a similar way to that described by Weidinger[83]. However, high expense is expected in this way for the instrumentation.

Apart from the NREL work reported by Walford[97], which is mentioned above, the author is not aware of other detailed publications that report the efficiency determination of a multi-MW wind turbine with the direct method. Some applications adopting this method have been only seen in the efficiency determination of small-size components of wind turbines[106–109].

2.3.2 Determination based on back-to-back test

In contrast to determining the efficiency directly with input and output powers, a method mentioned in the IEC 60034 standard[110] takes advantage of a back-to-back test set-up and thus obviates the need of torque measurement in the efficiency determination. In this set-up, two machines of the same type are coupled mechanically. While one machine acts as a motor, the other one runs in generator mode. By comparing the electrical input and output powers of the two machines, the over all power loss can be obtained. Assuming that the power losses in the two machines are identical or that the relationship between them is known, the power loss of each machine and hence the the corresponding efficiency can be determined accordingly. The method bypasses the torque measurement and is only based on the electrical measurement, making it a good alternative to the direct method.

A fundamental assumption of this method is that the two drivetrains in the back-to-back test are identical, or that the power loss distribution between the two is known. This assumption introduces additional uncertainty into the determined efficiency. Even when the drivetrains are identical in all respects and therefore also

have an identical efficiency behaviour, they still have different working points during a test. Take the example where both drivetrains have the efficiency around 90 %. This would mean that when the generator of the driving turbine (which operates here as a motor) runs at 100 % of the rated power, that of the driven turbine is only generating around 81 % of the rated power. Therefore, their efficiencies would not be the same.

An obstacle to applying this method to the wind turbine drivetrains is the large size of the drivetrains and hence the difficulties in the instrumentation of the back-to-back set-up. The drivetrain tilt angle and the axis misalignment between the two drivetrains also increase the challenge in instrumentation. It is hard to imagine that such a back-to-back set-up would be instrumented for wind turbines with a long drivetrain only for the efficiency determination. However, for a direct-drive turbine, where the drivetrain is very short or literally only a large generator, the instrumentation can be considerably easier. One possible way of instrumentation can be realised in a similar manner with the GE test bench shown in Figure 2.5.
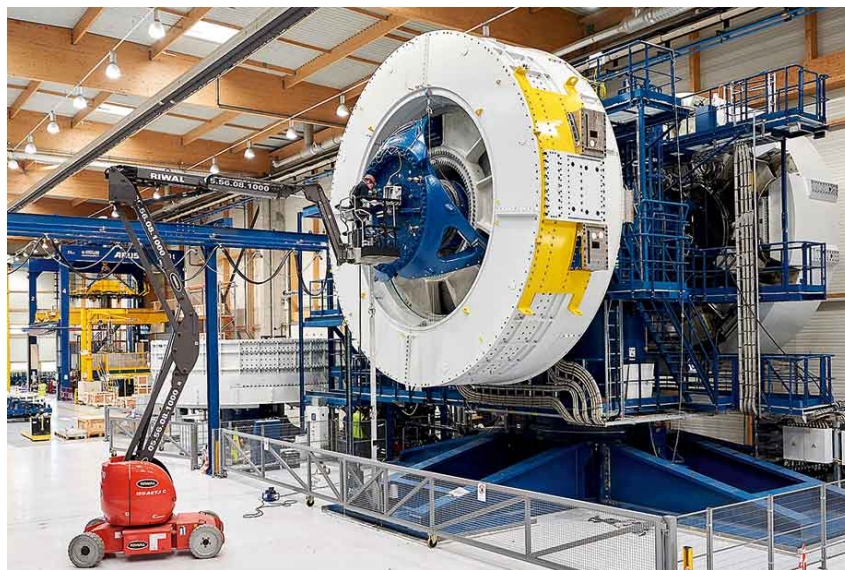
Figure 2.5: The generator of a GE Haliade 6-MW wind turbine being mounted to the test bench[111]

Despite the possibilities, the author is not aware of any publications that report explicitly and in detail about such an application of efficiency determination to wind turbine drivetrains. However, there are reports of the method being applied on the component level of the wind turbine, for example for determining the efficiency of a wind turbine gearbox[112]. Of course, for the gearbox efficiency determination, the power losses of the generators are no longer of interest. Therefore, a variant of the back-to-back method is applied with two small torque transducers installed on the high speed shaft of both gearboxes[113].

2.3.3 Determination with calorimetric method

Another method of efficiency determination is to measure the heat dissipation power of the drivetrain and consider it in the efficiency calculation as the power loss. This is also known as the calorimetric method as described in the IEEE 115-1995 standard[114]. Since nearly all the power loss occurring in the drivetrain is ultimately dissipated in the form of heat, the method utilises a very practical principle to measure the power loss. Theoretically the energy loss in the drivetrain can also dissipate to the environment in other energy forms, for example as mechanical energy through structure vibration and acoustic emission. However, they make very limited contributions to the overall power loss and are therefore neglected in the method.

To measure the heat dissipation, the DUT is often placed into a thermally insulated environment, where the heat is transported through a designed mechanism. During the test, the amount of heat can be determined through temperature and flow volume measurement[100]. The device for such thermal insulation and measurement is also referred to as a calorimeter. Calorimeters are widely used in the power loss measurement of electrical machines and power electronics[115–118]. As the calorimetric method focuses on the measurement of the power loss, it is especially suitable for determining high efficiencies close to 100 %, where the input and output powers of the DUT are very close and therefore determining the efficiency with direct method is not possible[119].

Proper thermal insulation around the DUT is often a vital requirement of the method. The insulation maximises the proportion of the heat that is transferred out through the designed route, where the thermal power can be properly measured. However, the insulation would be increasingly difficult as the size of the DUT increases. This is a major obstacle to be overcome for its applications on wind turbine drivetrains. An important approach in this field has been taken by the CWD of RWTH Aachen University in the study of a 3-MW gearbox-generator integration, the "HybridDrive" product from Winergy. The research is presented by Pagitsch et al.[120]. In the study, the DUT is contained in a thermal insulation box as shown in Figure 2.6, and the power loss is measured through the cooling system. The authors of the paper report satisfactory results with sufficient accuracy of the efficiency. For the efficiency at around 97 %, the associated error is determined by the study to be within ± 0.22 %. Because the measurement deals directly with the power loss, which is inversely proportional to the efficiency level, the uncertainty of the power loss drops when the efficiency increases. As a result, the efficiency uncertainty in this method also has an inverse relationship with the efficiency level. It is additionally reported in the paper that the a duration of several hours were needed for the system to reach the thermal equilibrium that is required by the method.

When proper thermal insulation is not possible or considered not necessary, there
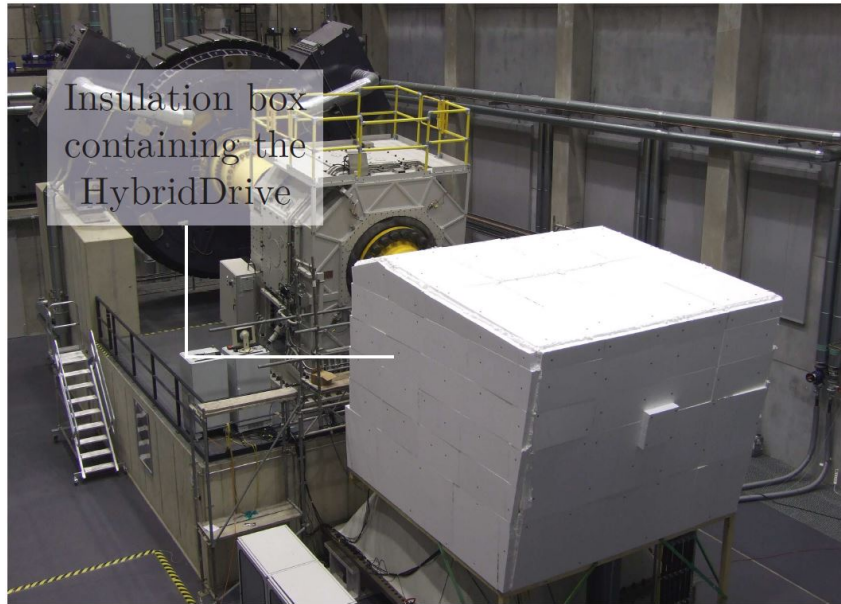
Figure 2.6: The calorimetric method adopted on the test bench of CWD[120] for efficiency determination of a 3-MW gearbox-generator integration named "HybridDrive" from Winergy

are also approaches calculating the heat emission based on temperature measurement of the DUT, for example in the hydropower industry[121,122]. One approach adopts infrared (IR) thermal imaging techniques for better temperature measurement for the emission analysis[123]. A similar approach on the wind turbine drivetrain was reported by NREL in 2002[97]. To determine the heat emission from the structure surface, an estimation is carried out in the study with the aid of a heat flux sensor for a single-point heat flux measurement, and thermal images for estimating the average temperature. The heat emission over the whole surface is obtained with the temperature and flux measurement from the signal point and the average temperature of the surface. However, the information of the uncertainty in the determined efficiency is not reported in the study.

3 Objectives and Outline

3.1 Objectives

The aim of the present work is to address a number of challenges related with different aspects of the torque measurement in the wind turbine drivetrain. Challenges in three aspects are dealt with in this dissertation: the measuring method, the calibration and an important application — drivetrain efficiency determination. To achieve the aim, four objectives are defined:

1. To develop a new torque measuring method based on rotary encoders and evaluate the measurement during a test campaign of a wind turbine drivetrain.

2. To assess and improve the conventional strain gauge based measuring method in term of signal quality.

3. To develop a new torque calibration method that uses the electrical power measurement as the reference while greatly reduces the uncertainty introduced by the drivetrain power loss.

4. To develop a new method for efficiency determination of the wind turbine drivetrain, where the accuracy of the determined efficiency is not sensitive to that of the torque measurement.

Objectives 1 and 2 focus in the aspect of measuring method, while objectives 3 and 4 dealt with challenges in torque calibration and in efficiency determination, respectively. The defined objectives are essential for a comprehensive solution of the torque measurement in a wind turbine drivetrain.

3.2 Outline

This dissertation comprises seven chapters. Chapter 1 and Chapter 2 explain the background of the research, including the motivation and state of the art. The current chapter presents the objectives and outline of the dissertation. The aforementioned objectives in this chapter are addressed in Chapter 4 to Chapter 6 in form of three research papers. Chapter 7 draws the conclusions at the end of the dissertation.

Subsequent to the current chapter, Chapter 4 proposes a new torque measurement method based on rotary encoders. The feasibility of the method is examined during a test campaign. At the same time, torque measurements with strain gauges are

also instrumented in different forms and positions in the test campaign. Through comparing and analysing signals from all the measurement channels, approaches of improvement in the signal quality are presented for the conventional method. Chapter 5 proposes a new torque calibration method based on electrical power and a special test process. Detailed uncertainty analysis is presented to quantify the accuracy of the new calibration method. The method is demonstrated on a back-to-back test between the two motors of a test bench. Chapter 6 proposes a new method for determining a wind turbine's drivetrain efficiency. The method utilises the same test process as proposed in Chapter 5. Detailed uncertainty analysis of the determined efficiency is also presented in this study. The method is demonstrated with a test on a scaled dynamometer test bench. The dissertation is finalised with comprehensive conclusions in Chapter 7, which comprises a summary of the research carried out for this dissertation and an outlook of further research directions.

4 Studies on Measuring Methods

Chapter 4 includes a research paper which presents a study of the methods of torque measurement. The paper was published by Wiley in the journal **Wind Energy** in December 2018.

H. Zhang, R. Ortiz de Luna, M. Pilas and J. Wenske. "A study of mechanical torque measurement on the wind turbine drive train — ways and feasibilities," Wind Energy, vol. 21, no. 12, pp. 1406–1422, 2018. https://doi.org/10.1002/we.2263

The author of this dissertation (Zhang, Hongkun) has carried out the main work and has composed the paper. Rubén Ortiz de Luna and Martin Pilas contributed to the realisation of the tests analysed in the paper during a test campaign. Jan Wenske contributed with advisory support.

In the paper, a comprehensive study of the torque measurement is carried out during a wind turbine test campaign, where the Adwen 8-MW wind turbine AD-8 was tested on the nacelle test bench DyNaLab at Fraunhofer IWES. During the test campaign, torque measurement was carried out with different forms of classical strain gauge methods, as well as with the newly proposed method that is based on rotary encoders.

Due to copyright restrictions, the full paper is not included in this publication of the dissertation.

A patent for the new torque measurement method proposed in the paper was applied for in Germany, and was granted in November 2018, with the patent number DE102017219886B3.

5 An Effective Way of Torque Calibration

Chapter 5 presents a research paper which proposes a new method of torque calibration especially on a test bench. The paper was published by Wiley in the journal **Wind Energy** in April 2020.

The author of this dissertation (Zhang, Hongkun) has carried out the main work and has composed the paper. Jan Wenske and Andreas Reuter contributed with advisory support, including support for the idea development; Mohsen Neshati carried out the tests that are analysed in the paper.

The study aims to develop a calibration method that is easy to realise and repeat on the test bench, and at the same time offers notably better accuracy than the commonly available methods in the industry. The proposed torque calibration method is based on the measurement of electrical power and the shaft rotation, which is similar to one of the traditional methods described in Section 2.2.2. In order to cope with the uncertainty in the traditional calibration method that is introduced by the unknown power loss in the drivetrain, a special test sequence is developed in the study. Through the new test sequence, it is possible to compensate the influence of the unknown drivetrain power loss to a great extent, and improve the accuracy of the calibration as a result.

A patent containing the calibration method proposed in this paper was applied in Germany and granted in July 2019. The patent number is DE102018203525B3.

RESEARCH ARTICLE

Proposals for a practical calibration method for mechanical torque measurement on the wind turbine drive train under test on a test bench

Hongkun Zhang[1] | Jan Wenske[1] | Andreas Reuter[2] | Mohsen Neshati[1]

[1]Fraunhofer Institute for Wind Energy Systems IWES, Bremerhaven, Germany
[2]Institut für Windenergiesysteme, Leibniz Universität Hannover, Hannover, Germany

Correspondence
Hongkun Zhang, Fraunhofer Institute for Wind Energy Systems IWES. Am Luneort 100, 27572 Bremerhaven, Germany.
Email: hongkun.zhang@iwes.fraunhofer.de

Abstract

The mechanical torque input into the wind turbine drive train is a very useful measurement for tests performed on a test bench. To ensure the accuracy and the reliability, an accurate calibration of the torque measurement must be carried out and repeated within a certain period of time. However, owing to the high torque level and large structure size, such a calibration is both expensive and time consuming. To overcome this challenge, a new calibration method is proposed here. The method is based on the electrical power measurement, where a high level of accuracy is much easier to achieve. With the help of a special test process, a relationship between the torque-measuring signal and the electrical power can be established. The process comprises two tests with the drive train running in different operating modes. The calibration is possible by carrying out the same test process on several different torque levels. Detailed uncertainty analysis of the method is presented, whereby the uncertainty can be calculated by means of matrix operation and also numerically. As a demonstration, the implementation of the method on a test bench drive train that contains two 5-MW motors in tandem with the motors operating in a back-to-back configuration is also presented. Finally, some variations on the method and possible ways of achieving better accuracy are discussed.

KEYWORDS

drive train, efficiency, test bench, torque calibration, torque measurement, wind turbine

1 | INTRODUCTION

The mechanical torque plays a very important role in the power transmission of wind turbines, transferring the mechanical power gained by the rotor all the way to the generator. Although due to certain restrictions the mechanical torque measurement (referred to simply as the "torque" below) is still not widely used in the everyday operation of wind turbines, it is indeed always an interesting variable for turbine tests both in a laboratory environment and in the field. Torque measurement is vital for the determination of the drive train efficiency, as well as the aerodynamic efficiency of the rotor. The enormous pressure to reduce costs in the wind energy industry makes efficiency a key parameter of the turbines on the market. Additionally, the level and variation of the input torque also have a strong influence on the fatigue damage of the components in the drive train, especially the gearbox.

Multi-MW wind turbines have one of the highest torque levels found in modern industries, along with hydro power and the shipbuilding, for example. For newer wind turbines with high rated power, the rated torque can be close to 10 MN·m, while the extreme torque is even higher. A calibration traceable to a national or international standard at this level is not possible at present, since the largest such calibration capacity available anywhere in the world is only 1.1 MN·m,[1] which is owned by the German national metrology institute PTB in Braunschweig. The governing calibration standard is the German DIN 51309 standard.[2] A new torque standard machine with a capacity of 5 MN·m is under development at the PTB.[3] Until adequate calibration capacity becomes available, the torque measurement can only be partially calibrated. Measurement behaviour beyond that has to be extrapolated.[4] Using this concept, the PTB has developed a 5-MN·m reference torque transducer

(also known as "torque transfer standard").[5,6] It is intended to be a movable reference torque measurement, which can be used to calibrate other torque-measuring devices, for example on a wind turbine test bench. The PTB 1.1-MW torque standard machine has a relative uncertainty of 0.1 %.[7] The partially calibrated and extrapolated 5-MN·m torque transfer standard (TTS) has been found to have a relative uncertainty of 0.15 %.[5] This level of torque accuracy would be more than sufficient for the efficiency determination of the drive train. However, in order to achieve this accuracy in the test, a state-of-the-art torque transducer similar to the PTB 5-MN·m TTS (or the TTS itself) has to be installed directly in front of the drive train. Since the design, manufacture, and calibration of such torque transducers require high levels of professionalism, and also because each transducer has to be individually customized for the specific application, the cost of such transducers can be a big challenge for industrial use.

As a fundamental variable, torque measurement is instrumented in almost all the nacelle and drive-train test benches for wind turbines. However, there is no standard method for torque measurement. The solution for the measurement is mostly individually designed or specified for each of the test benches. Some discussions about the different methods used on the nacelle test benches are given in the work of Foyer et al.[6]

For test benches that apply 6-DOF (degree of freedom) loads, the torque-measuring device is usually not located directly between the test bench and the turbine nacelle. Instead, in order to reduce the impact of the non-torque loads and protect the torque transducer against the shocks, the inherent torque-measuring devices of such test benches are often located behind the load application unit (LAU) that applies for example the bending moment. As a result, the friction torque of the LAU can introduce a major uncertainty to the input torque for the turbine, especially given that the friction torque is also highly temperature and load dependent. Research undertaken by Kock et al[8] has studied the friction behaviours of a specific LAU system on a 4-MW test bench,[9] aiming to quantify the friction torque and the uncertainty introduced by the LAU system. To measure the input torque to the turbine directly, the torque transducer needs to be very robust, in order to withstand the large non-torque loads. One possible way is to use the shaft adapter between the test bench and the nacelle as a torque-measuring device. Certain strain gauge connections can be applied on the cylindrical adapter to measure the torque-introduced strain on the adapter. A calibration of enough accuracy is then necessary in order to convert the strain signal into torque.

For simpler test benches that apply only the torque, for example, the common end-of-line test benches of the turbine manufacturer, the accompanying non-torque loads are not as critical as above. In this case, torque measurement with professional torque transducers would be possible, but measuring with strain gauges on the adapter or connection shaft is still very attractive with lower cost of both funding and time.

On both types of test benches, accurate and regular calibrations are vital for the torque measurement where the accuracy is important, for example, to determine the drive-train efficiency. However, the high cost and great effort required for the calibration often make it impossible to achieve the desired high accuracy. Therefore, it makes good sense to seek a calibration process that is cost effective, practical to perform, and easy to repeat. Even for those applications where an accurate torque measurement is not necessary, for example when an uncertainty below 5 % is sufficient, such a calibration process is also an important means of validation.

This paper proposes a new calibration method that establishes a relationship between the torque and the electrical power, so that the torque measurement is indirectly calibrated through the electrical measurement. The relationship is determined through a series of tests whereby the test bench and the turbine nacelle take turns to drive and generate power. Because no additional structural reconfigurations and only limited instrumentation are needed for carrying out the calibration, the method has a clear advantage in time and cost perspectives. Due to a parameter estimation adopted in the process, the method cannot be categorised as traceable calibration, which is strictly traced back to the national or international standards with known uncertainty. But for easier understanding, the term "calibration" is still used in this paper to describe the process of determining the linear relationship between the measured raw signal and the torque. As a countermeasure to the estimation, a detailed analysis of the uncertainty budget related with the method is presented in this paper.

2 | TEST PROCESS

In the previous study, a test process was proposed to determine the drive train efficiency with limited accuracy of the torque measurement.[10,11] A further study has shown that the same test process can also be used for the calibration of the torque measurement. A relationship between the torque and the power measurement can be obtained through the test.

Two tests are necessary for the process, which are named test A and test B, respectively. The layout and the configuration of the tests are illustrated in Figure 1, where the power losses through the drive train are demonstrated using the level change of the power curves. In the figure, $P_{mech.A}$ and $P_{mech.B}$ are the mechanical powers at the measuring point for test A and test B, while $P_{elec.A}$ and $P_{elec.B}$ are the corresponding electrical powers. Similarly, T_A and T_B denote the mechanical torques for the two tests, while ω_A and ω_B represent the speeds of rotation. Torque measurement is realised on the shaft adapter between the test bench and the nacelle. Electrical power is measured between the turbine generator and the converter. Additionally, position and rotational speed of the shaft are also measured by the incremental or absolute encoder near the shaft adapter.

- In test A, the test bench and the turbine nacelle both operate in their normal mode. The test bench drives the nacelle running at a specific operating point. A warm-up operation should be carried out prior to the test in order to achieve stable temperature conditions for the components that influence the transmission and power conversion efficiency of the nacelle. The test should be run for a period of time, so that influences from the non-torque loads and the structural dynamics can be well compensated in the mean measurement value.
- In test B, the power flows in the direction opposite to that in test A. The nacelle operates in motor mode while the test bench acts as a generator. The nacelle drives the whole set-up so it is running at the same speed but in the direction opposite to that in test A. The measured
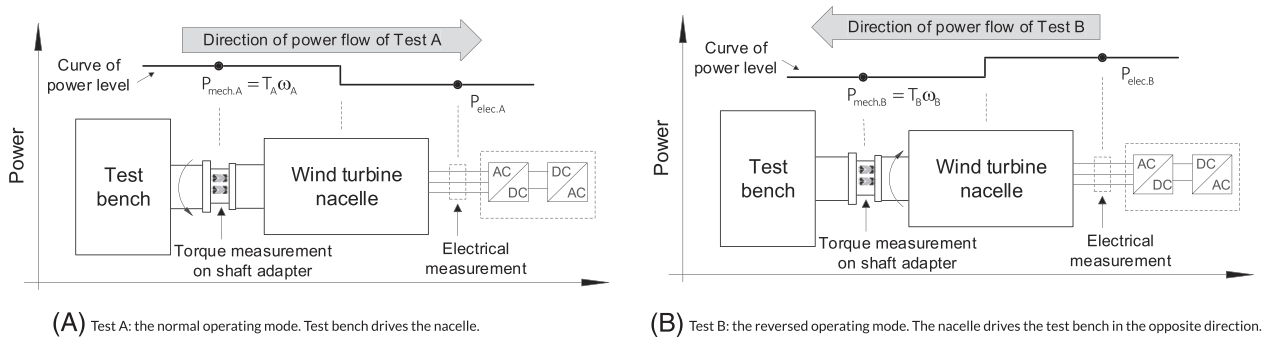
(A) Test A: the normal operating mode. Test bench drives the nacelle.

(B) Test B: the reversed operating mode. The nacelle drives the test bench in the opposite direction.

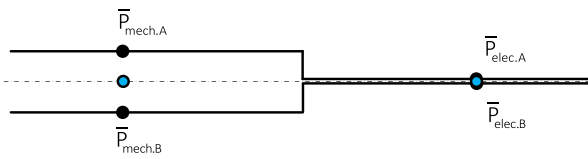**FIGURE 1** Layout and power loss demonstration of test A and test B

FIGURE 2 Levels of mechanical and electrical powers in test A and test B [Colour figure can be viewed at wileyonlinelibrary.com]

electrical power input to the nacelle generator should be carefully tuned to be as close as possible to the output power that is measured during test A. The test should also run for a similar time length as in test A.

For comparison, the input and output power levels of test A and test B can be plotted together as shown in Figure 2, where $\bar{P}_{mech.A}$ and $\bar{P}_{mech.B}$ are the mean values of the mechanical power in test A and test B, respectively, and $\bar{P}_{elec.A}$ and $\bar{P}_{elec.B}$ represent the mean values of the electrical power. It is worth emphasising that these four variables are the theoretical true values. The rotational speed is controlled to be stable throughout each test; therefore, the kinetic energy of the drive train inertia does not play a role in the equilibrium of the mean powers over a period of time.

The mean power loss in each of the tests can be expressed by definition as the difference between the input and output mean powers. This is shown in Equation (1), where $\bar{P}_{loss.A}$ and $\bar{P}_{loss.B}$ denote the mean value of the power loss in test A and test B, respectively. As the equation is expressed by the definition, $\bar{P}_{loss.A}$ and $\bar{P}_{loss.B}$ are also the true values without any uncertainty.

$$\begin{cases} \bar{P}_{loss.A} = \bar{P}_{mech.A} - \bar{P}_{elec.A} \\ \bar{P}_{loss.B} = \bar{P}_{elec.B} - \bar{P}_{mech.B}. \end{cases} \tag{1}$$

The factor k is introduced as the relationship between $\bar{P}_{loss.A}$ and $\bar{P}_{loss.B}$, as expressed in Equation (2). The equation can be further transformed into the expression in Equation (3), with the relationship from Equation (1).

$$\bar{P}_{loss.A} = k\bar{P}_{loss.B}, \tag{2}$$

$$\bar{P}_{mech.A} + k\bar{P}_{mech.B} = \bar{P}_{elec.A} + k\bar{P}_{elec.B}. \tag{3}$$

Other than drawing the relationship between the mechanical and electrical powers through the absolute drive train efficiency, Equation (3) forms the relationship based on the distribution of total power loss, which is depicted through a dash line in Figure 2. This is also the basis of the torque calibration method proposed in the present paper.

3 | METHOD OF TORQUE CALIBRATION

The mean values of the mechanical power $\bar{P}_{mech.A}$ and $\bar{P}_{mech.B}$ can be expressed as the accumulated energy divided by the corresponding duration, where the accumulated energy is the integrated torque in the angle domain. As a result, Equation (3) can be expressed further as Equation (4). In this equation, T denotes the torque, t_A and t_B are the durations of test A and test B, respectively, θ_A and θ_B are the corresponding accumulated angle displacements in test A and test B. Since the angular position is the raw signal from the encoder, it is more accurate to determine the power with the help of angle domain integration. Although encoders are often used on a wind turbine for measuring the rotational speed, the speed is in fact a derivative of the original position signal. For better accuracy, θ_A and θ_B can be chosen as integer multiples of 2π, so that the influence of the non-torque loads can be better compensated with signal from integer number of revolutions.

$$\frac{\int_0^{\theta_A} T d\theta}{t_A} + k\frac{\int_0^{\theta_B} T d\theta}{t_B} = \bar{P}_{elec.A} + k\bar{P}_{elec.B}. \tag{4}$$

Replacing the theoretical true variables with the measured values, T and P_{elec} can be expressed as in Equation (5), where

- ε represents the measured raw signal from the the torque measurement channel. In many cases, the raw signal is the strain measured by the strain gauges. Depending on the measurement principle and the channel configuration, the raw signal can also be other variables.
- a and b are the sensitivity and offset parameters that define the linear relationship between the measured raw signal ε and the true torque T. Due to the non-linear behaviour of the measurement and external influences, the real relationship can be more complicated than the linear one defined by a and b. The discrepancy from the linear behaviour is attributed to a time-varying quantity $r(t)$, which also includes the repeatability error of the measurement, for example the error caused by temperature change and the noise from EMI (Electromagnetic Interference).
- $\tilde{P}_{elec}$ is the measured signal of the electrical power. c and d are the sensitivity and offset errors of the measurement with respect to the true electrical power P. Similar to the $r(t)$ in the torque measurement, $q(t)$ denotes here the non-linearity and the repeatability errors of the electrical power measurement.

$$\begin{cases} T = a\varepsilon + b + r(t) \\ P_{elec} = (1+c)\tilde{P}_{elec} + d + q(t). \end{cases} \tag{5}$$

Using the definitions in Equation (5), the mean torque values can be expressed as Equation (6), where $\bar{\omega}_A$ and $\bar{\omega}_B$ are the mean rotational speeds in test A and test B, respectively. For the mean rotational speed, no distinction is made here between the theoretical true value and the measured value. The high positional accuracy provided by the encoder and the relatively long test period make it possible that the error of the measured mean speed can be regarded as zero. The right-hand side of Equation (4) can be expressed as Equation (7), with $\bar{\tilde{P}}_{elec.A}$ and $\bar{\tilde{P}}_{elec.B}$ being the mean values of the measured electrical power in test A and test B.

Defining $R_A = \frac{1}{t_A}\int_0^{\theta_A} r(\theta)d\theta$, $R_B = \frac{1}{t_B}\int_0^{\theta_B} r(\theta)d\theta$, $Q_A = \frac{1}{t_A}\int_0^{t_A} q(t)dt$, and $Q_B = \frac{1}{t_B}\int_0^{t_B} q(t)dt$, Equation (4) can be transformed into Equation (8).

$$\begin{cases} \dfrac{\int_0^{\theta_A} T d\theta}{t_A} = \dfrac{a}{t_A}\int_0^{\theta_A} \varepsilon(\theta)d\theta + b\bar{\omega}_A + \dfrac{1}{t_A}\int_0^{\theta_A} r(\theta)d\theta \\ \dfrac{\int_0^{\theta_B} T d\theta}{t_B} = \dfrac{a}{t_B}\int_0^{\theta_B} \varepsilon(\theta)d\theta + b\bar{\omega}_B + \dfrac{1}{t_B}\int_0^{\theta_B} r(\theta)d\theta, \end{cases} \tag{6}$$

$$\bar{P}_{elec.A} + k\bar{P}_{elec.B} = (1+c)(\bar{\tilde{P}}_{elec.A} + k\bar{\tilde{P}}_{elec.B}) + d(1+k) + \frac{1}{t_A}\int_0^{t_A} q(t)dt + \frac{1}{t_B}\int_0^{t_B} q(t)dt, \tag{7}$$

$$a\left(\frac{\int_0^{\theta_A} \varepsilon d\theta}{t_A} + \frac{k\int_0^{\theta_B} \varepsilon d\theta}{t_B}\right) + b(\bar{\omega}_A + k\bar{\omega}_B) + R_A + R_B = (1+c)(\bar{\tilde{P}}_{elec} + k\bar{\tilde{P}}_{elec}) + d(1+k) + Q_A + Q_B. \tag{8}$$

Denoting X and Y as expressed in Equations (9) and (10), the relationship defined in Equation (4) can be expressed in a concise form shown in Equation (11). A very clear linear relationship is seen in this equation, with a and b being the sensitivity and offset parameters. In fact, the aim of the calibration is exactly this—to determine the values of a and b.

It is obvious here that the parameters a and b can be determined with at least two sets of X and Y values at different torque levels. This means the test procedure described in Section 2 should be carried out on several different torque levels. If more than two sets of values are available, a and b can be determined through linear fit using the least squares method.

$$X = \frac{\int_0^{\theta_A} \varepsilon d\theta}{t_A(\bar{\omega}_A + k\bar{\omega}_B)} + \frac{k\int_0^{\theta_B} \varepsilon d\theta}{t_B(\bar{\omega}_A + k\bar{\omega}_B)}, \tag{9}$$

$$Y = \frac{(1+c)(\bar{\tilde{P}}_{elec.A} + k\bar{\tilde{P}}_{elec.B}) + d(1+k) + Q_A + Q_B - R_A - R_B}{\bar{\omega}_A + k\bar{\omega}_B}, \tag{10}$$

$$aX + b = Y. \tag{11}$$

As can be seen in Equations (9) and (10), the X and Y values are expressions of the mechanical and electrical measurement as well as the factor k. Additionally, some error terms are also in the expression, including c, d, Q_A, Q_B, R_A, and R_B. The measured mechanical and electrical values are of course known for the calculation. The factor k must be determined through analysis to become a known value, denoted as $\hat{k}$, with the uncertainty taken into account. Note that the k factor is not necessarily estimated as 1. In the calibration process, the error terms in the expression do not play any part, but they will be taken as uncertainty contributions in the following uncertainty analysis.

$$\begin{cases} \tilde{X} = \dfrac{\int_0^{\theta_A} \varepsilon d\theta}{t_A(\bar{\omega}_A + \hat{k}\bar{\omega}_B)} + \dfrac{\hat{k}\int_0^{\theta_B} \varepsilon d\theta}{t_B(\bar{\omega}_A + \hat{k}\bar{\omega}_B)} \\ \tilde{Y} = \dfrac{\bar{\tilde{P}}_{elec.A} + \hat{k}\bar{\tilde{P}}_{elec.B}}{\bar{\omega}_A + \hat{k}\bar{\omega}_B}. \end{cases} \tag{12}$$

For the calibration, the $\tilde{X}$-$\tilde{Y}$ value sets can be used for determining the parameters a and b. $\tilde{X}$ and $\tilde{Y}$ are defined in Equation (12). All the terms in the expressions are known values, and therefore, the calibration can easily be carried out. Suppose the test process in Section 2 is carried out on N different torque levels (N≥2), the estimated values of a and b, denoted as $\hat{a}$ and $\hat{b}$, can be obtained through the linear fit,[12, p246] and the results can be expressed as Equations (13) and (14), where i is the index number of a certain torque level, $\tilde{X}_i$ and $\tilde{Y}_i$ are the corresponding values obtained on the basis of that test. Note that the estimated value $\hat{k}$ may be different for tests with different torque levels.

$$\hat{a} = \frac{N \sum_{i=1}^{N} \tilde{X}_i \tilde{Y}_i - \sum_{i=1}^{N} \tilde{X}_i \sum_{i=1}^{N} \tilde{Y}_i}{N \sum_{i=1}^{N} (\tilde{X}_i^2) - (\sum_{i=1}^{N} \tilde{X}_i)^2}, \tag{13}$$

$$\hat{b} = \frac{\sum_{i=1}^{N} (\tilde{X}_i^2) \sum_{i=1}^{N} \tilde{Y}_i - \sum_{i=1}^{N} \tilde{X}_i \sum_{i=1}^{N} (\tilde{X}_i \tilde{Y}_i)}{N \sum_{i=1}^{N} (\tilde{X}_i^2) - (\sum_{i=1}^{N} \tilde{X}_i)^2}. \tag{14}$$

With the $\hat{a}$ and $\hat{b}$ known, and taking the definition in Equation (5) as the basis, the estimated torque $\hat{T}$ can be calculated in Equation (15). The term $r(t)$ contributes to the uncertainty of the torque calculation.

$$\hat{T} = \hat{a}\varepsilon + \hat{b} + r(t). \tag{15}$$

With $r(t)$ being considered as a source of uncertainty, the expression can be simplified to Equation (16).

$$\hat{T} = \hat{a}\varepsilon + \hat{b}. \tag{16}$$

4 | UNCERTAINTY CONSIDERATIONS

As a result of the calibration process, the torque measurement can be expressed as a function of the estimated $\hat{a}$, $\hat{b}$ and the measured raw signal ε. A time-varying variable $r(t)$ takes account of the repeatability error of the measured signal as well as the non-linearity error of the T-ε relationship. This situation is presented in Equation (15). The uncertainty in $\hat{T}$ is therefore dependent on $\hat{a}$, $\hat{b}$, ε and $r(t)$.

The uncertainty of the measured torque is ultimately composed of two parts. One part originates from the raw measurement itself, the other from the calibration. The uncertainty in the raw measurement represents the quality of the measured raw signal, which is affected by the signal noise, non-linear and hysteresis behaviour, signal drift due to temperature change and humidity, as well as other possible factors that make the signal less repeatable. The uncertainty from the calibration indicates how accurately the sensitivity and offset parameters are derived from the calibration. This paper will focus on the calibration uncertainty. Although the raw measurement uncertainty is not of great interest here, it does exert an influence on the calibration uncertainty, because the raw signals have to be used in the calibration process. A better calibration cannot improve the quality of the raw measurement, but better raw signals can indeed produce a more accurate calibration.

4.1 | Uncertainty of the raw measurement

Since the variable ε is defined as the value of the raw measurement, the uncertainty of ε itself should be considered to be zero. As a result, the uncertainty of the torque measurement directly owing to the raw signal is attributed to $r(t)$, which is introduced in Equation (5) to represent all the error contributions that cause the measured signal ε to deviate from the ideal linear response to the true torque. The error contributions can be grouped into two categories, namely, the non-linear behaviour and the repeatability errors. The total uncertainty contributed by $r(t)$ is denoted here as $u_{T,r}$. It characterises the quality of the measuring channel.

The non-linearity of a measurement is strongly dependent on the principle used and the measurement chain. In the case of a strain gauge-based measurement, it depends on the material and structural non-linear behaviour of the part to which the strain gauges are applied, as well as the non-linearity of the Wheatstone bridge circuit.[13] Further, non-linearity comes also from the data acquisition (DAQ) system of the measurement.

The repeatability error of the measurement comes from a number of sources that cause the measurement to be time-varying. A common source is the background noise in the measured signal due to EMI and the thermal noise[14] in the strain gauge resistors. Creep effect of the material and temperature change both cause a signal drift in the measurement and therefore also contribute to the repeatability error. Another contributor is the so-called "cross-talk" effect, which means that the load in other directions exert an influence on the torque measurement. Despite the effort and common methods available for the compensation against cross-talk,[15] a satisfactory compensation is usually very difficult on a wind turbine.[16] Fortunately, in some cases, the transient value of the measurement is of less interest, for example, in a stable operation on the test bench. The torque can then be determined by the mean of a period of time, or more precisely the mean value of an integer number of revolutions. This will be the case for a torque calibration test process as mentioned in Sections 2 and 3.

4.2 | Uncertainty associated with the calibration

The parameters $\hat{a}$ and $\hat{b}$ are the results of the linear fit of a number of ($\tilde{X}_i$-$\tilde{Y}_i$) points in the X-Y plane. This is schematically illustrated in Figure 3, where four points are available. For each point, both $\tilde{X}_i$ and $\tilde{Y}_i$ have uncertainties. The uncertainties are presented in the form of error bars, with
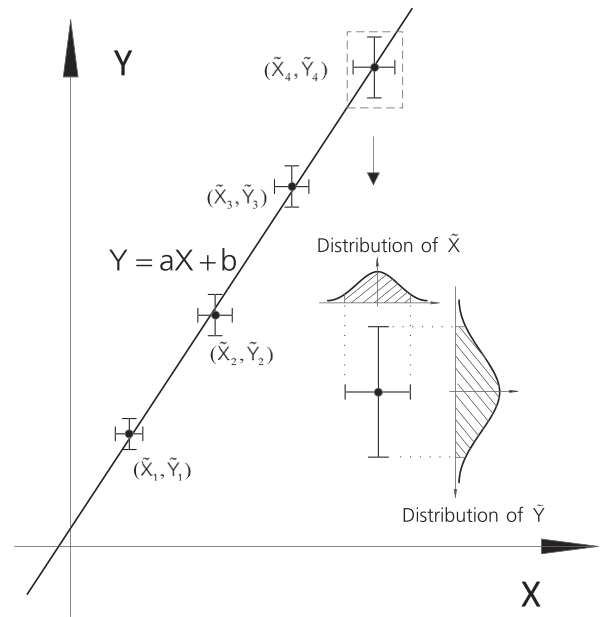
FIGURE 3 Linear fit in the X-Y plane

the corresponding estimated values $\tilde{X}_i$ and $\tilde{Y}_i$ located in the middle of the error bars. The length of the error bar represents the uncertainty of the corresponding variable, although this does not necessarily mean that the true value is located within the range defined by the bar. The probability distribution of the true value within and beyond the error bar can be of different types. The most common form is the normal distribution, as shown enlarged in the lower right part of Figure 3. Each individual uncertainty represented by the error bar makes a contribution to the uncertainty in $\hat{a}$ and $\hat{b}$ and hence the measured torque $\hat{T}$. Therefore, all the uncertainties of the $\tilde{X}_i$ and $\tilde{Y}_i$ values have to be considered in the uncertainty calculation for $\hat{a}$, $\hat{b}$.

Furthermore, the uncertainty covariances of each two values also exert influence on the overall uncertainties of $\hat{a}$, $\hat{b}$. These include the uncertainty covariance of each two different $\tilde{X}$ values, of each two different $\tilde{Y}$ values, and the uncertainty covariance of each $\tilde{X}$ and $\tilde{Y}$ combination. In fact, because the same k factor is used in the expression of both $\tilde{X}$ and $\tilde{Y}$, and also since the measurements on different torque levels are obtained from the same measurement chain, the covariances are of considerable significance. The standard uncertainty in $\hat{T}$ due to the linear fit parameters $\hat{a}$ and $\hat{b}$ (which are also the products of the calibration) is denoted in the following as $u_{T.cal}$.

The uncertainty $u_{T.cal}$ represents the uncertainty of the ($\hat{a}\varepsilon + \hat{b}$) part of Equation (15), where $\hat{a}$ and $\hat{b}$ are functions of N sets of $\tilde{X}_i$-$\tilde{Y}_i$ values. Following the principle of uncertainty propagation,[17] $u_{T.cal}$ can be determined,[12, p253] as expressed in Equation (17).

$$
\begin{aligned}
u_{T.cal}^2 = {} & \sum_{i=1}^{N}\left(\frac{\partial \hat{T}}{\partial \tilde{Y}_i}\right)^2 s_{\tilde{Y}_i}^2 + \sum_{i=1}^{N}\left(\frac{\partial \hat{T}}{\partial \tilde{X}_i}\right)^2 s_{\tilde{X}_i}^2 + \sum_{i=1}^{N}\left(\frac{\partial \hat{T}}{\partial \tilde{Y}_i}\right)^2 \sigma_{\tilde{Y}_i}^2 \\
& + 2\sum_{i=1}^{N-1}\sum_{k=i+1}^{N}\left(\frac{\partial \hat{T}}{\partial \tilde{Y}_i}\right)\left(\frac{\partial \hat{T}}{\partial \tilde{Y}_k}\right)\sigma_{\tilde{Y}_i\tilde{Y}_k} + \sum_{i=1}^{N}\left(\frac{\partial \hat{T}}{\partial \tilde{X}_i}\right)^2 \sigma_{\tilde{X}_i}^2 \\
& + 2\sum_{i=1}^{N-1}\sum_{k=i+1}^{N}\left(\frac{\partial \hat{T}}{\partial \tilde{X}_i}\right)\left(\frac{\partial \hat{T}}{\partial \tilde{X}_k}\right)\sigma_{\tilde{X}_i\tilde{X}_k} + 2\sum_{i=1}^{N}\sum_{k=1}^{N}\left(\frac{\partial \hat{T}}{\partial \tilde{X}_i}\right)\left(\frac{\partial \hat{T}}{\partial \tilde{Y}_k}\right)\sigma_{\tilde{X}_i\tilde{Y}_k}
\end{aligned}
\tag{17}
$$

where $s_{\tilde{X}_i}$ and $s_{\tilde{Y}_i}$ are the random standard uncertainties in the variables $\tilde{X}_i$ and $\tilde{Y}_i$, respectively.

$\sigma_{\tilde{X}_i}$ and $\sigma_{\tilde{Y}_i}$ similarly denote the systematic standard uncertainty of $\tilde{X}_i$ and $\tilde{Y}_i$.

$\sigma_{\tilde{Y}_i\tilde{Y}_k}$, $\sigma_{\tilde{X}_i\tilde{X}_k}$ and $\sigma_{\tilde{X}_i\tilde{Y}_k}$ are the covariance estimators for the correlated systematic errors of the corresponding variables in the subscript.

Examining the equation, it is seen that most of the terms are very easy to obtain:

- The partial derivatives of $\frac{\partial \hat{T}}{\partial \tilde{X}_i}$ and $\frac{\partial \hat{T}}{\partial \tilde{Y}_i}$ can be estimated numerically on the basis of the finite difference method. According to Equations (13), (14), and (16), the estimated torque $\hat{T}$ can be explicitly expressed with the estimated $\tilde{X}$, $\tilde{Y}$ values and the measured signal ε, all of which are known or already determined.

- The random uncertainties $s_{\tilde{X}_i}$ and $s_{\tilde{Y}_i}$ refer to the uncertainty components which are independent and have no correlation with other components. Based on the definition of X and Y in Equations (9) and (10), the random uncertainty $s_{\tilde{X}_i}$ can be considered as zero, because the accuracy of the time and angle position measurements (and hence the mean speed as well) are very high, and as a result, their uncertainties are negligible. The value of $s_{\tilde{Y}_i}$ is mostly dependent on the random uncertainty of the electrical power measurement.

- The systematic uncertainties $\sigma_{\tilde{X}_i}$ and $\sigma_{\tilde{Y}_i}$ are introduced by systematic reasons and can therefore be related with the uncertainties from other measurements. For example, the uncertainty in the measured electrical power on a certain power level can be related to the uncertainty on

another power level or on the same level from another test. The values of $\sigma_{\tilde{X}_i}$ and $\sigma_{\tilde{Y}_i}$ are dependent on the uncertainties from the estimated $\hat{k}$ factor and the electrical power measurement.

- The effect of the correlations between the systematic uncertainties is quantified in the calculation with covariances $\sigma_{\tilde{Y}_i\tilde{Y}_k}$, $\sigma_{\tilde{X}_i\tilde{X}_k}$, and $\sigma_{\tilde{X}_i\tilde{Y}_k}$. The covariance can be further expressed as a function of two systematic uncertainties and the corresponding correlation coefficient between them,[17] as expressed in Equation (18). Therefore, the task of determining the covariances is converted to the determination of correlation coefficients.

$$\begin{cases} \sigma_{\tilde{X}_i\tilde{X}_k} = \sigma_{\tilde{X}_i}\sigma_{\tilde{X}_k}r_{\tilde{X}_i\tilde{X}_k} \\ \sigma_{\tilde{Y}_i\tilde{Y}_k} = \sigma_{\tilde{Y}_i}\sigma_{\tilde{Y}_k}r_{\tilde{Y}_i\tilde{Y}_k} \\ \sigma_{\tilde{X}_i\tilde{Y}_k} = \sigma_{\tilde{X}_i}\sigma_{\tilde{Y}_k}r_{\tilde{X}_i\tilde{Y}_k}. \end{cases} \tag{18}$$

Although Equation (17) appears complicated with the large number of terms, most of the terms are in fact the diagonal and cross entries of a $2N \times 2N$ matrix. Therefore, the equation is suitable for processing with matrix operations. One possible way of establishing such a matrix operation is discussed in this section.

Define a row vector $\boldsymbol{v}$ as the array of partial derivatives with respect to $\tilde{X}$ and $\tilde{Y}$ at different torque levels. The vector has $2N$ elements, and is expressed in Equation (19). Similarly, define σ as a row vector containing $\sigma_{\tilde{X}}$ and $\sigma_{\tilde{Y}}$ at different torque levels as expressed in Equation (20). Vector σ also has $2N$ elements. Based on $\boldsymbol{v}$ and σ, two $2N \times 2N$ matrices ($\boldsymbol{v}^{\mathsf{T}}\boldsymbol{v}$) and ($\sigma^{\mathsf{T}}\sigma$) can be obtained by means of simple matrix operations. Each matrix contains all the possible products of two different elements from the corresponding vector (the cross entries of the matrix), as well as products of each vector element with itself (diagonal entries of the matrix). In matrix ($\sigma^{\mathsf{T}}\sigma$), each entry is a product of two standard systematic uncertainties. According to Equation (18), this product can be converted to the covariance of the two uncertainties after being multiplied by the relevant correlation coefficient. Inserting this correlation coefficient into the corresponding position of another $2N \times 2N$ matrix and repeating this for all the entries allows matrix of correlation coefficients to be obtained. This new matrix is denoted here as $\boldsymbol{R}$.

$$\boldsymbol{v} = \left(\frac{\partial \hat{T}}{\partial \tilde{X}_1}, \ \dots \ , \frac{\partial \hat{T}}{\partial \tilde{X}_N}, \frac{\partial \hat{T}}{\partial \tilde{Y}_1}, \ \dots \ , \frac{\partial \hat{T}}{\partial \tilde{Y}_N} \right), \tag{19}$$

$$\sigma = \left(\sigma_{\tilde{X}_1}, \ \dots \ , \sigma_{\tilde{X}_N}, \sigma_{\tilde{Y}_1}, \ \dots \ , \sigma_{\tilde{Y}_N} \right). \tag{20}$$

The Hadamard product of matrix ($\boldsymbol{v}^{\mathsf{T}}\boldsymbol{v}$), ($\sigma^{\mathsf{T}}\sigma$) and $\boldsymbol{R}$, denoted as $\boldsymbol{U}_{sys}$ in Equation (21), contains all the systematic uncertainty components in $u_{T.cal}^2$ as expressed in Equation (17). A summation of all the entries of matrix $\boldsymbol{U}_{sys}$ is easy to achieve in the calculation and can be expressed analytically as $\boldsymbol{e}\boldsymbol{U}_{sys}\boldsymbol{e}^{\mathsf{T}}$, where $\boldsymbol{e}$ is a row vector with all elements being 1. Therefore, with the help of matrix operations, the expression of $u_{T.cal}^2$ in Equation (17) can be converted into a concise form shown in Equation (22).

$$\boldsymbol{U}_{sys} = (\boldsymbol{v}^{\mathsf{T}}\boldsymbol{v})\circ(\sigma^{\mathsf{T}}\sigma)\circ\boldsymbol{R}, \tag{21}$$

$$u_{T.cal}^2 = \sum_{i=1}^{N}(\frac{\partial \hat{T}}{\partial \tilde{Y}_i})^2 s_{\tilde{Y}_i}^2 + \sum_{i=1}^{N}(\frac{\partial \hat{T}}{\partial \tilde{X}_i})^2 s_{\tilde{X}_i}^2 + \boldsymbol{e}\boldsymbol{U}_{sys}\boldsymbol{e}^{\mathsf{T}}. \tag{22}$$

In summary, the systematic uncertainty can be obtained using the two vectors $\boldsymbol{v}$ and σ, together with the correlation matrix $\boldsymbol{R}$. The calculation process is suitable for matrix operations, which can be effectively carried out with computer programmes or commercial mathematical software. While $\boldsymbol{v}$ and σ can be easily obtained through numerical calculation, the matrix $\boldsymbol{R}$ requires more analysis of the uncertainty source. Due to space limitation, the analysis is not discussed in detail in this paper. Nevertheless, the matrix $\boldsymbol{R}$ is not difficult to obtain as most of its entries are close or equal to zero or one.

5 | EXPERIMENT WITH THE METHOD ON A 10-MW NACELLE TEST BENCH

During a re-commissioning of the motors on the nacelle test bench "DyNaLab,"[18] the mechanical torque on the structure between the two tandem motors is needed for the validation of the electrical model of the motors, which is a basis of the motor controller. In order to measure the torque between the motors, strain gauges are applied to the intermediate shaft between the motors, and thus the measured signal from the strain gauges needs to be calibrated. One possible calibration method is the FEM analysis of the intermediate shaft, where the relationship between structure strain and torque can be established. However, the accuracy is considered insufficient due to the accumulated uncertainty from the strain measurement and the FEM analysis. Another method is to apply torque on one side of the drive train with a lift crane over a lever of known length. The problem with this method is the logistic expense and the difficulty to lock the drive train on the other side.

After evaluation of possible ways of calibration, the method proposed in this paper is considered to be the most convenient and accurate way of calibration. Additionally, the efficiencies of the motors at different operation points can be also determined as by-products. The method and test process are therefore carried out during the re-commissioning.
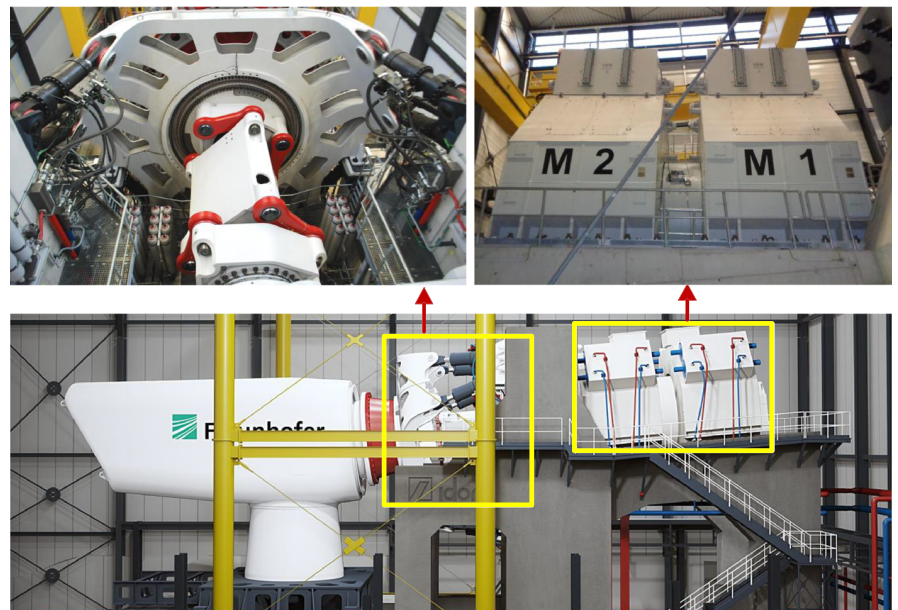
FIGURE 4 The 10 MW nacelle test bench "DyNaLab" at Fraunhofer IWES in Bremerhaven. Top left: the coupling and load application system (LAU) with a moment bearing. Top right: two tandem motors and the intermediate shaft. Bottom: overview of the test bench [Colour figure can be viewed at wileyonlinelibrary.com]

TABLE 1 Parameters per one motor

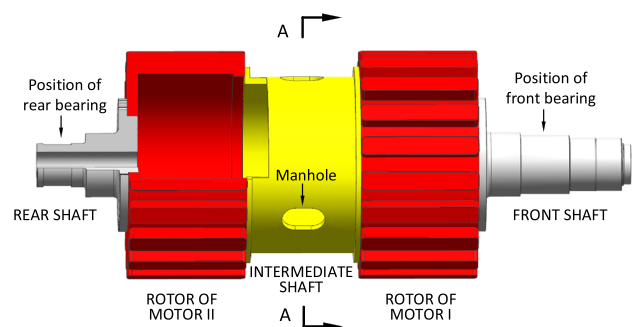| Motor Type	Rated power	Rated torque	Overload Torque	Rated speed	Speed range
Synchronous	5000 kW	4.3 $MN \cdot m$	6.5 $MN \cdot m$	11 rpm	2.5 - 25 rpm

FIGURE 5 Drive train layout of the drive system [Colour figure can be viewed at wileyonlinelibrary.com]

The motors and the test bench "DyNaLab" are shown in Figure 4. Two motors are connected together in tandem by an intermediate shaft between them. The basic information about a single motor is listed in Table 1. In the normal operation, the two motors work together to provide the driving torque of the test bench. During the re-commissioning, the motors run in back-to-back mode instead. In application of the new method, motor I and motor II correspond to the test bench and the turbine, respectively, as described in Sections 2 and 3.

5.1 | Instrumentation of the measurement system

The drive train layout of the two motors is shown in Figure 5. The rotors are connected together and supported by two bearings on the front and rear shafts. The intermediate shaft as well as the rotors have a hollow structure. Three manholes are available on the intermediate shaft, which enable operations to be carried out inside the rotating part, for example, applying the strain gauges on the inner surface from inside the structure. Owing to the large diameter of the intermediate shaft, this has clear logistic advantages over applying the strain gauges on the outer surface.

The strain gauges and the instrumentation for the measurement are illustrated in detail with a cross-sectional sketch of the middle of the intermediate shaft in the A-A direction, as shown in Figure 6.

Three identical wheatstone strain gauge full bridges are applied at three different positions on the inner surface of the structure, labelled as $60°$, $180°$, and $300°$ in the figure. The positions are chosen to be as far away from the manholes as possible, which means that they are located at the mid-points between the manholes. This keeps the strain gauges away from the strain concentration and complexity at the vicinity of the manholes. The full bridges are applied so as to measure the local shear strain. Each full bridge is located at a single position, and therefore, the temperature difference within the full bridge is minimised. In order to compensate the strain component that is introduced by the shear force, the average of the three full bridge signals should be taken as the signal for the torque measurement. This can be demonstrated with a simple equation as shown in Equation (23), where γ_{torque} denotes the shear strain that is introduced purely by the torque, while $\gamma_{60°}$, $\gamma_{180°}$, and $\gamma_{300°}$ are
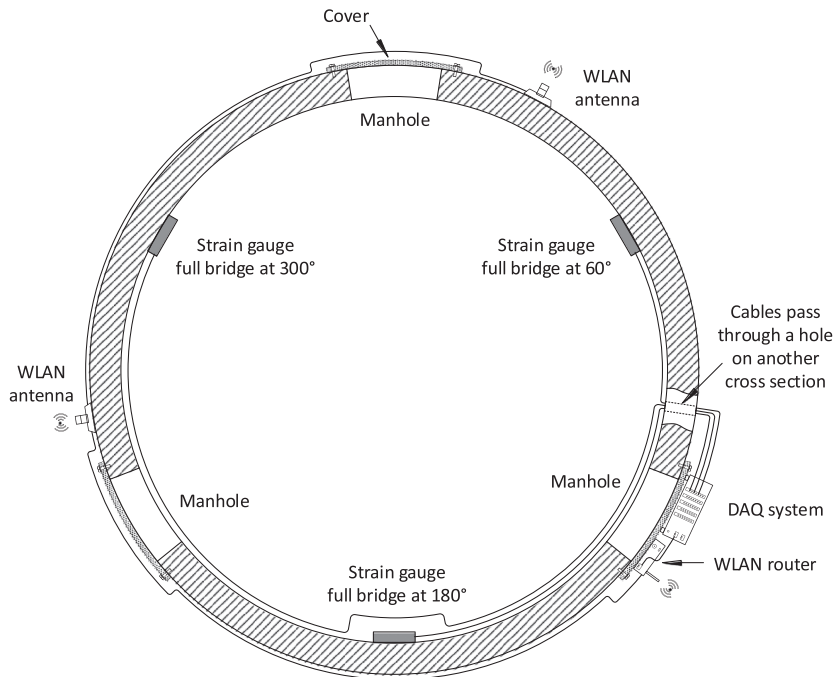
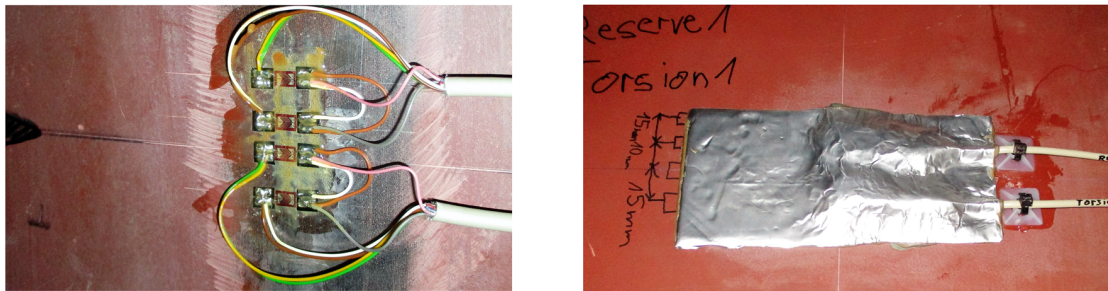**FIGURE 6** Cross section A-A on the intermediate shaft

FIGURE 7 Examples of the strain gauges before and after the protective covering is affixed. At each position, two identical full bridges are used to provide redundancy. This explains why two output cables can be seen in each photo [Colour figure can be viewed at wileyonlinelibrary.com]

the corresponding local shear strains. Two photos showing how the strain gauge is mounted are presented in Figure 7.

$$\gamma_{torque} = (\gamma_{60°} + \gamma_{180°} + \gamma_{300°})/3. \tag{23}$$

During the test, the manholes have to be closed with the covers. Therefore, the cables of the full bridge channels are led out through a small hole (available on another cross-section) to the data acquisition (DAQ) system, shown in Figure 6. The DAQ system is fixed to one of the manhole covers, with the help of the bolts for the cover. Since the strain gauges together with the DAQ system are located on the rotating part, a WLAN (Wireless LAN) connection is utilised for the communication between the rotating system and the stationary parts, including the data and time synchronisation server, as well as the remote measurement controller. Time synchronisation on the rotating DAQ system is realised through the WLAN connection in the network time protocol (NTP). The router of the WLAN system is also fixed to the cover. To ensure the quality of the wireless connection, three antennas are placed at equal separations along the circumference of the intermediate shaft.

In addition to the torque measurement, the speed and angular position are measured by an absolute encoder at the end of the test bench drive train. The encoder measures the rotation of the rear shaft relative to the adjacent bearing housing. This encoder is part of the test bench and has a resolution of 16384 CPR (counts per revolution). The signal is connected to a stationary DAQ system, with the same time reference as the rotating DAQ system.

To measure the electrical power, voltage and current sensors are installed on the input power cables of the two motors. A high sampling frequency DAQ system is used to measure the alternating voltage and current signals. The electrical power can be processed on the basis of the voltage and current measurements. The same source of time reference is also used in this system for the signal time stamps.

5.2 | Back-to-back test and torque calibration

Back-to-back tests are carried out following the method explained in Section 2. The electrical measurement of motor II is chosen as the reference during the test process. Since motor I is connected to a number of other components in the front, including the moment bearing of the load

TABLE 2 The whole test sequence for the torque calibration

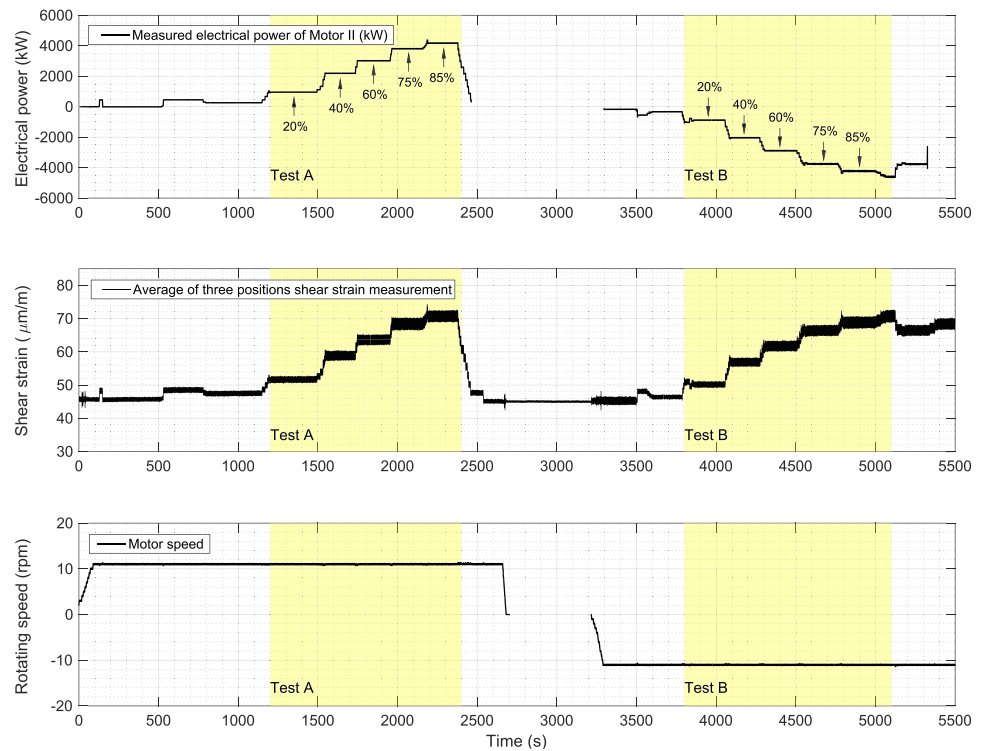| Test Step	1	2	3	4	5	6	7	8	9	10
Motor II electrical power in relation to rated	20 %	40 %	60 %	75 %	85 %	20 %	40 %	60 %	75 %	85 %
Operating mode	A	A	A	A	A	B	B	B	B	B
Rotational speed, rpm	11	11	11	11	11	-11	-11	-11	-11	-11

FIGURE 8 The measured raw signal of motor II electrical power (top), shear strain for the torque measurement (middle), and the rotational speed (bottom) [Colour figure can be viewed at wileyonlinelibrary.com]

application system, the friction loss is greater than motor II and will additionally increase the uncertainty in the calibration; therefore, the electrical measurement of motor II is preferred in the test and calibration process.

A test sequence of 10 steps is carried out with the motors run first in normal mode (test A), and later in reversed mode (test B). For each mode, the test is run in five different power levels. Motor II is taken as the reference, so that the electrical power of motor II is at a similar level in the corresponding steps of test A and test B. The test drive train rotates at the same speed, but in the opposite direction for the two modes. Detailed information about the test sequence is listed in Table 2. The values given in the table should be considered as the nominal. The actual values are controlled or tuned close to the nominal ones, and small discrepancies are allowed which deviate from the nominal values. Nevertheless, keeping the discrepancies as small as possible does help reduce the uncertainty in the calibration, especially the electrical power difference of motor II in mode A and mode B. Due to software limitations during the early phase of the commissioning, motor II is not run to 100 % of the rate power. The torque calibration is then calibrated in the range of 20 % to 85 % of the rated torque.

The raw data of the measured electrical power, the strain, and the rotational speed are shown in Figure 8, where the real time series of the complete test sequence are displayed. The segments corresponding to the test in mode A and mode B are highlighted in yellow in the figure. The system needs to come to a halt between the two operating modes because the drive train needs to change the direction of rotation. At the same time, the motor controllers also need to be reconfigured for the reversed operating mode. Although blank segments are seen in the signals of the electrical power and rotational speed, the test and the measurements are indeed carried out sequentially and continuously. Here, the speed signal is shown to provide a better indication of the operating condition, although the angle position instead of rotational speed is used in the calibration.

In Figure 8, the steps of different power levels can be clearly seen. For each step, the operation is kept on a stable state for at least 180 seconds, in order to have a stable measurement of sufficient length for the subsequent signal averaging. The power levels are marked on the plot of the electrical power. A positive electrical power stands for active power output (generator mode), while the negative power values indicate power input and that the machine is operating in motor mode. The motor speed stays at a very stable amplitude during both test A and test B. The rotating direction in test B can be seen to be opposite to the direction of test A. This ensures that the mechanical torque measured by the strain gauges is in the same direction for both test modes.

Before the torque calibration is possible, the k factor that describes the relationship between the power losses in the different operating modes as defined in Equation (2) must be estimated. In this test, the $\hat{k}$ factor is assumed to be 1.0 for all five test levels. Afterwards, the estimated $\tilde{X}$ and $\tilde{Y}$ can be obtained on each test level using the measured data as per Equation (12). From the same equation, it is possible to derive that $\tilde{X}$ has the

Power Level	I (20 %)	II (40 %)	III (60 %)	IV (75 %)	V (85 %)
$\tilde{X}$ (μm/m)	50.890	57.780	62.639	67.375	69.775
$\tilde{Y}$ (kN $\cdot$ m)	796.9	1836.4	2563.1	3282.2	3645.4

TABLE 3 Estimated $\tilde{X}$ and $\tilde{Y}$ on different test levels
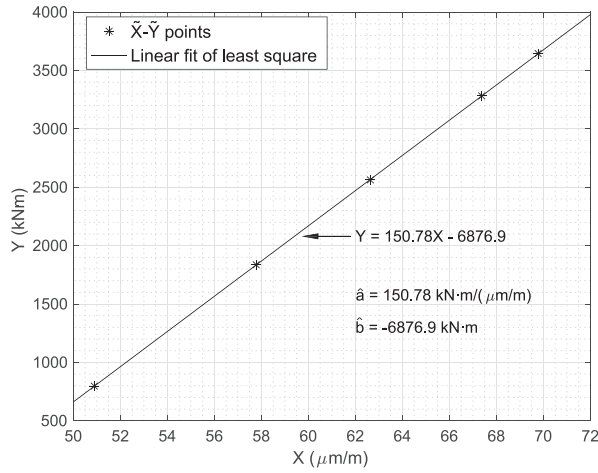
FIGURE 9 $\tilde{X}$ - $\tilde{Y}$ points and the linear fit with the least squares method

same unit as the raw measurement ε, a strain signal. The widely used unit micro-strain is adopted here as the unit of $\tilde{X}$ and expressed as $\mu m/m$ in accordance with the common practice in the industry. The $\tilde{Y}$ is the result of power divided by rotational speed and therefore has the dimension of torque. The unit $kN \cdot m$ is adopted here as the unit of $\tilde{Y}$. The values are listed in Table 3.

Each set of $\tilde{X}$ - $\tilde{Y}$ values in Table 3 can be plotted as one point in the X-Y plane. Five points corresponding to the five test levels can be drawn as shown in Figure 9. A linear fit of the five points is then possible. The slope and intercept of the line can be determined as $\hat{a} = 150.78\ kN \cdot m/(\mu m/m)$ and $\hat{b} = -6876.9\ kN \cdot m$, as per Equations (13) and (14). The calibrated torque measurement can be expressed as in Equation (24), with the unit of estimated torque $\hat{T}$ being $kN \cdot m$ and the unit of raw signal ε being $\mu m/m$.

$$\hat{T} = 150.78 \frac{kN \cdot m^2}{\mu m} \cdot \varepsilon - 6876.9\ kN \cdot m. \tag{24}$$

Unlike the conventional calibration methods that generate an accurate reference torque, the method described in this paper uses the electrical power as the reference and is based on the fact that the electrical power can be measured easily and with good accuracy. To present a better, visual explanation of the principle, the mean values of the mechanical, and electrical powers will be calculated and presented below. As the torque measurement is already calibrated and expressed in Equation (24), the average mechanical powers $\bar{\hat{P}}_{mech.A}$ and $\bar{\hat{P}}_{mech.B}$ on a certain test level can be expressed in Equation (25). The mean measured electrical powers $\bar{\hat{P}}_{elec.A}$ and $\bar{\hat{P}}_{elec.B}$ can easily be calculated in the normal way of averaging over the time domain.

$$\begin{cases} \bar{\hat{P}}_{mech.A} = \dfrac{\int_0^{\theta_A} \hat{T}d\theta}{t_A} \\[2ex] \bar{\hat{P}}_{mech.B} = \dfrac{\int_0^{\theta_B} \hat{T}d\theta}{t_B} \end{cases} \tag{25}$$

The mean mechanical and electrical powers $\bar{\hat{P}}_{mech.A}$, $\bar{\hat{P}}_{mech.B}$, $\bar{\hat{P}}_{elec.A}$, and $\bar{\hat{P}}_{elec.B}$ can be calculated for each of the five test levels listed in Table 3. For a better understanding, the values are plotted in Figure 10 together with level lines, similar to the procedure adopted in Figure 2. The plots for the five test levels are placed in turns along the horizontal axis according to the value of the nominal electrical power. The exact position along the horizontal axis is however not significant and therefore no grid or ticks are plotted on that axis. In contrast, the position along the vertical axis does have a concrete meaning and indicates the absolute value of test power.

From Figure 10, an equation linking the electrical power and the mechanical power can be obtained on each test level with the help of Equation (3). The calibration is therefore theoretically possible with two or more test levels. A potential improvement to the test process in this calibration can be seen in the figure. The electrical powers of motor II in the motor and generator modes can be tuned to be closer to each other, in order to have a lower uncertainty later on in the calibration. To achieve that, an on-line power analyser of the electrical measurement could be helpful.

5.3 | Uncertainty of the torque calibration

The uncertainty of the torque calibration comes mainly from the raw torque measurement, the electrical power, and the estimated k factor. Basic parameters used in the calculation are listed in Table 4. The notations of the error components are given in accordance with the definition in
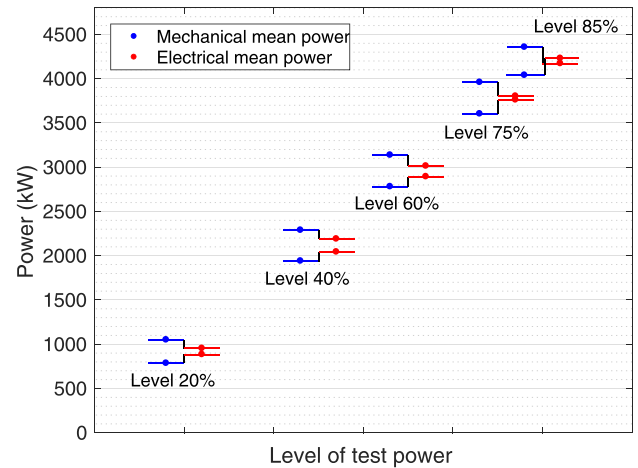
FIGURE 10 Mechanical mean power $\bar{\bar{P}}_{mech.A}$, $\bar{\bar{P}}_{mech.B}$ and electrical mean power $\bar{\bar{P}}_{elec.A}$, $\bar{\bar{P}}_{elec.B}$ of each test level displayed together [Colour figure can be viewed at wileyonlinelibrary.com]

TABLE 4 Basic uncertainty parameters related to the calibration

Uncertainty Component	Notation	Error Range	Standard Uncertainty u	Type
Sensitivity error of electrical power	c	$\pm 0.20\,\%$	$\pm 0.12\,\%$	Systematic
Offset error of electrical power	d	$\pm 3\,kW$	$\pm 1.73\,kW$	Systematic
Miscellaneous electrical power	Q	$\pm 2\,kW$	$\pm 1.15\,kW$	Random
Miscellaneous mechanical power	R	$\pm 8\,kW$	$\pm 4.62\,kW$	Random
Error of estimated $\hat{k}$ factor	δk	$\pm 20\,\%$	$\pm 11.55\,\%$	Systematic

TABLE 5 Standard uncertainty of $\tilde{X}$ and $\tilde{Y}$ at different torque levels

Standard Uncertainty	Unit	i=1	i=2	i=3	i=4	i=5
$\tilde{X}_i$ systematic	$\mu m/m$	0.0109	0.0144	0.0148	0.0148	0.0131
$\tilde{Y}_i$ systematic	$kN \cdot m$	1.8147	2.7568	3.4033	4.0856	4.4844
$- \tilde{Y}_i$ systematic due to c	$kN \cdot m$	0.9202	2.1205	2.9596	3.7899	4.2094
$- \tilde{Y}_i$ systematic due to d	$kN \cdot m$	1.5035	1.5035	1.5035	1.5035	1.5035
$- \tilde{Y}_i$ systematic due to δk	$kN \cdot m$	0.8623	1.8362	1.5007	0.5224	0.7227
$\tilde{X}_i$ random	$\mu m/m$	0	0	0	0	0
$\tilde{Y}_i$ random	$kN \cdot m$	0.8179	0.8179	0.8179	0.8179	0.8179

Section 3. All the uncertainty components shown in the table are assumed to obey the rectangular distribution[17] within the corresponding error range.

The electrical power measurement result from the three-phase voltage and current measurement, where high accuracy industrial sensors are used. The whole measurement chain is considered for the uncertainties of the voltage and current measurement channels, whereby the uncertainty of the sensors turns out not to play a major role. One of the important reasons is that the power factor of the motor is close to 1, which makes the otherwise very important phase error of the sensors less relevant to the overall power uncertainty. The miscellaneous errors of the electrical and mechanical powers Q and R are integrated over a period of time or angular rotation, as defined in Section 3. As mentioned in Section 5.2, the estimated factor $\hat{k}$ is adopted as 1 for all the five test levels. A uniform error of δk is also assumed for all the levels. Of course, both the estimated factor $\hat{k}$ and its error δk can be considered individually for each test level. Here, a uniform assumption is adopted for the sake of simplicity. As a result, a larger error range δk is also taken into consideration.

With the error parameters in Table 4 and according to the expressions for $\tilde{X}$ and $\tilde{Y}$ in Equations (9) and (10), the uncertainties of $\tilde{X}$ and $\tilde{Y}$ can be calculated as shown Table 5. The subscript i in the table denotes different test levels. The five levels from 20 % up to 85 % presented in Table 3 correspond to i being 1 to 5, respectively. In accordance with the discussion in Section 4.2, the systematic and random uncertainties are listed separately. Three contributions of the systematic uncertainty of $\tilde{Y}$ are also listed in the table. Note that the random uncertainties of $\tilde{X}$ are all zero, because the relevant uncertainties are attributed to the Y side, as shown in the definitions of the X and Y in Equations (9) and (10).

The correlation coefficient matrix **R** used in the calculation is presented in Table 6. The matrix **R** is defined in Section 4.2, and each of the entries represents the correlation coefficient between the corresponding standard systematic uncertainties. In Table 6, the corresponding standard systematic uncertainties are indexed in the first row and the first column. The values are taken with conservative considerations, and therefore, most of the entries are 1 or 0.

The estimated torque $\hat{T}$ is a function of the measured signal ε, with the estimated â and $\hat{b}$ as the sensitivity and offset parameters, shown in Equation (15). Therefore, the uncertainty of $\hat{T}$ comes from the uncertainties of â and $\hat{b}$, which are in turn dependent on the uncertainties of the $\tilde{X}$ and $\tilde{Y}$ values. Although by definition no uncertainty is attributed to the raw signal ε, it does exert an influence on the uncertainty of $\hat{T}$ by affecting and scaling the contribution of â. This influence is reflected in the partial derivatives of $\hat{T}$ with respect to $\tilde{X}$ and $\tilde{Y}$ in Equation (17). The partial derivatives have different values on different torque levels. An example is given in Table 7, where the measured raw signal ε equals 65 $\mu m/m$,

TABLE 6 The matrix of correlation coefficient R

	$\sigma_{\tilde{X}_1}$	$\sigma_{\tilde{X}_2}$	$\sigma_{\tilde{X}_3}$	$\sigma_{\tilde{X}_4}$	$\sigma_{\tilde{X}_5}$	$\sigma_{\tilde{Y}_1}$	$\sigma_{\tilde{Y}_2}$	$\sigma_{\tilde{Y}_3}$	$\sigma_{\tilde{Y}_4}$	$\sigma_{\tilde{Y}_5}$
$\sigma_{\tilde{X}_1}$	1	1	1	1	1	0	0	0	0	0
$\sigma_{\tilde{X}_2}$	1	1	1	1	1	0	0	0	0	0
$\sigma_{\tilde{X}_3}$	1	1	1	1	1	0	0	0	0	0
$\sigma_{\tilde{X}_4}$	1	1	1	1	1	0	0	0	0	0
$\sigma_{\tilde{X}_5}$	1	1	1	1	1	0	0	0	0	0
$\sigma_{\tilde{Y}_1}$	0	0	0	0	0	1	0.92	0.86	0.79	0.73
$\sigma_{\tilde{Y}_2}$	0	0	0	0	0	0.92	1	0.98	0.94	0.88
$\sigma_{\tilde{Y}_3}$	0	0	0	0	0	0.86	0.98	1	0.98	0.95
$\sigma_{\tilde{Y}_4}$	0	0	0	0	0	0.79	0.94	0.98	1	0.99
$\sigma_{\tilde{Y}_5}$	0	0	0	0	0	0.73	0.88	0.95	0.99	1

TABLE 7 Partial derivatives of $\hat{T}$ with respect to the $\tilde{X}_i$ and $\tilde{Y}_i$ when $\varepsilon = 65\ \mu m/m$

Partial Derivative	Unit	i = 1	i = 2	i = 3	i = 4	i = 5	Sum
$\partial\hat{T}/\partial\tilde{X}_i$	$kN \cdot m/(\mu m/m)$	−6.776	−21.679	−32.282	−42.449	−47.615	−150.80
$\partial\hat{T}/\partial\tilde{Y}_i$	$kN \cdot m/(kN \cdot m)$	0.0450	0.1439	0.2136	0.2816	0.3160	1

Note. The values in the table are dependent on the torque level.

TABLE 8 Torque uncertainty owing to the calibration on several torque levels

Torque Level, $kN \cdot m$	Standard Uncertainty $u_{T.cal}$, $kN \cdot m$	Expanded Uncertainty U_{95}, $kN \cdot m$	U_{95} Relative to the Torque Level, %
1000	10.59	21.17	2.12
2000	10.90	21.79	1.09
3000	11.43	22.87	0.77
3600	11.85	23.71	0.66

corresponding to around 2920 $kN \cdot m$ of torque. Note that the summation of all the partial derivatives w.r.t. $\tilde{X}$ in the table is roughly equal to the inverse of the sensitivity â, while the summation of the partial derivatives w.r.t. $\tilde{Y}$ is exactly 1.

For the entire uncertainty of $\hat{T}$, the component $r(t)$ in Equation (15) also plays a role. It can be considered to be the uncertainty related to the signal quality. Again, since this paper focuses on the calibration method, only the uncertainty due to the calibration process will be analysed here. As defined in Section 4.2, the standard uncertainty of (15) caused by the calibration is denoted as $u_{T.cal}$. The expanded uncertainty with the 95 % confidence level is twice the value of $u_{T.cal}$, and is denoted as U_{95}. The uncertainty results of $\hat{T}$ due to the calibration on several torque levels are given in Table 8, where $u_{T.cal}$, U_{95} as well as the percentage of the U_{95} relative to the nominal torque are also presented.

It is seen in Table 8 that the uncertainty stays at a relatively stable level as the torque level increases. This is partly due to the conservative assumption made in Table 6 for the correlation coefficients. As the uncertainties $\sigma_{\tilde{X}_i}$ and $\sigma_{\tilde{X}_k}$ are assumed to be well correlated, this also means the $\tilde{X}$-$\tilde{Y}$ points in Figure 9 deviate more collectively from the true positions. Other reasons are the constant components that are not dependent on the torque level, for example, the offset error of the electrical power. Considering the percentage of the uncertainty (U_{95}) in relation to the measured torque, 0.66 % is achieved near the calibration upper limit around 3600 $kN \cdot m$. At lower torque levels, the percentage of uncertainty will be higher. However, for the majority of the measuring range, an uncertainty of less than 2 % of the nominal torque is achieved.

6 | DISCUSSION

The calibration process described in this paper focuses on the measurement and behaviour on the turbine side. Both the electrical and mechanical powers input and output of the the turbine are measured. In fact, the method can also be realised on the measurements on the test bench side with the electrical power of the test bench being measured. The method actually requires only two electrical machines that can both run in motor and generator modes and also in different directions. In this sense, the calibration method can also be used in other industries and applications where a similar test layout can be realised. One advantage of focusing on the test bench is that the properties of this object are stable regardless if a different turbine is under test. The disadvantage is the potentially greater uncertainty due to the large friction torque on the test bench.

The method can be carried out on turbines with or without a gearbox. As the turbine changes its operating mode and rotational speed at the same time in the reversed test mode, the gear teeth inside the gearbox always mesh on the same side. This eliminates the concern that the gearbox should not run under load in the opposite direction because the teeth are manufactured differently on the two sides. Nevertheless, it is recommended to consult the gearbox supplier regarding potential problems and the efficiency difference in the two test modes.

To increase the calibration accuracy, efforts should be taken on the whole measurement chains of all electrical and mechanical raw measurements. For the electrical power, special attention should be paid to the time delay and hence the phase errors between the voltage and the current signals. For the torque measurement, the signal drift resulting from temperature change and creep has a direct impact on the calibration results. Furthermore, a proper time-synchronisation is imperative, in order to avoid time and phase shift between different signal channels.

For the test process, several efforts can be taken in the preparation and during the test. First, a preheating prior to the calibration test process is necessary in order to reach a relatively stable temperature and lubrication status for the whole drive train and the measurement system. Second, the ambient temperature should be kept as stable as possible during the whole test process, so that temperature changes in all systems are kept under control. Third, the electrical power input and output amplitudes should be kept as close to each other as possible. In the case shown in Figure 10, further improvement could be achieved by better controlling the electrical powers to be at the same level. Another effort is to try to have the power factor of the electrical machine as close to 1 as possible, which helps reduce the uncertainty in the electrical power.

The biggest contribution to the uncertainty for the calibration is in many cases the uncertainty in the assumed $\hat{k}$ factor. As the k factor cannot realistically be determined by a test, it must be chosen either with the help of detailed analysis of the drive train and the electrical machine or with an approximate assumption which results in a large uncertainty. Therefore, for a smaller uncertainty of the $\hat{k}$ factor, a detailed analysis of the power loss and the efficiency of the drive train is necessary.

7 | CONCLUSIONS

The proposed new calibration method takes advantage of the high accuracy of the electrical power measurement while at the same time it greatly reduces the uncertainty introduced by the power losses in the drive train. Based on the fact that the drive train tends to have a similar power loss in both motor and generator mode, the effect of the power loss can be largely compensated by carrying out the test in both the normal mode and in the reversed mode. With measured data from both test modes, an equilibrium can be drawn between the electrical and mechanical powers. The calibration can be carried out with the help of several such equilibriums on different torque levels.

No special instrumentation is needed for the method. All the sensors and equipment used in the calibration are produced in series and commercially available. The necessary test process can be carried out with the same mechanical layout as the normal test, which means that no additional structural reconfigurations or logistical effort is necessary. As a result, the calibration is low cost and time efficient. It can also be easily repeated whenever necessary.

One prerequisite of the calibration method is the ability of the test bench and the DUT (device under test) to run in reversed mode and operate in both directions up to the rated power. The calibration method is demonstrated on a torque measurement between two 5-MW driving motors of a nacelle test bench for the wind turbine, where both the calibration parameters and the accompanying uncertainties are determined. With conservative considerations, the uncertainty due to calibration is, in this case, within 0.7 % at upper limit of the calibration range. Better calibration accuracy can be achieved by reducing the electrical power uncertainty, improving the quality of the raw torque-measuring signal, and most importantly, by a better analysis of the drive train and therefore a smaller uncertainty in the k factor estimation.

ORCID

Hongkun Zhang https://orcid.org/0000-0001-5172-4867
Jan Wenske https://orcid.org/0000-0001-7035-1947
Mohsen Neshati https://orcid.org/0000-0001-6701-0666

REFERENCES

1. Schlegel C, Kahmann H, Kumme R. MN·m torque calibration for nacelle test benches using transfer standards. *ACTA IMEKO*. 2016;5(4):12-18.
2. DIN 51309:2005-12, Materials testing machines — Calibration of static torque measuring devices.
3. Kahmann H, Schlegel C, Kumme R, Röske D. Principle and design of a 5MNm torque standard machine. In: *IMEKO TC3, TC5 and TC22 International Conference 2017*; 2017.
4. Weidinger P, Foyer G, Kock S, Gnauert J, Kumme R. Development of a torque calibration procedure under rotation for nacelle test benches. *J Phys Conf Ser*. 2018;1037(5):052030–052039. https://doi.org/10.1088/1742-6596/1037/5/052030
5. Weidinger P, Schlegel C, Foyer G, Kumme R. *Characterisation of a 5 MN·m torque transducer by combining traditional calibration and finite element method simulations*. In: *AMA Conferences*; 2017.
6. Foyer G, Kock S. Measurement uncertainty evaluation of torque measurements in nacelle test benches. In: *23rd IMEKO TC3, 13th TC5 and 4th TC22: International Conference, TC3, TC5 and TC22 International Conference*; 2017.
7. Peschel D, Mauersberger D, Schwind D, Kolwinski U. The new 1.1 MNm torque standard machine of the PTB Braunschweig/Germany. In: *19th IMEKO TC3: TC3 International Conference on Force, Mass and Torque, TC3 International Conference on Force, Mass and Torque, Cairo, Egypt*; 2005:19-25.
8. Kock S, Jacobs G, Bosse D, Sharma A. Friction as a major uncertainty factor on torque measurement in wind turbine test benches. *J Phys Conf Ser*. 2018;1037(6):062001–062008. https://doi.org/10.1088/1742-6596/1037/6/062001
9. Averous NR, Stieneker M, Kock S, et al. Development of a 4 MW full-size wind-turbine test bench. In: *2015 IEEE 6th International Symposium on Power Electronics for Distributed Generation Systems (PEDG)*:1-8; 2015. https://doi.org/10.1109/PEDG.2015.7223108.
10. Zhang H, Neshati M. An effective method of determining the drive-train effciency of wind turbines with high accuracy. *J Phys Conf Ser*. 2018;1037(5):052013–052023. https://doi.org/10.1088/1742-6596/1037/5/052013
11. Zhang H, Eich N, Pilas M, Wenske J. Verfahren zum Ermitteln einer Effizienz und/oder zum Kalibrieren eines Drehmoments eines Antriebsstrangs, insbesondere einer Windenergieanlage. Patent DE102018203525 (in German); 2019.
12. Coleman HW, Steele WG. *Experimentation, validation, and uncertainty analysis for engineers*. 4th ed. Wiley; 2018.

13. Errors due to Wheatstone bridge nonlinearity. Tech Note TN-507-1: Vishay Precision Group; 2010. http://www.vishaypg.com/doc?11057.

14. Schäck MM. High-precision measurement of strain gauge transducers at the physical limit without any calibration interruptions. In: *IMEKO-TC3 International Conference*. Cape Town, South Africa; 2014.

15. Plane-shear measurement with strain gages. Tech Note TN-512-1: Vishay Precision Group; 2010. http://www.vishaypg.com/docs/11062/tn5121tn.pdf.

16. Zhang H, Ortiz de Luna R, Pilas M, Wenske J. A study of mechanical torque measurement on the wind turbine drive train — ways and feasibilities. *Wind Energy*. 2018;21(12):1406-1422. https://doi.org/10.1002/we.2263

17. Evaluation of measurement data — Guide to the expression of uncertainty in measurement (GUM 2008). JCGM - Joint Committee for Guides in Metrology; 2008.

18. *Web page DyNaLab, Nacelle Testing and Examination of Electrical Characteristics*. : Frauhofer IWES; https://www.iwes.fraunhofer.de/en/test-centers-and-measurements/nacelle%-testing-and-certification-of-electrical-characteristics. Accessed October 2018.

6   A New Method of Efficiency Determination

Chapter 6 presents a research paper which introduces a new method of efficiency determination for wind turbines. The paper was first presented at the conference "The Science of Making Torque from Wind" in Milan 2018 (**TORQUE 2018**), and was later published in Journal of Physics.

__H. Zhang__ and M. Neshati, "An effective method of determining the drive-train efficiency of wind turbines with high accuracy," Journal of Physics: Conference Series, vol. 1037, no. 5, p. 052013, 2018. https://doi.org/10.1088/1742-6596/1037/5/052013

The author of this dissertation (Zhang, Hongkun) has carried out the main work and has composed the paper. Mohsen Neshati supported the work by carrying out the tests that are analysed in the paper.

The paper deals with the problem that the drivetrain efficiency determination of a wind turbine is strongly dependent on the accuracy of the torque measurement. A method with special test process is developed in the study that makes it possible to notably improve the accuracy of the determined efficiency without the need to improve the accuracy of the torque measurement.

The method of efficiency determination presented in this paper is also part of the German patent DE102018203525B3 mentioned in Chapter 5.

An effective method of determining the drive-train efficiency of wind turbines with high accuracy

Hongkun Zhang, Mohsen Neshati

Fraunhofer IWES, Am Luneort 100, 27572 Bremerhaven, Germany

E-mail: `hongkun.zhang@iwes.fraunhofer.de, mohsen.neshati@iwes.fraunhofer.de`

Abstract. Measurement of efficiency under various load conditions is an important prerequisite for the validation of wind turbine drive train systems. Current measurement methods rely highly on the accuracy of the mechanical torque measurement, which is substantially limited by the high level of torque as well as the available calibration capacity. This paper proposes a new method of test and measurement procedures, aiming to substantially reduce the dependency of the efficiency accuracy on the torque and electrical power measurement. Instead of measuring the efficiency directly, the new method focuses on measuring the loss of power and in this way reduces the uncertainty of the determined efficiency. At rated power, an uncertainty lower than 0.5 % is considered as achievable. The efficiency uncertainty is analysed in detail in the paper with considerations of different sources of measurement uncertainties and their contributions. An example of the uncertainty calculation with typical parameters is presented as a demonstration. The study shows that the new method can effectively reduce the effect of the torque (as well as the electrical power) uncertainty on the overall uncertainty of the determined efficiency, and therefore achieve a better accuracy despite of the unfavourable accuracy of the torque and electrical power measurement. Finally, experimental tests have been performed on a scaled dynamometer test bench, where the efficiencies at different operation points are determined with the new method. The efficiency results as well as their uncertainties are presented in the paper.

1. Introduction

Drive train efficiency is a key property of a wind turbine. Since stochastic wind loads and varying environmental conditions are the basic operation conditions for the wind turbine, measuring the efficiency under various load cases and environmental conditions provides manufacturers with an comprehensive evaluation of the turbine's efficiency property. This knowledge forms the basis of a more targeted further development.

Drive train effciency is normally determined experimentally on test benches in a laboratory environment, where the drive train is driven up throughout the whole operation range upto rated power. More advanced test benches can apply loads in 6-DOF and emulate different load cases. One example of such test benches is the 10-MW dynamic nacelle test laboratory DyNaLab [1] of Fraunhofer IWES in Germany. For the measurement on the test bench, the input mechanical torque and electrical power output are necessary for the efficiency determination. However, accurate torque measurement is hindered by the multi-MN·m torque level and the limited calibration capacity of the high accuracy calibration machines. The currently largest calibration capacity is 1.1 MN·m, which is owned by the PTB [2]. Additionally, professional torque transducers with high level of torque measurement usually come together with high cost.

One alternative way is to use a partially calibrated part (e.g. the input shaft adapter) for the measurement, instead of a fully calibrated transducer. For doing that, a calibrated torque transducer can be used as reference, to calibrate the shaft adapter between the test bench and the turbine drive train. It is of course also possible to calibrate the shaft adapter directly under a professional calibration machine. The shaft adapter can be calibrated to the capacity of the reference transducer or the calibration machine. The behaviour beyond the calibration range has to be obtained via extrapolation. With professional handling and favourable conditions, the method does deliver a good measurement accuracy [3, 4]. However, the cost and reliability can be big problems especially for the common application in the industry. The calibration has to be carried out to a torque level as high as possible and needs to be repeated regularly. Furthermore, since the shaft adapter is not a designed transducer, the professional instrumentation and compensation procedures are difficult to be guaranteed, for example the compensation against temperature change and creep, the protection against humidity and so on.

Another alternative avoids the need of toque measurement, using two identical drive trains running in a back-to-back setup. One of the drive trains operates in motor mode and the other in generator mode. In this case, the total power loss (of the whole setup) can be measured through the input and output electrical power difference on both sides. This method is also outlined in the IEC 60034 standard [5]. However, there are some limitations with this method. First, due to power losses along the drive train, the turbine in generator mode operates at a lower power level than the turbine in motor mode. The electrical output power can be, depending on the turbine efficiency, over 10 %. This means the electrical machines from both sides have different operation points. Furthermore, there may also be behaviour discrepancies between the two individual drive trains. These facts lead to an increase of uncertainty in the determination of the power loss from each drive train. Second, the assembling and instrumentation of the test have to be designed for every different type of wind turbine and it would be difficult to apply additional loads (e.g. the bending moment) to the turbine drive train in order to study the influences of parasitic loads on the efficiency.

2. New Method of Efficiency Determination
On a nacelle test bench, the turbine drive train can be run in a number of designed test scenarios, with various load cases, specific control and system configurations and on different operational points. Turbine behaviours in different scenarios can be thoroughly studied through a series of tests.

The uncertainty of the drive train efficiency is a combination of the uncertainties from both mechanical torque and electrical power measurement. The efficiency determination has a very high requirement on the measurement accuracy. An uncertainty of for example 2 % would very likely make the determination meaningless for the designer when the efficiency is about 95 %. For a test bench similar as DyNaLab, the shaft adapters have to be designed capable of withstanding large bending moments (up to 20 MN·m). This makes an accurate torque measurement even more difficult.

The new method presented in this paper aims to solve this problem and determine the efficiency with sufficient accuracy. The method is all based on the currently available torque and power measurement techniques. A preliminary analysis within the scope of this paper shows that at rated power, an uncertainty less than 1 % is expected. With more accurate instruments and detailed analysis of the components, an uncertainty lower than 0.5 % is also considered as achievable.

Instead of relying on the absolute measured torque and power values, the new method focuses on the changes of the measured values. In fact, the percentage of power loss is measured first and the efficiency is calculated as a result. The torque change is measured between two different tests with opposite transmission directions. Since the power loss is much smaller than the transmission

power, the influence of the absolute measurement uncertainties are essentially reduced.

2.1. Test configuration and the major assumption

Two tests with opposite power transmission directions are needed for this method:

- Test A (normal mode). The turbine drive train works in normal generator mode at a certain operating point (speed, power, etc.) where the efficiency needs to be determined. The test bench also runs in the normal mode and drives the turbine drive train. Torque measurement is instrumented on the shaft adapter between the test bench and the drive train; the electrical measurement is carried out between the generator and the power converter. The transmission direction and power losses are shown in the upper part of Figure 1. A warm up running of the whole test setup should be carried out in advance of the test.

- Test B (reversed mode). The turbine drive train works in motor mode and drives the test bench, while the test bench works as a generator. The operating point of the turbine is tuned to be as close to test A as possible, which means the same electrical power, the same rotating speed (but with opposite direction) and similar control parameters. The reason for the opposite rotating direction is to have the same direction of mechanical torque. The bearing and generator temperatures should be monitored and kept to be similar to test A. The mechanical and electrical measurements are carried out at the same positions as in Test A. The transmission direction and power losses in case of test B are shown in the lower part of Figure 1.
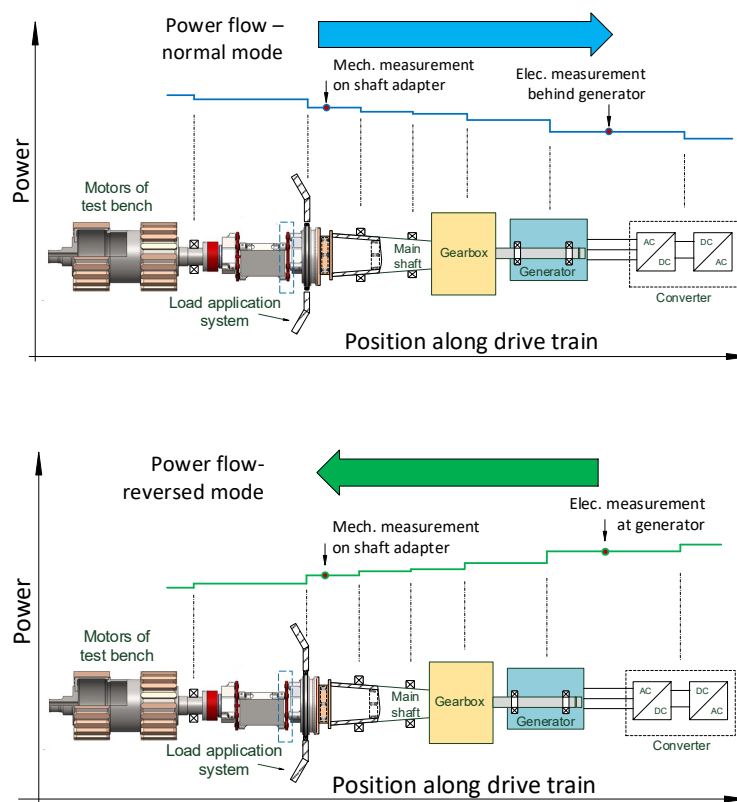

Figure 1. Drive train power loss in normal mode (upper) and reversed mode (lower).

An important foundation of the method is that the relation of drive train losses in test A and test B are known or can be assumed at the price of introducing additional Uncertainty. A simple assumption would be that the total power loss is equally shared by the two tests. The major power losses in the turbine drive train are related to the bearings, the generator and the gearbox when available. The bearing friction depends mainly on external loads, rotating speed, temperature and the lubrication condition. For test A and B, all these conditions are the same or similar. The change of rotating direction might have some effect on the lubrication condition, but the overall impact to the friction is very limited. Electrical machines generally have a good consistency of efficiency between generator and motor mode. The power loss within the gearbox comes mainly from the friction of bearings, the meshing of teeth and the viscosity of the lubricant. Because both the rotating direction and the power transmission direction change in test B, the gear teeth still contact on the same side as in test A. However, depending on the individual gearbox structure and lubrication design, there might be some efficiency difference on the gearbox and this needs to be individually considered in the uncertainty calculation.

2.2. Processing and calculation

The mean values from measurement of both mechanical and electrical powers are used for calculating the efficiency. The power loss diagrams of both tests shown individually in Figure 1 are illustrated together in Figure 2. $\bar{P}_{mech.A}$, $\bar{P}_{elec.A}$ denote the mean mechanical and electrical powers in test A, while similarly $\bar{P}_{mech.B}$, $\bar{P}_{elec.B}$ describe the mean powers in test B.
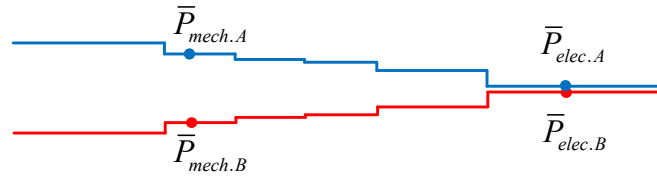

Figure 2. Mean value of mechanical and electrical power in test A and test B

The mean value of electrical power can be easily obtained with averaging in the time domain. For the case of mechanical power, it is easier and more accurate to integrate the measured torque signal first in the angle domain to get the mechanical energy first, before obtaining the mean value over the corresponding time period, as demonstrated in Equation (1) and (2).

$$\bar{P}_{mech.A} = \frac{E_{mech.A}}{t_A} = \frac{\int_0^{\theta_A} T d\theta}{t_A} \tag{1}$$

$$\bar{P}_{mech.B} = \frac{E_{mech.B}}{t_B} = \frac{\int_0^{\theta_B} T d\theta}{t_B} \tag{2}$$

where, $E_{mech.A}$ and $E_{mech.B}$ denote the mechanical energy of test A and test B, integrated over θ_A and θ_B in the angle domain respectively. T is the mechanical torque, while t_A and t_B stand for the corresponding time periods.

The total power loss of the two tests (in the mean value perspective) can be expressed as Equation (3). It's composed of the mechanical and electrical power changes between test A and test B. The accuracy of the total power loss is therefore not depended on the absolute uncertainty of every single torque or power measurement, but on the uncertainties of the torque and power differences. This is also the main reason of the uncertainty reduction in this method.

It is actually the power loss that is being measured, rather than the efficiency itself. As it is not possible to control the electrical power in test B to be exactly the same as in test A, the equation still contains electrical power terms.

$$\bar{P}_{Loss.total} = \bar{P}_{mech.A} - \bar{P}_{mech.B} + \bar{P}_{elec.B} - \bar{P}_{elec.A} \tag{3}$$

In order to determine the efficiency of the drive train in each operating mode, the total power loss needs to be divided into components contributed by test A and test B. As a general case, the proportion of power loss in test A out of the whole power loss is defined as k_A, thus $\bar{P}_{Loss.A}$ can be expressed as in Equation (4). The efficiency of the drive train in normal operating mode can be then obtained following Equation (5).

$$\bar{P}_{Loss.A} = k_A \bar{P}_{Loss.total} \tag{4}$$

$$\eta = \frac{\bar{P}_{elec.A}}{\bar{P}_{mech.A}} = \frac{\bar{P}_{elec.A}}{\bar{P}_{elec.A} + \bar{P}_{Loss.A}} = \frac{\bar{P}_{elec.A}}{\bar{P}_{elec.A} + k_A \bar{P}_{Loss.total}} \tag{5}$$

3. Uncertainty consideration

The efficiency of test A as expressed in Equation (5) is determined by the electrical power measurement $\bar{P}_{elec.A}$, the total power loss $\bar{P}_{Loss.total}$ and the proportion factor k_A. Therefore, the uncertainty of the efficiency is depending on the uncertainties of these three variables.

$\bar{P}_{Loss.total}$ is calculated from the mechanical and electrical powers as expressed in Equation (3), where the mechanical powers are in turn functions of torque and angle position and the time stamp of the measurement, as expressed in Equation (1) and (2). Because of the high accuracy of the angle position (from incremental or absolute encoder) and the time stamp, the corresponding uncertainties are considered to be zero. Therefore the uncertainty of $\bar{P}_{Loss.total}$ is contributed by torque and electrical power measurement. Taking the measurement errors into consideration, the measured torque and electrical power can be expressed as Equation (6).

$$\begin{cases} \tilde{T} = aT + b + r(t) \\ \tilde{P}_{elec} = cP_{elec} + d + q(t) \end{cases} \tag{6}$$

where, $\tilde{T}$ and $\tilde{P}_{elec}$ are the measured values of torque and electrical power, while T and P_{elec} are the true values. A number of parameters are introduced here to describe the sources of measurement errors:

- a and c are the sensitivity errors of corresponding measurements. Sensitivity error is also known as gain error or slope error.
- b and d are the offset errors.
- $r(t)$ and $q(t)$ represent the summation of miscellaneous errors, including the linearity, the hysteresis and repeatability errors. As a result, they are time dependent.

The sensitivity and offset errors defined above are considered to be constant. Additional sensitivity change and offset drift due to environment change (temperature, humidity, etc.) are accounted in the miscellaneous items $r(t)$ and $q(t)$.

The mean value of the calculated mechanical powers in the two tests, namely $\bar{\tilde{P}}_{mech.A}$ and $\bar{\tilde{P}}_{mech.B}$, can be expressed as in Equation (7). Similarly, the mean value of measured electrical

power $\bar{\tilde{P}}_{elec.A}$ and $\bar{\tilde{P}}_{elec.B}$ are expressed in Equation (8).

$$
\begin{cases}
\bar{\tilde{P}}_{mech.A} = \left[\int_0^{\theta_A} (aT + b + r(t))d\theta \right] / t_A = a\bar{P}_{mech.A} + b\bar{\omega}_A + R_A \\
\bar{\tilde{P}}_{mech.B} = \left[\int_0^{\theta_B} (aT + b + r(t))d\theta \right] / t_B = a\bar{P}_{mech.B} + b\bar{\omega}_B + R_B
\end{cases}
\tag{7}
$$

where, $\bar{P}_{mech.A}$ and $\bar{P}_{mech.B}$ are the true mean values of the mechanical power. $\bar{\omega}_A$ and $\bar{\omega}_A$ are the mean speed of test A and test B, while R_A and R_B are the power errors caused by $r(t)$ in the two tests.

$$
\begin{cases}
\bar{\tilde{P}}_{elec.A} = \left[\int_0^{t_A} (cP_{elec} + d + q(t))dt \right] / t_A = c\bar{P}_{elec.A} + d + Q_A \\
\bar{\tilde{P}}_{elec.B} = \left[\int_0^{t_B} (cP_{elec} + d + q(t))dt \right] / t_B = c\bar{P}_{elec.B} + d + Q_B
\end{cases}
\tag{8}
$$

where, $\bar{P}_{elec.A}$ and $\bar{P}_{elec.B}$ are the true mean values of the electrical power. Q_A and Q_B represent the power errors caused by $q(t)$ in the two tests.

The measured total power loss $\bar{\tilde{P}}_{Loss.total}$ can be expressed therefore as in Equation (9), which shows that the sensitivity errors a and c apply only on the restrained mechanical and electrical power differences. The offset error of the mechanical measurement is multiplied by the small speed difference, while the offset error of the electrical measurement is balanced out. The miscellaneous errors, on the contrary, can barely be reduced and as a result apply important influences on the uncertainty of $\bar{\tilde{P}}_{Loss.total}$.

$$
\begin{aligned}
\bar{\tilde{P}}_{Loss.total} = {}& a\left(\bar{P}_{mech.A} - \bar{P}_{mech.B}\right) + b\left(\bar{\omega}_A - \bar{\omega}_B\right) + R_A - R_B \\
& + c\left(\bar{P}_{elec.A} - \bar{P}_{elec.B}\right) + Q_A - Q_B
\end{aligned}
\tag{9}
$$

To derive the power loss of each test from $\bar{\tilde{P}}_{Loss.total}$, a proportion factor k_A is introduced in Section 2.2. The value of k_A should be around 0.5, which means test A and B have the sameamount of power loss. In the calculation, a concrete k_A value has to be assumed and the error of this assumption, namely the difference between the assumed value k_A and the real proportion, can be defined as k'_A. Correspondingly, the assumed power loss in test A, considering the error of the assumption, can be expressed as in Equation (10). In further calculations of this paper, k_A is assumed to be 0.5.

$$
\bar{\tilde{P}}_{Loss.A} = (k_A + k'_A)\bar{\tilde{P}}_{Loss.total}
\tag{10}
$$

where, k_A is the assumed proportion value and k'_A is the error of assumption.

The uncertainty of the efficiency is determined by the uncertainty of power loss as well as the uncertainty of the electrical power measurement together, as shown in Equation (5). In order to demonstrate the uncertainty calculation, an example is given here, where typical parameters of the wind turbine and conservative measurement uncertainties are adopted. Details of the parameters are listed in Table 1. The standard uncertainty of each error source is calculated based on uniform distribution within the error range. Uncertainty calculations in the paper are carried out in accordance with the GUM guide line [6].

For the uncertainty calculation of $\bar{\tilde{P}}_{Loss.total}$, all components in Equation (9) are listed and analysed in Table 2. For the purpose of demonstration, an efficiency of 95 % is assumed. The corresponding power loss can be determined in Equation (11). As mentioned in Section 2.1,

Table 1. Adopted parameters and corresponding standard uncertainty calculation

Adopted parameters	Value	Standard uncertainty u
Rated power	5 MW	-
Rated rotor speed	9.5 rpm	-
Rated torque	∼5000 kN·m	-
Efficiency (rated power)	∼95 %	-
Sensitivity error of torque measurement a (of reading)	±5 %	$u_a = 2.89$ %
Offset error of torque measurement b	±50 kN·m	$u_b = 28.87$ kN·m
Miscellaneous errors of torque measurement r	±15 kN·m	$u_r = 8.66$ kN·m
Sensitivity error of electrical power c (of reading)	±2.0 %	$u_c = 1.15$ %
Offset error of electrical power d	∼0	$u_d = 0$
Miscellaneous errors of electrical power q	±10 kW	$u_q = 5.78$ kW
Error of power loss distribution assumption $k_A^{'}$	±5 %	$u_{k_A} = 2.89$ %

the electrical power of the turbine in test B is kept as close as possible to the power in test A. But since the powers cannot be controlled to be exactly the same, a 0.5 % difference of electrical power (25 kW) is adopted. As a result, Equation (11) can be split into the electrical and mechanical parts, expressed in Equation (12). The difference of mean rotating speed in the two tests can be easily measured and calculated. Here, a difference of 1 % is considered to be conservative, as expressed in Equation (13).

$$\bar{P}_{Loss.total} = \bar{P}_{mech.A} - \bar{P}_{mech.B} + \bar{P}_{elec.B} - \bar{P}_{elec.A} \approx 2 \times 5000 \times 5\ \% = 500\ \text{kW} \qquad (11)$$

$$\begin{cases} \bar{P}_{mech.A} - \bar{P}_{mech.B} = 475\ \text{kW} \\ \bar{P}_{elec.B} - \bar{P}_{elec.A} = 25\ \text{kW} \end{cases} \qquad (12)$$

$$\bar{\omega}_A - \bar{\omega}_B = 0.011\ \text{rad/s} \qquad (13)$$

Table 2. Standard uncertainty of the measured total power loss

Uncertainty components	Calculation of uncertainty	Standard uncertainty/kW
$a\left(\bar{P}_{mech.A} - \bar{P}_{mech.B}\right)$	$475u_a$	13.73
$c\left(\bar{P}_{elec.A} - \bar{P}_{elec.B}\right)$	$25u_c$	0.29
$b\left(\bar{\omega}_A - \bar{\omega}_B\right)$	$0.011u_b$	0.32
R_A	$u_r\bar{\omega}_A$	9.07
R_B	$u_r\bar{\omega}_B$	9.07
Q_A	u_q	5.78
Q_B	u_q	5.78
	Resultant $u_{Loss.total} = 20.50$ kW	

The results in Table 2 show that, the uncertainty components caused by the sensitivity and offset errors are dramatically reduced and as a result, the other sources of error (referred as "miscellaneous errors" in Table 1) become very important. In fact, the most important benefit of the presented solution is to sharply reduce the influence of the sensitivity and offset errors

of the measurement. This has a great meaning especially for the torque measurement without professional calibration. For the other errors in the measurement however, this method has limited improvement.

The standard uncertainty of the mean measured electrical power in test A is calculated in Equation (14).

$$u_{elec.A} = \sqrt{(5000 \times 1.15~\%)^2 + 10^2} = 58.37~\text{kW} \tag{14}$$

$$\eta = \frac{\bar{P}_{elec.A}}{\bar{P}_{elec.A} + k_A \bar{P}_{Loss.total}} \tag{15}$$

The efficiency calculation Equation (5) can be expressed as a function of $\bar{P}_{Loss.total}$, k_A and $\bar{P}_{elec.A}$ in Equation (15). With the uncertainties of all the three variables already known, the uncertainty of the efficiency can be determined in Table 3 as $U = 0.66~\%$, with the level of confidence at about 95 % (coverage factor of 2). It is worth pointing out that, the variables $\bar{P}_{elec.A}$ and $\bar{P}_{Loss.total}$ are not independent and according to the GUM guideline, the cross term between these two variables needs to be considered. However, because the covariance of them are equivalent to the covariance between $\bar{P}_{elec.A}$ and $\bar{P}_{elec.B} - \bar{P}_{elec.A}$, the contribution of the cross term to the overall uncertainty is very small or even negative. Therefore, for simplicity and conservative reasons, the variables in Table 3 are considered to be independent from each other.

Table 3. Uncertainty calculation of the efficiency

Variable	Standard uncertainty	Partial derivative	Uncertainty contribution
$\bar{P}_{elec.A}$	58.37	9.07E-06	0.053 %
$\bar{P}_{Loss.total}$	20.50	9.07E-05	0.158 %
k_A	2.89 %	0.0907	0.263 %

Resultant standard uncertainty $u = 0.33~\%$

Expanded uncertainty $U = 0.66~\%$, with coverage factor 2.

Table 3 shows that the largest contribution of the efficiency uncertainty comes from the k_A factor, which denotes the proportion of the power loss of test A in the total power loss. This is also the reason why the electrical power, instead of the mechanical torque of test B, is kept as close as possible to test A. Because in this way the electrical machine of the turbine will have the most similar power loss. In this paper, the error range of k_A are conservatively assumed as $\pm 5~\%$. In case of $k_A = 0.5$ (the losses of test A and B are the same), this assumption implies a difference of roughly $\pm 10~\%$ between the power losses. In case of better knowledge of the turbine and therefore a smaller uncertainty of k_A, better accuracy of the efficiency calculation can be achieved. Thanks to the new test solution presented in this paper, the uncertainty of the total power loss only plays a secondary role in the overall efficiency uncertainty in this case.

4. Test on a scaled test bench

As an example of the proposed test and measurement method, experimental tests are performed on a 50 kW laboratory dynamometer test bench described in [7]. Figure 3 shows a picture as well as the schematic diagram of the test bench. Three electrical machines are available in the drive train, denoted as machine 1, 2 and 3 in the figure. Machine 1 and 2 emulate the tandem drive motors of a turbine test bench and operate always in the same mode (either motor or

generator mode). Machine 3 emulates the turbine drive train under test, and works as a counter part of the other two machines. A mechanical torque measurement is located between machine 2 and 3. Electrical power measurement on machine 3 is used for the efficiency calculation.
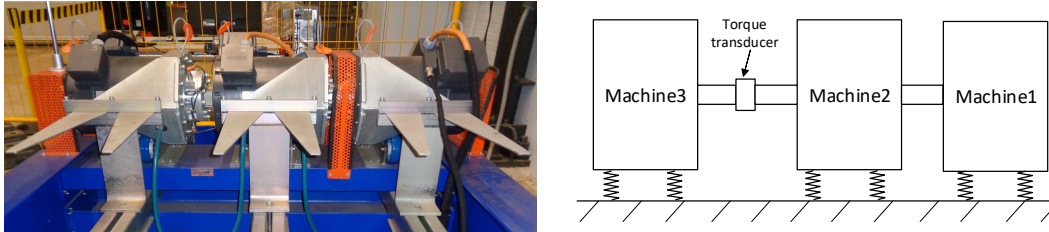

Figure 3. The 50kW small dynamometer test bench used in the tests

Two tests are carried out for measuring the efficiency of machine 3. In accordance with the test process in Section 2.2, machine 3 runs during test A in generator mode, and afterwards during test B in motor mode. In each test, three different load levels (level I, II and III) are reached and stayed on for about 3 minutes each. The load steps are shown in Table 4. On each load level, the demanded torque of machine 3 is set to be the same between the two tests. The rotating speed is controlled constant through out the tests, while the drive train rotates in opposite directions between test A and B. The opposite rotating speed ensures that the direction of mechanical torque stays the same and therefore the torque signal experiences a small change.

Table 4. Test process of the normal and reversed modes

Test	Load step	Speed/rpm	Demanded torque of machine 3 /N·m	Mode of machine 3
A (Normal mode)	StepA.I	200	-50	generator
	StepA.II	200	-150	generator
	StepA.III	200	-300	generator
B (Reversed mode)	StepB.I	-200	-50	motor
	StepB.II	-200	-150	motor
	StepB.III	-200	-300	motor

Measured results of both electrical and mechanical powers from the two tests are shown in Figure 4. The mechanical power is calculated as the measured mechanical torque multiplied by the rotational speed, while the electrical power is given by the measurement in the electrical converter. Corresponding uncertainties are considered according to the sensor data sheets and assumptions. Both the torque and the electrical power measurement here have a large uncertainty of over 3 %. The efficiency determined by the conventional method (with output power divided by input power) makes no sense, as it may even give an efficiency over 100 %. However, because most of the uncertainty is contributed by the sensitivity and offset errors of the measurement, the new method can give a much smaller uncertainty and therefore also meaningful efficiency values, as shown in Table 5.

It can be observed from Figure 4 that the electrical power remains roughly the same in both modes, while the mechanical power experiences a clear amplitude change. Here the mechanical power change is a result of the power loss of machine 3 in the two tests. Assuming that the
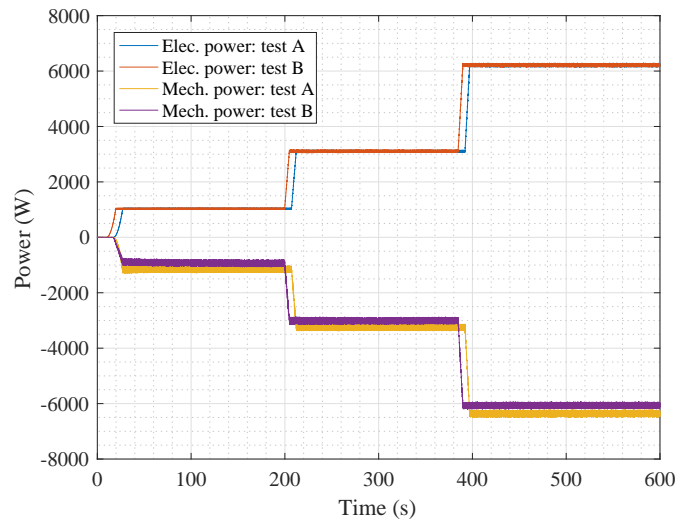
Figure 4. Results of the mechanical and electrical power in both test modes. Electrical powers are displayed as positive and mechanical powers displayed as negative.

losses in the two tests are identical, the efficiency at each load level can be calculated in Table 5. As mentioned above in the paper, how to divide the total power loss into each individual test can be decided according to analysis and experience. A proper uncertainty has to be considered according to the corresponding assumption.

Table 5. Efficiency calculation of machine 3

Quantity	Unit	Level I	Level II	Level III
Mechanical power difference, $\bar{\bar{P}}_{mech.A} - \bar{\bar{P}}_{mech.B}$	W	232.30	241.45	291.01
Electrical power difference, $\bar{\bar{P}}_{elec.A} - \bar{\bar{P}}_{elec.B}$	W	0.03	-0.10	-0.33
Total power loss, $\bar{\bar{P}}_{Loss.total}$	W	232.27	241.55	291.34
Power loss in test A, $\bar{\bar{P}}_{Loss.A}$	W	116.14	120.78	145.67
Electrical power of machine 3, $\bar{\bar{P}}_{elec.A}$	W	1035.5	3108.1	6217.2
Efficiency η	-	89.9 %	96.3 %	97.7 %
Uncertainty U, with coverage factor 2	-	1.45 %	0.57 %	0.33 %

An important feature of the proposed solution can be recognised in Table 5, that the efficiency uncertainty decreases very evidently while the efficiency goes higher. This comes mainly from the uncertainty consideration of the k_A factor and makes sense because higher accuracy is more important for the high efficiencies.

5. Conclusion

A new test and measurement method has been proposed for efficiency determination of the wind turbine drive trains without the requirement on the high accurate torque and electrical power measurements. The uncertainty of the determined efficiency at rated power is expected be lower than 1 %, while further reduction to below 0.5 % is also considered as possible. The method determines the power losses in the tests that based on the changes of the

torque and electrical power measurements, and therefore dramatically reduces the importance of their accuracy. Detailed test and calculation procedures are presented in the paper for the efficiency determination. Uncertainty analysis shows that the influence caused by the sensitivity and offset errors of the measurements can be dramatically reduced. An example with typical and conservative parameters are presented in the paper, demonstrating the uncertainty consideration. The method is tried out on a scaled test bench with the tests run in three different power levels. Efficiency of the studied machine is determined on each of the levels, while the corresponding efficiency is also given. Overall, the proposed method provides a way of efficiency determination for wind turbine drive trains. The method is expected to sharply reduce the uncertainty of the determined efficiency compared to the conventional method, while still based on the conventional measurement techniques that are commonly used in the industry.

Reference

[1] Pilas M. and Riezu M., 2017, Functional prototype testing of an 8 MW wind turbine, German Wind Energy Conference DEWEK 2017, Bremen.
[2] Schlegel C., Kahmann H. and Kumme R., 2016, MN·m torque calibration for nacelle test benches using transfer standards, ACTA IMEKO, 12-18.
[3] Kock S., Jacobs G., Bosse D. and Weidinger P., 2017, Torque measurement uncertainty in multi-MW nacelle test benches, Conference for Wind Power Drives 2017.
[4] Weidinger P., Schlegel C., Foyer G. and Kumme R., 2017, Characterisation of a 5 MN·m torque transducer by combining traditional calibration and finite element method simulations, AMA Conferences 2017.
[5] 2010 IEC 60034-2 rotating electrical machines - Part 2-1: Standard methods for determining losses and efficiency from tests.
[6] Committee Guides Metrology J, 2008, Evaluation of measurement data, Guide to the Expression of Uncertainty in Measurement (GUM 2008), vol. 100.
[7] Neshati M., Curioni G., Karimi H. R. and Wenske J., 2017, H-∞ drive train control for hardware-in-the-loop simulation with a scaled dynamometer test bench, 43rd Annual Conference of the IEEE Industrial Electronics Society (IECON), 8578-8583.

7 Conclusions

7.1 Summary

This dissertation has proposed and evaluated solutions to a number of challenges faced by applications of the torque measurement in wind turbine drivetrains. Technical improvement and new methods are developed in torque measurement and calibration, as well as in the efficiency determination of a wind turbine drivetrain.

Addressing the missing of practical long-term torque measurement method for operating wind turbines, the research proposed a new measurement method based on the signal of rotary encoders. The utilises the angular deformation in a drivetrain caused by the torque. The deformation can be determined by the angular signals from two encoders at different positions along the drivetrain. As an example, one encoder locates on main shaft and the other one on the generator. Since the encoder on the generator is commonly already available in a modern wind turbine for speed measurement, only one encoder normally needs to be additionally installed. Because the signal of the encoder comes from the stationary part, the data acquisition is not dependent on a slip ring or telemetry system. Since the encoders are normally designed to have a long life, the method is a good candidate for long-term torque measurement in the wind turbine. The method was implemented and compared with the classical strain gauge-based torque measurement during a test campaign of the AD-8 wind turbine on the nacelle test bench DyNaLab. The results show that the encoders are capable of capturing the angular deformation caused by the torque with good resolution. Compared with the traditional measurement with strain gauges, the measurement with encoders is considerably less sensitive to the influence of the non-torque loads in the drivetrain. However, the method requires a relatively long and soft drivetrain to produce enough angular deformation and hence sufficient measurement resolution. This makes the application in a direct-drive turbine very difficult, where the drive train is normally short and stiff. Additionally, depending on the materials of the components between the encoders, the measurement may exhibit a certain level of non-linear behaviour in response to the torque; and the measurement may need regular re-calibration due to the signal drift of the angular deformation. Nevertheless, for many applications of the operating wind turbine, the accuracy of the torque measurement is not of crucial importance. In this case, small non-linear behaviour in the torque measurement can either be charted and compensated or be tolerated, while the re-calibration can be carried out during the normal operation with the electrical power.

Although strain gauges are not considered suitable for long-term measurement on operating wind turbines, they are the most frequently adopted method in other applications. Therefore, it is also important to investigate and make improvement in this method. One problem with the method is the considerable influence of non-torque loads on the torque signal. This research studied this effect and looked for a practical method of compensation. During the afore-mentioned AD-8 nacelle test campaign, several channels of torque measurement from different types of strain gauge circuits have been instrumented at a number of positions on the shaft. The post-processing have confirmed large influence of the non-torque loads on all the instrumented torque measurement channels. The results show that the signal influence oscillates along with the shaft rotation in all channels of torque measurement, but the phase of the influence in each channel is dependent on the specific angular positions along the shaft circumference where the strain gauges are installed. It have been found the non-torque loads component cannot be totally compensated in the torque measurement with the regular two-position strain gauge full bridge, as commonly adopted in applications on a wind turbine. Based on the results of the test campaign, the research has drawn attention to the fact that torque measurement should be instrumented with more strain gauges distributed along the shaft circumference, in order that the influence of non-torque loads can be better compensated.

In response to the demand for regular re-calibration of the torque measurement on a nacelle test bench, the research developed a new calibration method that is based on the conservation of energy in the wind turbine drivetrain. Theoretically, the input torque of the wind turbine can be obtained by dividing the mechanical input power by the rotational speed, whereby the input power is often determined from the electrical output power together with the estimated power loss in the drivetrain. To reduce the calibration uncertainty introduced by the power loss estimation, the new method proposed utilises a sequence of designed tests, where the drivetrain first operates in normal generator mode and then reversed in motor mode in the opposite rotational direction. A relationship between the torque and the electrical power measurements can be established by combining the measurements in the two test modes. In this way, the power loss plays only a secondary role in the calibration, and the calibration uncertainty due to the unknown power loss can be greatly reduced. A comprehensive uncertainty analysis for the torque calibration has been carried out in the research. Two major uncertainty sources are identified for the calibration. The first one is the uncertainty in the electrical power measurement, which acts as the reference for the calibration; the second one is the uncertainty in the ratio estimation between the power losses in the normal and reversed operating modes. The calibration method proposed has been realised in a back-to-back test campaign of the two motors of the DyNaLab nacelle test bench, where the calibration uncertainty was determined at 95 % confidence level to be within 1 % around the rated torque. In general, the

method proposed allows the torque calibration to be carried out on a nacelle test bench with much higher accuracy without a great deal of additional reconfiguration or instrumentation. With the method, the calibration can also be repeated regularly with manageable effort. One important prerequisite for applying the method is that the DUT can operate in both generator mode and motor mode. To ensure this, it may be necessary to adapt specific software and control strategy of the turbine.

The efficiency of the DUT can be determined as a by-product of the test sequence for the torque calibration. In fact, the sequence was originally developed aiming for the efficiency determination while the possibility of using it for the torque calibration was discovered and developed during the research afterwards. Nevertheless, in cases where the torque measurement is not calibrated in advance, the task of torque calibration does indeed need to be carried out prior to the efficiency determination. The method proposed utilises the same test sequence as described above for the torque calibration. The total power loss of the DUT in both generator mode and motor mode can be determined and expressed at the end as a function of the torque difference in the two operating modes. The uncertainty in the absolute torque values is in this way greatly constrained into a much smaller range of the torque difference. The efficiency can be then determined by combining the power loss and the electrical power measurement. Moreover, because the electrical power measurement is only present in the denominator of the efficiency expression, it exerts thus less influence on the efficiency uncertainty compared with the direct method. To determine the efficiency for the drivetrain in generator mode and in motor mode individually, a ratio is adopted to divide the total power loss into losses from both modes. Since the ratio has to be obtained through analysis, it can introduce a major part of uncertainty into the determined efficiency. An example of the uncertainty calculation has been presented in the dissertation. With conservative considerations, the uncertainty (95 % confidence level) in the efficiency of a wind turbine drivetrain is expected to be within 1 % at rated power. The limitation of the method is, again, that the DUT also needs to be able to operate in motor mode. The proposed method was demonstrated in the dissertation using an application on a dynamometer test bench.

7.2 Outlook

This dissertation have proposed solutions to a number of important problems in applications of torque measurement in the wind turbine. The aim is to enhance the utilisation of torque measurement in the wind energy. On the other hand, more applications of the proposed methods are also important future work, where more technical details can be cleared and improvement can be made.

The AD-8 wind turbine whose drivetrain was tested in DyNaLab was subsequently

installed as a test turbine in a wind field in Bremerhaven. Same encoders are instrumented in the test turbine in the same way as during the test in DyNaLab. Further research will be carried out to study the long-term feasibility of the torque measurement using the encoders. Signal drift and stiffness change of the drivetrain over long periods of operation are very important factors for the torque measurement. Data analysis will also be carried out to compare the measurements from the field and from the test bench.

Apart from torque measurement, one further potential application of the encoder measurement is to measure the transmission error caused by the teeth meshing in the gearbox. The overall angular deformation inside the gearbox in total could be sensed by two encoders directly in front of and behind the gearbox. If the deformation can be captured clearly by the encoders, the signal could act as an information input for the condition monitoring of the gearbox. Similarly, another further application is the detection of possible slip in the drivetrain, for example the slip at the torque limiter of the high speed shaft. Since the slip will occur over a very short period, it can be clearly distinguished from the long-term signal drift of the measurement.

As for the methods used for the torque calibration and the efficiency determination, future work will focus on further reducing the corresponding uncertainties. The most promising direction is to achieve better estimation for the distribution ratio of the power loss in motor and generator modes of the DUT. The current status of the research is that no specific method is developed to determine the ratio. When limited information is available, it is advisable to assign a relatively large uncertainty to the ratio. In the case studies conducted in this research, the uncertainty in the distribution ratio is the largest or even dominant source of the overall uncertainty of the task. For better estimation of the ratio, more information on the component level of the DUT must be taken into consideration. For example, the power losses of the generator at specific working points in motor mode and generator mode should be analysed in detail. Because both the gearbox and generator of the wind turbine are optimised for the normal generator mode, the ratio can be very different to 1. The uncertainty can only be reduced through a careful and detailed analysis for each component of the drivetrain. However, as the ratio is obtained through analysis and can scarcely be determined through measurement, it would be an ultimate limitation to the accuracy of the method.

The measurement of the electrical power is normally easier and more accurate than the torque measurement. Therefore, the uncertainty in the electrical power was not discussed in this research to the same extent as those of the torque. However, a thorough analysis of the electrical power measurement could help make determining the efficiency in an alternative way possible. In the cases where the torque is calibrated with the method proposed in this dissertation, the errors in the electrical power mea-

surement will also be inherited by the torque measurement, since the electrical power is taken as the reference in the calibration. This makes the uncertainty of the torque measurement correlated with that of the electrical power measurement. As the efficiency is a comparison result between the mechanical power (based on torque) and the electrical power, the correlated uncertainties in the torque and electrical power measurements would be largely balanced out. As a result, the efficiency can be potentially determined with sufficient accuracy using the direct method comparing the input and output powers, where the torque should be calibrated with the electrical power following the calibration method proposed in Chapter 5. However, to examine if the correlated part of uncertainties in the torque and electrical power can be balanced out and to check if sufficient accuracy can be met with the direct method of efficiency determination, comprehensive study on the behaviour and uncertainty of the electrical power measurement are still necessary to be carried out in the future.

Publications

JOURNAL ARTICLES

[J1]   **H. Zhang**, R. Ortiz de Luna, M. Pilas and J. Wenske, "A study of mechanical torque measurement on the wind turbine drive train — ways and feasibilities," *Wind Energy*, vol. 21, no. 12, pp. 1406–1422, 2018. doi:10.1002/we.2263.

[J2]   **H. Zhang**, J. Wenske, A. Reuter, and M. Neshati, "Proposals for a practical calibration method for mechanical torque measurement on the wind turbine drive train under test on a test bench," *Wind Energy*, vol. 23, no. 4, pp. 1048–1062, 2020. doi:10.1002/we.2472.

CONFERENCE PAPERS

[C1]   **H. Zhang** and M. Neshati, "An effective method of determining the drive-train efficiency of wind turbines with high accuracy," *Journal of Physics: Conference Series*, vol. 1037, no. 5, p. 052013, 2018. doi:10.1088/1742-6596/1037/5/052013.

[C2]   **H. Zhang**, M. Pilas, N. Eich and R. Ortiz de Luna, "Mechanical torque measurement during a wind turbine nacelle test," *German Wind Energy Conference DEWEK 2017*, http://publica.fraunhofer.de/dokumente/N-480098.html.

PATENTS

[P1]   **H. Zhang** and J. Wenske, "Verfahren und Vorrichtung zur Drehmomentmessung im Antriebsstrang einer Windenergieanlage," German patent DE10201 7219886B3, Dec. 2018. Status: granted, in force.

       PCT international publication: WO2019/091777A1. "Method and device for measuring the torque in the drivetrain of a wind power plant," Status: published.

[P2]   **H. Zhang**, N. Eich, M. Pilas and J. Wenske, "Verfahren zum Ermitteln einer Effizienz und/oder zum Kalibrieren eines Drehmoments eines Antriebsstrangs, insbesondere einer Windenergieanlage," German patent DE102018203525B3, Jul. 2019. Status: granted, in force.

PCT international publication: WO2019/170539A1. "Method for determining an efficiency and/or for calibrating a torque of a drive train, in particular of a wind energy installation," Status: published.

OTHERS

Conference Presentation
H. Zhang, "A practical way of high level torque calibration for the wind turbine nacelle test," *Offshore Wind R&D Conference*, Bremerhaven 2018

Bibliography

[1] World Wind Energy Association WWEA, "Wind power capacity worldwide reaches 597 GW, 50.1 GW added in 2018," February 2019.

[2] WindEurope, "Wind energy in Europe in 2018 - Trends and statistics," February 2019.

[3] G. Corbetta, "Wind energy scenarios for 2030," , WindEurope, August 2015.

[4] W. Yang, P. Tavner, C. Crabtree, Y. Feng, and Y. Qiu, "Wind turbine condition monitoring: technical and commercial challenges," *Wind Energy*, vol. 17, no. 5, pp. 673–693, 2014. doi: 10.1002/we.1508.

[5] E. A. Bossanyi, "Individual blade pitch control for load reduction," *Wind Energy*, vol. 6, no. 2, pp. 119–128, 2003. doi: 10.1002/we.76.

[6] E. Bossanyi, P. Fleming, and A. Wright, "Field test results with individual pitch control on the NREL CART3 wind turbine," in *50th AIAA Aerospace Sciences Meeting*, January 2012. doi: 10.2514/6.2012-1019.

[7] T. Mikkelsen, N. Angelou, K. Hansen, M. Sjöholm, M. Harris, C. Slinger, P. Hadley, R. Scullion, G. Ellis, and G. Vives, "A spinner-integrated wind lidar for enhanced wind turbine control," *Wind Energy*, vol. 16, no. 4, pp. 625–643, 2013. doi: 10.1002/we.1564.

[8] M. Pilas and M. Riezu, "Functional prototype testing of an 8 MW wind turbine," in *German Wind Energy Conference DEWEK*, (Bremen, Germany), 2017.

[9] "Nacelle testing and examination of electrical characteristics," Test bench homepage, Frauhofer IWES, Bremerhaven, Germany. https://www.iwes.fraunhofer.de/en/test-centers-and-measurements/nacelle-testing-and-certification-of-electrical-characteristics.html. Accessed: April 2020.

[10] Vishay Precision Group, "Plane-shear measurement with strain gages," Tech Note TN-512-1, 2010. [Online]. Available: http://www.vishaypg.com/docs/11062/tn5121tn.pdf.

[11] K. Hoffmann, *An introduction to stress analysis and transducer design using strain gauges*. Darmstadt, Germany: HBM Test and Measurement, 2012. [Online]. Available: https://www.hbm.com/en/0112/reference-literature-on-measurements-using-strain-gauges/. Accessed: April 2020.

[12] *The route to measurement transducers: A guide to the use of the HBM K series, foil strain gauges and accessories*. Darmstadt, Germany: HBM Test and Measurement, 1991. [Online]. Available: https://www.hbm.com/en/3736/tips-tricks-transducer-design/. Accessed: April 2020.

[13] R. Schicker and G. Wegener, *Measuring torque correctly*. Darmstadt, Germany: HBM Test and Measurement, 2002. [Online]. Available: https://www.hbm.com/en/3108/torque-measurement-in-wind-turbines. Accessed: April 2020.

[14] R. Schicker, "Torque measurement in wind turbines - as relevant today as it was in the past," , HBM Test and Measurement. [Online]. Available: https://www.hbm.com/en/3108/torque-measurement-in-wind-turbines. Accessed April 2020.

[15] *"Wind turbines — Part 13: Measurement of mechanical loads,"* IEC Standard 61400-13, International Electrotechnical Commission, Geneva, Switzerland, 2015.

[16] "Strain gage thermal output and gage factor variation with temperature," Tech Note TN-504-1, Vishay Precision Group, 2014. [Online]. Available: http://www.vishaypg.com/doc?11054. Accessed: April 2020.

[17] K. Hoffmann, *An introduction to measurements using strain gages*. Darmstadt, Germany: Hottinger Baldwin Messtechnik GmbH, 1989.

[18] K. Khaled, D. Röske, A. Abuelezz, and M. Elsherbiny, "Humidity and temperature effects on torque transducers, bridge calibration unit and amplifiers," *Measurement*, vol. 74, pp. 31 – 42, 2015. doi: 10.1016/j.measurement.2015.07.007.

[19] H. Söker, S. Kieselhorst, and R. Royo, "Load monitoring on a mainshaft. A case study," in *German Wind Energy Conference DEWEK*, (Wilhelmshaven, Germany), 2004.

[20] U. Schmidt Paulsen, "Performance of meta power rotor shaft torque meter," Risoe-R, No. 1255(EN), Forskningscenter Risø, Roskilde, Denmark, 2002.

[21] "Telemetry for wind energy applications," Webpage, KMT Telemetry, Otterfing, Germany. [Online]. Available: https://www.kmt-telemetry.com/applications-measurement/wind-energy/. Accessed: April 2020.

[22] S. Oh, "Extracting condition monitoring information from a wind turbine drive train," in *First International Symposium on Flutter and its Application*, (Tokyo, Japan), pp. 697–704, May 2016.

[23] M. Bezziccheri, P. Castellini, P. Evangelisti, C. Santolini, and N. Paone, "Measurement of mechanical loads in large wind turbines: Problems on calibration of strain gage bridges and analysis of uncertainty," *Wind Energy*, vol. 20, no. 12, pp. 1997–2010, 2017. doi: 10.1002/we.2136.

[24] T. Verbruggen, "Wind turbine operation maintenance based on condition monitoring WT-Ω," ECN-C–03-047, ECN, April 2003. [Online]. Available: https://publicaties.ecn.nl/PdfFetch.aspx?nr=ECN-C--03-047. Accessed: April 2020.

[25] M. Kreuzer, "Strain measurement with fiber bragg grating sensors," Tech Note S2283-1.0en, HBM Test and Measurement, Darmstadt, Germany, 2006.

[26] Y. Wang, L. Liang, Y. Yuan, G. Xu, and F. Liu, "A two fiber bragg gratings sensing

system to monitor the torque of rotating shaft," *Sensors*, vol. 16, p. 138, January 2016. doi: 10.3390/s16010138.

[27] T. Li, C. Shi, Y. Tan, and Z. Zhou, "Fiber bragg grating sensing-based online torque detection on coupled bending and torsional vibration of rotating shaft," *IEEE Sensors Journal*, vol. PP, pp. 1–1, February 2017. doi: 10.1109/JSEN.2017.2669528.

[28] R. Rolfes, S. Tsiapoki, and M. Häckell, "19 - Sensing solutions for assessing and monitoring wind turbines," in *Sensor Technologies for Civil Infrastructures* (M. Wang, J. Lynch, and H. Sohn, eds.), vol. 56 of *Woodhead Publishing Series in Electronic and Optical Materials*, pp. 565 – 604, Woodhead Publishing, 2014. doi: 10.1533/9781782422433.2.565.

[29] T. Verbruggen, "Load monitoring for wind turbines — fibre optic sensing and data processing," ECN-E–09-071, ECN Wind Energy, 2010. [Online]. Available: https://publications.ecn.nl/ECN-E--09-071. Accessed: April 2020.

[30] K. Kragh, M. Hansen, and L. Henriksen, "Sensor comparison study for load alleviating wind turbine pitch control," *Wind Energy*, vol. 17, no. 12, pp. 1891–1904, 2014. doi: 10.1002/we.1675.

[31] E. Bossanyi, P. A. Fleming, and A. D. Wright, "Validation of individual pitch control by field tests on two- and three-bladed wind turbines," *IEEE Transactions on Control Systems Technology*, vol. 21, pp. 1067–1078, July 2013. doi: 10.1109/TCST.2013.2258345.

[32] K. Selvam, S. Kanev, J. W. van Wingerden, T. van Engelen, and M. Verhaegen, "Feedback–feedforward individual pitch control for wind turbine load reduction," *International Journal of Robust and Nonlinear Control*, vol. 19, no. 1, pp. 72–91, 2009. doi: 10.1002/rnc.1324.

[33] H. joon Bang, M. Jang, and H. Shin, "Structural health monitoring of wind turbines using fiber Bragg grating based sensing system," in *Sensors and Smart Structures Technologies for Civil, Mechanical, and Aerospace Systems 2011* (M. Tomizuka, ed.), vol. 7981, pp. 716 – 723, International Society for Optics and Photonics, SPIE, 2011. doi: 10.1117/12.880654.

[34] M. Mieloszyk and W. Ostachowicz, "An application of structural health monitoring system based on FBG sensors to offshore wind turbine support structure model," *Marine Structures*, vol. 51, pp. 65 – 86, 2017. doi: 10.1016/j.marstruc.2016.10.006.

[35] C. Hübler, W. Weijtjens, R. Rolfes, and C. Devriendt, "Reliability analysis of fatigue damage extrapolations of wind turbines using offshore strain measurements," *Journal of Physics: Conference Series*, vol. 1037, p. 032035, June 2018. doi: 10.1088/1742-6596/1037/3/032035.

[36] D. Zappala, M. Bezziccheri, C. Crabtree, and N. Paone, "Non-intrusive torque measurement for rotating shafts using optical sensing of zebra-tapes," *Measurement Science and Technology*, vol. 29, March 2018. doi: 10.1088/1361-6501/aab74a.

[37] J. Westerkamp, M. Sorg, and A. Fischer, "High-resolution speckle sensor for contactless

torque measurement in wind energy systems," AMA Conferences 2017, pp. 233–237, 2017. doi: 10.5162/sensor2017/B4.4.

[38] "Bearingless encoders," Webpage product portfolio, Baumer GmbH, Friedberg, Germany. [Online]. Available: https://www.baumer.com/de/en/product-overview/rotary-encoders-angle-sensors/bearingless-encoders/c/320. Accessed: April, 2020.

[39] A. Vath, "Dynamische Drehmomentmessung im Antriebsstrang zur Ertragssteigerung und Lastreduzierung," in *Windmesse Technik-Symposium Review*, (Hamburg, Germany), May 2014.

[40] "T-Sense," Product webpage, VAF Instruments, Dordrecht, The Netherlands. https://www.vaf.nl/products-solutions/overview/t-sense-shaft-power-torque-meter. Accessed: April 2020.

[41] "Thrust-Torque Measuring System EVOthrust," Product webpage, Leutert, Adendorf, Germany. https://www.leutert.com/maritime-division/en/products/thrust-torque-meter. Accessed: April 2020.

[42] D. Peschel, D. Mauersberger, D. Schwind, and K. U, "The new 1.1 MNm torque standard machine of the PTB Braunschweig/Germany," in *Proceedings of 19th IMEKO-TC3 Conference on Force, Mass and Torque Measurement*, (Cairo, Egypt), 2005.

[43] K. Ohgushi, T. Ota, K. Ueda, and E. Furuta, "Design and development of 20 kNm deadweight torque standard machine," in *Proceedings of 18th IMEKO TC3 Conference on Force, Mass and Torque*, 2002. doi: 10.1109/DEMPED.2007.4393125.

[44] R. M. Lorente-Pedreille, M. A. Sebastián, M. A. Sáenz-Nuño, and M. N. Medina-Martín, "A metrological characterization approximation for the new torque measurement system in wind turbines test benches," *IEEE Access*, vol. 7, pp. 73469–73479, 2019. doi: 10.1109/access.2019.2920261.

[45] H. Kyling, N. Eich, and P. Feja, "Measuring MNm torques as part of a prototype testing campaign of a high-temperature superconducting generator for wind turbine application in the scope of the ecoswing project," *Journal of Physics: Conference Series*, vol. 1222, p. 012018, May 2019. doi: 10.1088/1742-6596/1222/1/012018.

[46] S. Kock, G. Jacobs, D. Bosse, and J. Gnauert, "Conception of 5 MNm torque transducer for wind turbine test benches," in *Tagungsband der 5. Tagung Innovation Messtechnik*, (Aachen, Germany), pp. 7–12, 5. Tagung Innovation Messtechnik, Vienna, Shaker, May 2017. doi: 10.18154/RWTH-2017-04437.

[47] J. Gnauert, G. Jacobs, S. Kock, and D. Bosse, "Measurement uncertainty estimation of a novel torque transducer for wind turbine test benches," *Journal of Physics: Conference Series*, vol. 1065, p. 042050, August 2018. doi: 10.1088/1742-6596/1065/4/042050.

[48] I. J. Garshelis, "Torque and power measurement," in *The measurement, instrumentation and sensors handbook* (J. G. Webster, ed.), ch. 24, CRC Press LLC, 1999.

[49] J. Andrae, W. Nold, and G. Wegener, "Traceability of rotating torque transducers calibrated under non-rotating operating conditions," in *Proceedings of the 17th IMEKO World Conference*, 2003.

[50] "DT Dynos," Webpage product information, Horiba Automotive Test Systems, Kyoto, Japan. https://www.horiba.com/de/automotive-test-systems/products/mechatronic-systems/engine-test-systems/details/dt-dynos-1955/. Accessed: April, 2020.

[51] A. Berger, T. Trebitsch, and F. Otto, "Measuring torque on an engine test stand," in *Reports in applied measurement*, pp. 6–14, 2001. Published by HBM, Darmstadt, Germany.

[52] *"Wind turbines — Part 22: Conformity testing and certification,"* IEC Standard 61400-22, International Electrotechnical Commission, Geneva, Switzerland, 2010.

[53] M. R. Wilkinson and P. J. Tavner, "Extracting condition monitoring information from a wind turbine drive train," in *39th International Universities Power Engineering Conference*, vol. 2, (Bristol, UK), pp. 591–594, September 2004.

[54] M. R. Wilkinson, F. Spinato, and P. J. Tavner, "Condition monitoring of generators & other subassemblies in wind turbine drive trains," in *2007 IEEE International Symposium on Diagnostics for Electric Machines, Power Electronics and Drives*, pp. 388–392, September 2007. doi: 10.1109/DEMPED.2007.4393125.

[55] N. Perišić, P. Kirkegaard, and B. Pedersen, "Cost-effective shaft torque observer for condition monitoring of wind turbines," *Wind Energy*, vol. 18, no. 1, pp. 1–19, 2015. doi: 10.1002/we.1678.

[56] W. Yang, "18 - condition monitoring of offshore wind turbines," in *Offshore Wind Farms* (C. Ng and L. Ran, eds.), pp. 543 – 572, Woodhead Publishing, 2016. doi: 10.1016/B978-0-08-100779-2.00018-0.

[57] N. R. Averous, M. Stieneker, S. Kock, C. Andrei, A. Helmedag, R. W. De Doncker, K. Hameyer, G. Jacobs, and A. Monti, "Development of a 4 MW full-size wind-turbine test bench," *IEEE Journal of Emerging and Selected Topics in Power Electronics*, vol. 5, pp. 600–609, June 2017. doi: 10.1109/JESTPE.2017.2667399.

[58] G. Foyer and S. Kock, "Measurement uncertainty evaluation of torque measurements in nacelle test benches," in *Proceedings of 23rd IMEKO-TC3 Conference on Force, Mass and Torque Measurement*, (Helsinki, Finland), 2017.

[59] J. J. C. for Guides in Metrology, *International vocabulary of metrology – Basic and general concepts and associated terms (VIM)*. 2012.

[60] B. I. des Poids et Mesures, *Le Système International d'Unités (SI) – The International System of Units (SI), 9th edition*. 2019. https://www.bipm.org/en/publications/si-brochure/.

[61] P. De Bièvre, "Metrological traceability is a prerequisite for evaluation of measurement uncertainty," *Accreditation and Quality Assurance*, vol. 15, pp. 437–438, August 2010. doi: 10.1007/s00769-010-0680-y.

[62] P. Howarth and F. Redgrave, *Metrology - In Short (3rd Edition)*. EURAMET, 2008.

[63] D. Röske, "Torque measurement: From a screw to a turbine," *PTB-Mitteilungen*, no. 118, pp. 48–55, 2008.

[64] D. Peschel, "The state of the art and future development of metrology in the field of torque measurement in Germany," in *New Measurements - Challenges and Visions, XIV. IMEKO World Congress*, pp. 65–71, 1997.

[65] S. Merlo, C. Ferrero, C. Marinari, and E. Martino, "Metrology of torque: New development at the CNR-IMGC," in *XV IMEKO World Congress*, 1999.

[66] K. Ohgushi, T. Tojo, and A. Furuta, "Development of the 1 kN·m torque standard machine," in *XVI. IMEKO World Congress*, 2000.

[67] T. Li, M. Dai, J. Lin, Y. Zhang, and Z. Zhang, "The torque standard machines in China," in *Fundamental and Applied Metrology, XIX IMEKO World Congress*, pp. 347–350, 2009.

[68] P. Averlant, P. Lacipiere, and J.-M. David, "Development of the new LNE 5 kN.m deadweight torque standard machine," in *IMEKO 22nd TC3, 12th TC5 and 3rd TC22 International Conferences*, 2014.

[69] A. Robinson, "The design, development and commissioning of a 2 kNm torque standard machine," *CalLab*, pp. 31–35, January-March 2007.

[70] H. Kahmann, C. Schlegel, R. Kumme, and D. Röske, "Principle and design of a 5 MNm torque standard machine," in *Proceedings of 23rd IMEKO-TC3 Conference on Force, Mass and Torque Measurement*, June 2017.

[71] A. Schäfer, "TN torque transfer standard with improved usability for inter-laboratory comparisons," *Journal of Physics: Conference Series*, vol. 1065, p. 042007, August 2018. doi: 10.1088/1742-6596/1065/4/042007.

[72] F. Meng, Z. Zhang, and J. Lin, "Comparison between a reference torque standard machine and a deadweight torque standard machine to be used in torque calibration," *International Journal of Modern Physics: Conference Series*, vol. 24, p. 1360022, 2013. doi: 10.1142/S2010194513600227.

[73] D. Röske and D. Mauersberger, "On the stability of measuring devices for torque key comparisions," in *XVIII IMEKO World Congress*, 2006.

[74] G. Wegener and L. Stenner, "A guide for choosing the right calibration for torque transducers," vol. II of *SENSOR+TEST Conference 2009*, pp. 265–270, 2009. doi: 10.5162/sensor2017/B4.4.

[75] "Materials testing machines — calibration of static torque measuring devices," (in German). DIN Standard 51309:2005-12, Deutsches Institut für Normung DIN, 2005. doi: 10.31030/9653229.

[76] *"Guidelines on the Calibration of Static Torque Measuring Devices,"* EURAMET/cg-14/v.01,

Previously EA-10/14, EURAMET - European Association of National Metrology Institutes, 2007.

[77] "Characteristics of torque transducers," Guideline VDI/VDE 2639:2008-10, Verein Deutscher Ingenieure VDI, 2008.

[78] A. Robinson, "Guide to the calibration and testing of torque transducers," Good Practice Guide 107, National Physical Laboratory (NPL), 2008. [Online]. Available: https://www.npl.co.uk/special-pages/guides/mgpg107.

[79] C. Schlegel, H. Kahmann, P. Weidinger, and R. Kumme, "New perspectives for MN·m torque measurement at PTB," in *IMEKO 23rd TC3, 13th TC5 and 4th TC22 International Conference*, 2017.

[80] R. Kumme, "Final publishable report of EMPIR project: torque measurement in the MN·m range," 14IND14, EURAMET, 2018.

[81] C. Schlegel, H. Kahmann, and R. Kumme, "MN·m torque calibration for nacelle test benches using transfer standards," *ACTA IMEKO*, vol. 5, pp. 12–18, December 2016.

[82] C. Schlegel, H. Kahmann, and R. Kumme, "Traceable torque calibration for nacelle test benches in the MN·m range," in *14th IMEKO TC10 Workshop Technical Diagnostics*, 2016.

[83] P. Weidinger, C. Schlegel, G. Foyer, and R. Kumme, "Characterisation of a 5 MN·m torque transducer by combining traditional calibration and finite element method simulations," in *AMA Conferences*, 2017. doi: 10.5162/sensor2017/D6.2.

[84] P. Weidinger, G. Foyer, J. Ala-Hiiro, C. Schlegel, and R. Kumme, "Investigations towards extrapolation approaches for torque transducer characteristics," *Journal of Physics: Conference Series*, vol. 1065, p. 042057, August 2018. doi: 10.1088/1742-6596/1065/4/042057.

[85] P. Weidinger, G. Foyer, S. Kock, J. Gnauert, and R. Kumme, "Procedure for torque calibration under constant rotation investigated on a nacelle test bench," in *Sensors and Measuring Systems; 19th ITG/GMA-Symposium*, June 2018.

[86] P. Weidinger, G. Foyer, S. Kock, J. Gnauert, and R. Kumme, "Development of a torque calibration procedure under rotation for nacelle test benches," *Journal of Physics: Conference Series*, vol. 1037, p. 052030, jun 2018. doi: 10.1088/1742-6596/1037/5/052030.

[87] P. Weidinger, G. Foyer, S. Kock, J. Gnauert, and R. Kumme, "Calibration of torque measurement under constant rotation in a wind turbine test bench," *Journal of Sensors and Sensor Systems*, vol. 8, no. 1, pp. 149–159, 2019. doi: 10.5194/jsss-8-149-2019.

[88] R. M. Lorente, N. Medina, M. A. Sáenz, and M. A. Sebastián, "Torque traceability for nacelle's test benches: A design proposal," in *IMEKO 23rd TC3, 13th TC5 and 4th TC22 International Conference*, 2017.

[89] G. Foyer and H. Kahmann, "Design of a force lever system to allow traceable calibration of mn?m torque in nacelle test benches," in *Sensors and Measuring Systems; 19th ITG/GMA-Symposium*, (Nuremberg, Germany), pp. 1–4, June 2018.

[90] G. Foyer and H. Kahmann, "A finite element analysis of effects on force lever systems under nacelle test bench conditions," *Journal of Physics: Conference Series*, vol. 1065, p. 042006, August 2018. doi: 10.1088/1742-6596/1065/4/042006.

[91] "Guideline for the certification of wind turbines," Guideline GL 2010, Hamburg, Germany, 2010.

[92] "Guideline for the certification of offshore wind turbines, edition 2012," Guideline GL 2012, Hamburg, Germany, 2012.

[93] L. Cuadros-Rodríguez, M. G. Bagur-González, M. Sánchez-Viñas, A. González-Casado, and A. M. Gómez-Sáez, "Principles of analytical calibration/quantification for the separation sciences," *Journal of Chromatography A*, vol. 1158, no. 1, pp. 33 – 46, 2007. doi: 10.1016/j.chroma.2007.03.030.

[94] K. Gil, C. Chung, and J.-S. Bang, "Mechanical calibration for the load measurement of a 750 kW direct-drive wind turbine generator system (KBP-750D)," *Renewable Energy*, vol. 79, pp. 177 – 186, 2015. Selected Papers on Renewable Energy: AFORE 2013.

[95] D. J. Lekou and F. Mouzakis, "WT Load Measurement Uncertainty: Load-Based Versus Analytical Strain-Gauge Calibration Method," *Journal of Solar Energy Engineering*, vol. 131, pp. 011005 1–8, January 2009. doi: 10.1115/1.3027508.

[96] A. Grauers, "Efficiency of three wind energy generator systems," *IEEE Transactions on Energy Conversion*, vol. 11, pp. 650–657, September 1996. doi: 10.1109/60.537038.

[97] C. Walford, K. Lybarger, T. Lettenmaier, and D. Roberts, "Midium-speed drivetrain test report," NREL/SR-5000-51175, National Renewable Energy Laboratory NREL, 2012.

[98] "Brochure of LMG671 precision power analyzer," , ZES ZIMMER Electronic Systems GmbH, Oberursel, Germany. [Online]. Available: https://www.zes.com/en/Products/Precision-Power-Analyzers/LMG671. Accessed: April 2020.

[99] "Specifications of WT5000 precision power analyzers," , Yokogawa Test & Measurement, Tokyo, Japan. [Online]. Available: https://tmi.yokogawa.com/solutions/products/power-analyzers/wt5000/. Accessed: April 2020.

[100] M.-M. Kepsu, "Uncertainty of efficiency measurements in electric drives," Master's thesis, Lappeenranta University of Technology, Lappeenranta, Finnland, 2015.

[101] S. M. Schneider, *Test bench design for power measurement of inverter-operated machines in the medium voltage range*. Universitätsverlag der TU Berlin, 2018.

[102] B. Kemink, "The effect of internal phase shift on power measurement uncertainty," , Yokogawa Europe & Africa – Test & Measurement. [Online]. Available: https://cdn.tmi.yokogawa.com/EPE.pdf.

[103] "Datasheet of DS2000ICLA fluxgate current sensor," , Danisense A/S, Taastrup, Denmark. [Online]. Available: http://www.danisense.com/files/DS2000ICLA.pdf. Accessed: April 2020.

[104] "Brochure of hst wideband precision high voltage divider," , ZES ZIMMER Electronic Systems GmbH, Oberursel, Germany. [Online]. Available: https://www.zes.com/en/products/sensors/HST. Accessed: April 2020.

[105] "Evaluation of measurement data – guide to the expression of uncertainty in measurement (gum)," Standard JCGM 100:2008, Joint Committee for Guides in Metrology JCGM, 2008.

[106] K. Stockman, S. Dereyne, P. Defreyne, E. Algoet, and S. Derammelaere, "Efficiency measurement campaign on gearboxes," in *Energy efficiency in motor driven systems, Proceedings*, p. 11, EEMODS, 2015.

[107] P. M. Marques, C. M. Fernandes, R. C. Martins, and J. H. Seabra, "Efficiency of a gearbox lubricated with wind turbine gear oils," *Tribology International*, vol. 71, pp. 7 – 16, 2014. 10.1016/j.triboint.2013.10.017.

[108] S. Derammelaere, S. Dereyne, P. Defreyne, E. Algoet, F. Verbelen, and K. Stockman, "Energy efficiency measurement procedure for gearboxes in their entire operating range," in *2014 IEEE Industry Application Society Annual Meeting*, pp. 1–9, October 2014. doi: 10.1109/IAS.2014.6978376.

[109] D. Kim, B. Park, and J. Jang, "Wind turbine generator efficiency based on powertrain combination and annual power generation prediction," *Applied Sciences*, vol. 8, no. 6, 2018. doi: 10.3390/app8060858.

[110] *"Rotating electrical machines - Part 2-1: Standard methods for determining losses and efficiency from tests,"* IEC Standard 60034-2, International Electrotechnical Commission, Geneva, Switzerland, 2014.

[111] T. Kellner and M. Egan, "This massive magnet will generate power at America's first offshore windfarm," GE Renewable Energy, March 2016. [Online]. Available: https://www.ge.com/reports/this-massive-magnet-will-generate-power-at-americas-first-offshore-windfarm/. Accessed: April 2020.

[112] C. M. Fernandes, L. Blazquez, J. Sanesteban, R. C. Martins, and J. H. Seabra, "Energy efficiency tests in a full scale wind turbine gearbox," *Tribology International*, vol. 101, pp. 375 – 382, 2016. doi: 10.1016/j.triboint.2016.05.001.

[113] "Laboratory testing of drivetrain component efficiencies for constant-speed and variable-speed wind turbines," NREL/SR-500-30117, National Renewable Energy Laboratory NREL, January 2002.

[114] *"IEEE Guide* for Test procedures for synchronous machines - Part I Acceptance and performance testing," IEEE Std 115-2009.

[115] L. Aarniovuori, A. Kosonen, M. Niemelä, and J. Pyrhönen, "Calorimetric measurement of variable-speed induction motor," in *2012 XXth International Conference on Electrical Machines*, pp. 872–878, September 2012. doi: 10.1109/ICElMach.2012.6349979.

[116] L. Aarniovuori, J. Kolehmainen, A. Kosonen, M. Niemelä, H. Chen, W. Cao, and J. Pyrhönen, "Application of calorimetric method for loss measurement of a SynRM drive system," *IEEE Transactions on Industrial Electronics*, vol. 63, April 2016. doi: 10.1109/TIE.2015.2499252.

[117] D. Christen, U. Badstuebner, J. Biela, and J. W. Kolar, "Calorimetric power loss measurement for highly efficient converters," in *The 2010 International Power Electronics Conference - ECCE ASIA -*, pp. 1438–1445, June 2010. doi: 10.1109/IPEC.2010.5544503.

[118] C. Xiao, G. Chen, and W. G. H. Odendaal, "Overview of power loss measurement techniques in power electronics systems," *IEEE Transactions on Industry Applications*, vol. 43, pp. 657–664, May 2007. doi: 10.1109/TIA.2007.895730.

[119] W. Cao, K. J. Bradley, and A. Ferrah, "Development of a high-precision calorimeter for measuring power loss in electrical machines," *IEEE Transactions on Instrumentation and Measurement*, vol. 58, pp. 570–577, March 2009. doi: 10.1109/TIM.2008.2005083.

[120] M. Pagitsch, G. Jacobs, R. Schelenz, D. Bosse, C. Liewen, S. Reisch, and M. Deicke, "Feasibility of large-scale calorimetric efficiency measurement for wind turbine generator drivetrains," *Journal of Physics: Conference Series*, vol. 753, p. 072011, September 2016. doi: 10.1088/1742-6596/753/7/072011.

[121] Z. Bertalanic, M. Pavlica, and Z. Maljkovic, "Analysis of hydro-generator's losses determined by calorimetric method," in *The XIX International Conference on Electrical Machines - ICEM 2010*, pp. 1–6, September 2010. doi: 10.1109/ICELMACH.2010.5608105.

[122] W. Li, "Efficiency measuring of the hydro-turbine generator by calorimetry method," *Hydropower and New Energy*, pp. 36–40, March 2016.

[123] E. C. Bortoni, R. T. Siniscalchi, and J. A. Jardini, "Hydro generator efficiency assessment using infrared thermal imaging techniques," in *IEEE PES General Meeting*, pp. 1–6, July 2010. doi: 10.1109/PES.2010.5589946.
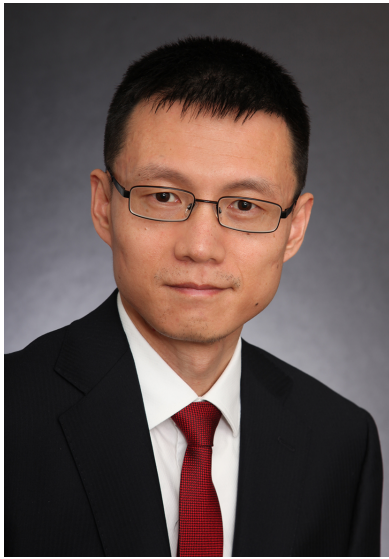
Curriculum Vitae

Personal details

Surname, Given name:	Zhang, Hongkun
Date of birth:	19. April 1985
Place of birth:	Liaoning, China

Education

1991 - 2003:	School education
2003 - 2007:	Bachelor of Science in Engineering: Aircraft Design and Engineering Beijing University of Aeronautics and Astronautics
2007 - 2010:	Master of Science in Engineering: Aeronautical and Astronautical Science & Technology Tsinghua University, Beijing

Career and research experience

2010 - 2014:	R&D Engineer Guodian United Power Ltd., Beijing China
Since 2014:	Research Associate (Wissenschaftlicher Mitarbeiter) Fraunhofer IWES, Bremerhaven Germany